HYDROLOGICAL AND BIOGEOCHEMICAL RESPONSE OF A HIGH ARCTIC GLACIERIZED CATCHMENT TO CLIMATE CHANGE;

A LONG TERM STUDY FROM BAYELVA WATERSHED;

SVALBARD

Thesis submitted for the degree of

Doctor of Philosophy

By

Agnieszka Nowak-Zwierz

(MSc)

Department of Geography

The University of Sheffield

December 2013

ABSTRACT

This thesis examines the Bayelva watershed (Svalbard) between 1974 and 2010 in order to investigate its response to climate change. Hydrological changes are revealed that are most significant during the last ten years, when winters have become warmer and wetter. Water balance modelling shows that more rainfall is offsetting any reduction in flow caused by continued glacier shrinkage. An optimised water budget for 1974/75 to 2009/10 shows that inter-annual changes in water storage can no longer be ignored, despite permafrost and cold-based glaciers being present. Hydrograph analysis suggests that since the transfer of meltwater through the channel network is becoming increasingly efficient, then the deepening active layer is responsible for the new delayed water flowpaths.

To explore the biogeochemical consequences of the above hydrological changes, long-term datasets in Bayelva were examined and new data from separate moraine, talus and soil micro-catchments were collected. Unlike the main river, a significant microbial effect upon runoff geochemistry was seen in all the micro-catchments, causing high NO_3^- and SO_4^{2-} concentrations and contributing to high pCO_2, especially during end of summer low flows. Evidence for the deepening active layer was clear in the soil micro-catchment, because uplifted marine sediments were found to enrich runoff Cl^- concentrations. However, the recently exposed glacier forefield emerges as the most chemically active part of the watershed, for example, when causing a prolonged “flush” of ions and significant pCO_2 depletion following sudden channel migration at the immediate glacier margin. In addition, solute acquisition from glacial sediments in the downstream floodplain contributes significantly to watershed solute export. This means that the overall watershed biogeochemical response to climate change is dominated by a ‘glacial signal’ resulting from rapid chemical weathering reactions. Therefore, understanding Arctic landscape biogeochemical response to climate change can only be uncovered by studying small-scale environments within it.

ACKNOWLEDGEMENTS

This research was funded by a Marie Curie Initial Stage Training Network (NSINK-Sources, sinks and impacts of atmospheric nitrogen deposition in the Arctic, project number R/123386).

I would like to thank both the Norwegian Water Resources and Energy Directorate (NVE) and the Norwegian Meteorological Institute (DNMI) for the provision of runoff and meteorological data respectively. I also thank Jack Kohler of the Norwegian Polar Institute for the provision of mass-balance data, Richard Hodgkins for providing guidance on water balance modelling and Jan Kaiser and Alina Marca from School of Environmental Sciences at the University of East Anglia for determination of NO_3^- isotopes. Furthermore, I would like to thank NERC for providing accommodation and support during the fieldwork in Ny-Ålesund and Kath Taylor and Bill Crowe for help in the labs at Sheffield.

Phil Blaen and Tristram Irvine-Fynn were very supportive during both of my field seasons in Ny-Ålesund therefore a special thanks goes to both of them for excellent field assistance and fantastic company. I will always treasure your friendship.

Sonal Choudary, Aimeric Blaud thanks for your company during long hours of labwork that very frequently stretched well into the night.

Time I have spent in Ny-Ålesund will be always in my heart thanks to all those who turned my stay there into an amazing adventure, a fantastic bunch of people from Birmingham, Bristol, Sheffield and Innsbruck Universities.

I would also like to thank my lovely distraction from work – all my friends from Sheffield Uni. *Guys you know who you are – Dziękuję!*

Finally, Dad, you've always told me to follow my dreams, I bet you didn't expect that.. ☺

I dedicate this work to the person, who made all this possible &
gave me Svalbard, the new love in my life;
to my Supervisor, Andy Hodson

TABLE OF CONTENTS

LIST OF FIGURES

CHAPTER ONE

LIST OF TABLES

CHAPTER TWO

CHAPTER THREE

CHAPTER FOUR

LIST OF PLATES

CHAPTER ONE:
THESIS SUMMARY

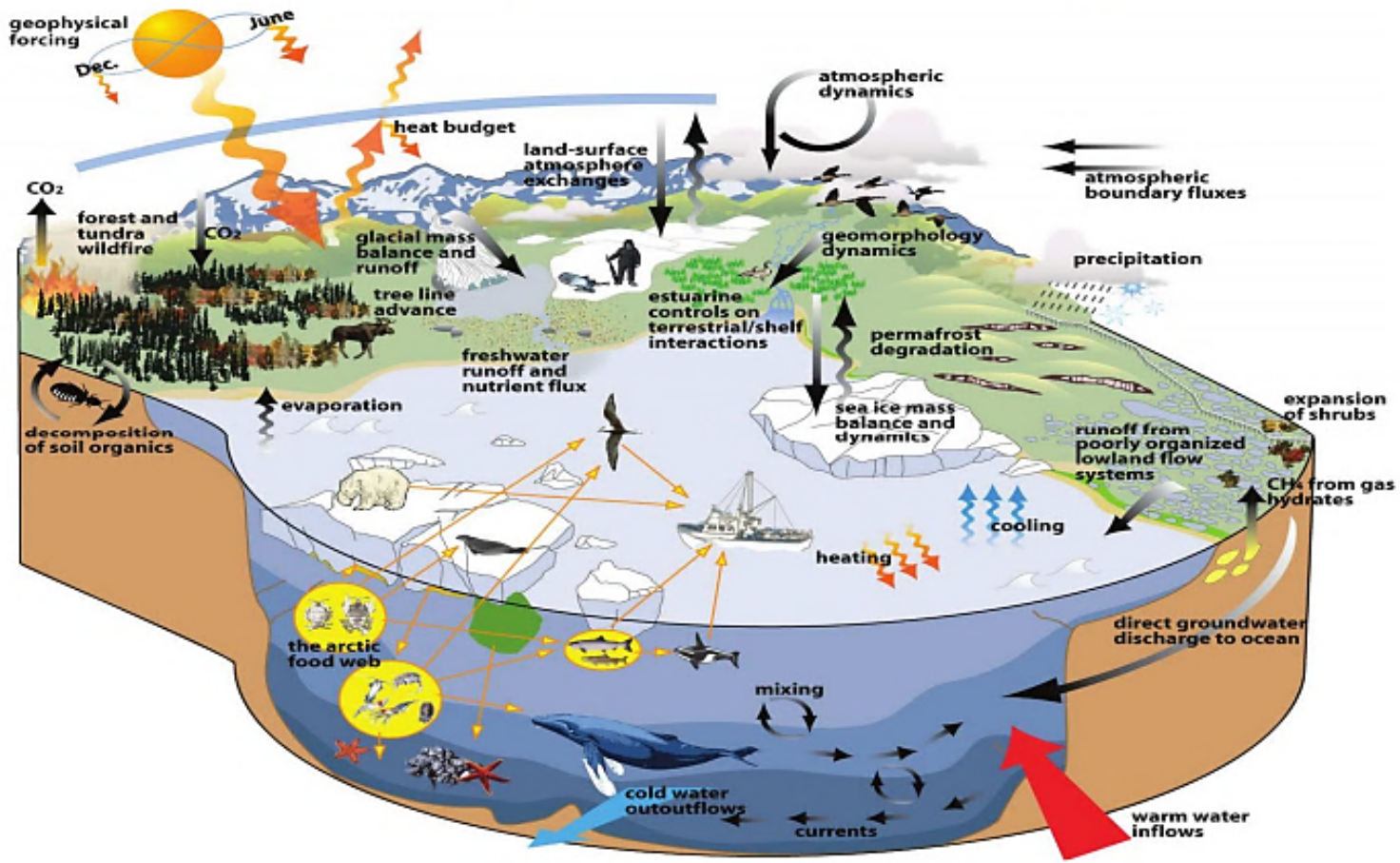

Plate 1 The complexity of dependencies between different meteorological, hydrological and biological factors influenced by climate change in the Arctic. After Döscher 2010

1.1 INTRODUCTION

1.1.1 Arctic climatic setting

"The Arctic is now experiencing some of the most rapid and severe climate change on earth. Over the next 100 years climate change is expected to accelerate contributing to major physical, ecological social and economic changes, many of which have already begun" (ACIA 2005).

Although the above statement is just a part of the summary of the Arctic Climate Impact Assessment, it depicts the breadth of the changes occurring in the Arctic very well. The reasons behind such a severe response to rise in air temperature (hereafter T_a) include not only the geographical pattern in climate warming but also several feedback mechanisms that affect polar regions (IPCC 2007). Therefore, studies indicate that Northern Hemisphere is warming faster that the Southern Hemisphere (IPCC 2007), which is mainly attributed to the ocean-atmosphere circulation. Warming of Northern Hemisphere is caused by northward cross-equatorial ocean heat transport, a concept which was first introduced by Croll in 1870 and explained as follows: *"Since there is a constant flow of water from the southern hemisphere to the northern in the form of surface currents, it must be compensated by undercurrents of equal magnitude from the northern hemisphere to the southern. The currents however which cross the equator are far higher in temperature than their compensating undercurrents; consequently there is constant transference of heat from the southern hemisphere to the northern".* Although Croll presented his idea nearly 150 years ago, his concept explained the processes of northern ocean heat transfer very well. Modern studies (such as Styszyńska 2005, Jie et al. 2008, Marsz and Styszyńska 2009) not only confirmed the importance of that statement but also showed that North Atlantic circulation is the most important factor influencing T_a changes in the Arctic. Moreover, Marsz (2010) showed that the atmospheric heat transfer to the Arctic from Atlantic (30 - 50^{o}N) and Mediterranean/central Europe can only contribute to interannual variations in Arctic T_a temperature, rather than be responsible for its long term changes. For example, if we assume that sea surface temperature and the heat stored in water mass is high then the atmospheric transport of warm air from temperate latitudes, mentioned above, will result in strong T_a rise. Furthermore, transport of cold air from higher latitudes will result in its warming over warmer waters and therefore T_a in the Arctic will decrease only slightly. Contrastingly, if we assume that the same water mass contains less heat, warmer air transported from lower latitudes will lose the heat faster and in

consequence T_a rise over the Arctic will be much slower. However, the decline in T_a caused by transport of cold air from the North over colder waters will be much more severe.

The natural pattern of inter-hemisphere heat transfer is also influenced by the anthropogenic emissions of greenhouse gasses. The latest climate model simulations indicate that the release of such gasses is responsible for the acceleration of climate warming observed over the last century (Gillett et al. 2008). However, Gillett et al. (2012) show that estimates of the Transient Climate Response for the 21st century from T_a observations between 1851 and 2010 range between 1.3 – 1.8^{o}C and are therefore lower than formerly predicted (1.3 – 3.5^{o}C according to Hegerl et al. 2007).

However, what makes the polar regions especially vulnerable to rising T_a are the feedback mechanisms that follow that change. Therefore, warming of the Arctic has been nearly twice as rapid as other regions in the past few decades (ACIA 2005). Thus, as T_a rises, the duration of the winter season changes. For example, Magnuson et al. (2000) found that since 1846 the freeze-up and break-up of ice on lakes and rivers is starting later/earlier by c. 5.8/6.5 days per 100 years. Warmer air that prolongs the melting season is also responsible for increased precipitation (Hanssen-Bauer 2002) especially during winter season (Beldring 2009) and the reduction in the extent for sea-ice and snow cover (Groisman et al. 1994; Brown 2000; Serreze et al. 2000).

Since the freshwater budget in the Arctic is primarily driven by precipitation (Walsh et al. 1998) any changes in precipitation volume and type influence the Arctic ecosystem and may have an effect on North Atlantic Deep-water formation and consequently, upon the global thermohaline circulation (Aagaard & Carmack 1989; Mysak et al. 1990). For example, freshwater runoff to the Arctic Ocean (that contains about 1.5% of the world ocean water) is circa 10% of the total global runoff. Therefore, the local production of freshwater contributes strongly to the stratification of the upper Arctic Ocean (Walsh et al. 1998). As Brooks and Budyka's model shows (Styszyńska 2007), this has a direct effect upon formation of the sea-ice, a key element of Arctic climate that influences the heat exchange between water and the atmosphere. In the Arctic, sea-ice is influenced by the presence and depth of the Arctic Surface Waters created by freshwater surface runoff (from precipitation, rivers, glacial melt) as well as snow and sea-ice melt. Therefore, the Arctic Surface Waters have lower salinity (c. 34.4 PSU), temperature and density than underlying North Atlantic Deep Waters (c 34.9 - 35.2 PSU). As a consequence, those two water layers are separated by a thermocline and pycnocline which prohibit mixing

between them. Additionally, during spring/summer, when multiannual sea-ice and its overlying snowpack melts, an additional layer of 'fresh' waters is created, that is separated by a pycnocline from the underlying Arctic Surface Waters. Increased input of fresh waters from various sources indicated above, results in faster creation of sea-ice which prohibits turbulent heat transfer between water and the atmosphere and increases albedo. During the Arctic winter, when there is no solar radiation, 75 - 88% of the T_a changes are driven by sea-ice presence (heat transferred by non-frozen waters), sea ice thickness (if > 30cm, heat transfer ceases) and atmospheric circulation (Styszyńska 2007). Furthermore, Lawrence et al. (2008) show, that sea-ice loss (circa 7% per decade since the 1970's Johannesseent al. 1999; NSIDC 2013; Fig. 1.1) strongly accelerates Arctic land warming, especially during autumn and early winter.

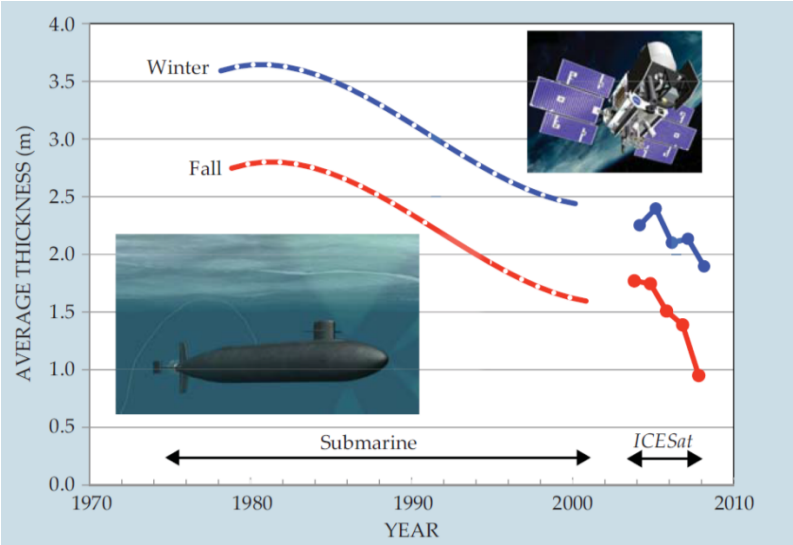

Fig. 1.1 Thinning of the sea ice in the central Arctic between 1978 and 2008. Data from US Navy submarine sonar and NASA's Ice, Cloud and Land Elevation Satellite (ICEsat). Modified from Kwok & Untersteiner (2011)

Areas that are newly exposed by seasonal melting and are darker than snow or ice absorb far more solar radiation than they reflect. The albedo decreases and the heat budget of polar region changes. As a consequence, seasonally and perennially frozen zones on the ground surface (the active layer and permafrost respectively) are subjected to increased heat inputs from solar radiation. The importance of permafrost state as an indicator of climatic changes was recognized during the International Polar Year 2007-2009 when a Permafrost Observatory Network was created (Fig 1.2). Continuation of measurements at existing and reinstated observatory sites and the drilling of new

boreholes resulted in a detailed observation of the state of permafrost and identified a complex relationship between factors controlling its thermal regime such as snow conditions, vegetation types, climate, ground material and landforms (Romanovsky et al. 2010).

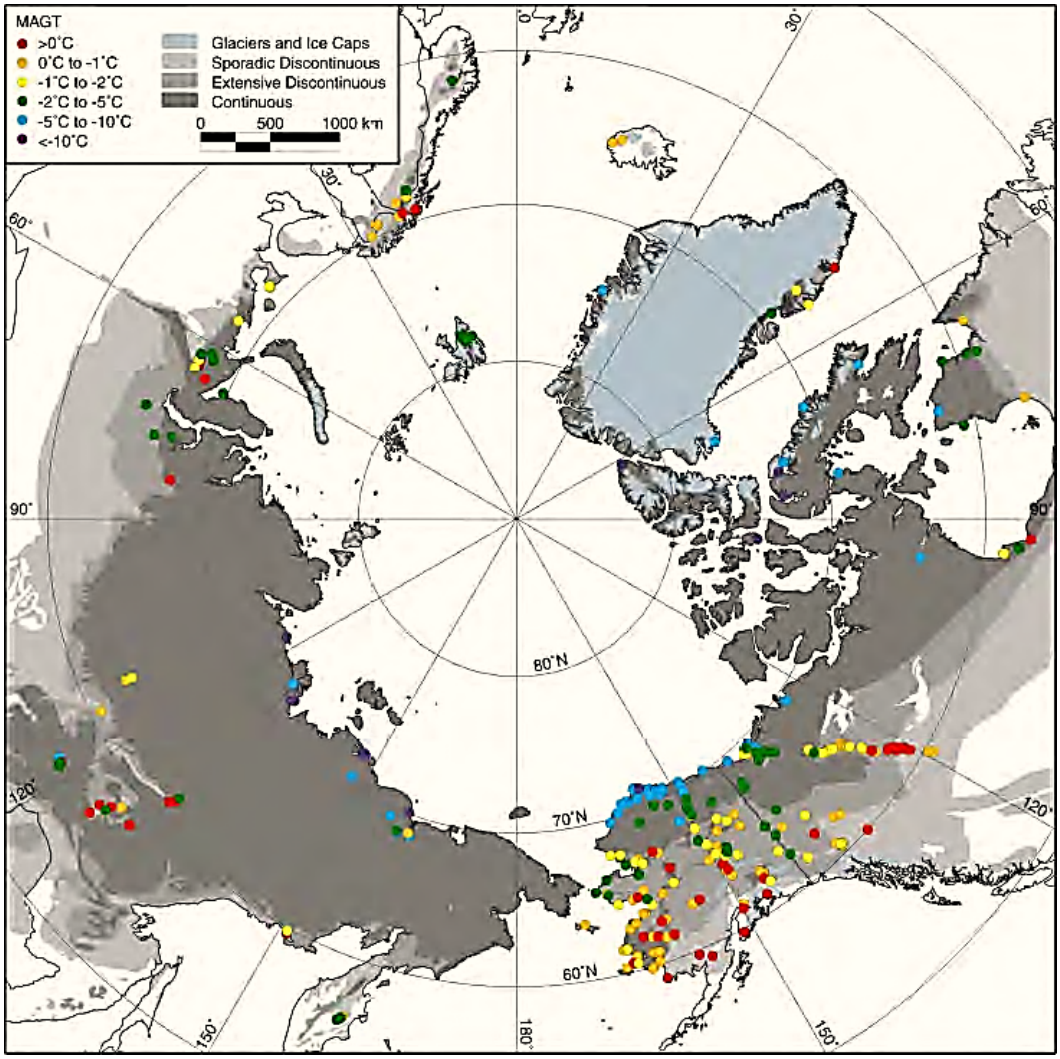

Fig. 1.2 Permafrost monitoring sites established in the Northern Hemisphere before and during International Polar Year (IPY). Colour dots represent Mean Annual Ground Temperature (MAGT) at the depth of zero annual amplitude. In greyscale permafrost zones are presented after Brown et al. (1997). Modified from Romanovsky et al. (2010)

For example, Smith et al. (2010) show that the increase in snowfall observed in northern Alaska may be responsible for the warming of permafrost there due to the insulating properties of snowpack. Conversely, the reduction in snowcover recorded in southern and central parts of Alaska may be partially responsible for the lack of change or even cooling. However, as research shows, the thickness of snowcover is also dependent

upon the type of the vegetation cover. For instance, increasingly abundant Arctic shrubs (Sturm et al. 2005) favour accumulation of snow (Kokelj et al. 2007; Burn and Kokelj 2009). Thicker snowcover is also more likely to persist longer throughout the season. This not only has an impact on thermal regime of the active layer (hereafter AL) and permafrost, but also on microbial communities enclosed in such environments. Insulated from frigid winter conditions, microbes remain active and are responsible for higher net nitrogen mineralization rates. It is also suspected that the changes in the carbon to nitrogen ratio that follows such increased microbial activity may be responsible for increased decomposability of the leaf litter in the following season (Schimel et al. 2004; Sturm et al. 2005).

The state of permafrost is also influenced by the thermal conductivity of the subsurface material. Sites composed of high thermal conductivity material such as quartzite, transfer surface heat into deeper layers of permafrost more effectively than gravel and clays and in consequence, are subjected to more pronounced inter-seasonal temperature variations (Williams& Smith 1989; Yershov, 1998). Water that can be trapped within sediments or in permafrost aquifers also has the same effect on heat transfer. The energy exchange between the atmosphere and permafrost is therefore influenced by the latent heat involved in freezing/thawing processes that occur as permafrost approaches 0^{o}C. Research shows that in such areas a smaller proportion of energy goes into deeper permafrost resulting in slower rates of permafrost warming. By contrast, in colder permafrost (<-2^{o}C) the effect of latent heat can be negligible, resulting in greater temperature changes (Riseborough 1990). Thus, in addition to snowcover, the warming of permafrost depends on its current thermal conditions and the presence of water in its uppermost part, which can preclude annual energy exchange with the atmosphere and therefore restrict further warming.

Additionally, extreme winter rainfalls that follow climate change in the Arctic (Beldring 2009; Førland et al. 2009) can influence ground surface temperatures due to the release of latent heat when the rain freezes below the snowpack. Such events are capable of maintaining the surface temperature close to 0◦C for several weeks, and when repeated regularly over a course of three to five years, can be responsible for the formation of unfrozen zones within permafrost (Westermann, Boike et al. 2011).

As shown above, the response of the AL and permafrost to changing climate depends on multiple factors. Despite that, permafrost has typically warmed across the Arctic during the second half of the 20^{th} and beginning of the 21^{st} century by 0.5 - 4.0^{o}C. The exact

estimate depends on period of record, location and depth of the measurements (see Lemke et al. 2007). Studies investigating the consequences of such a change link permafrost thaw to adaptations in microbial ecosystem functioning (especially with respect to key biogeochemical cycles), local watershed hydrology and the composition of terrestrial vegetation (Smith et al. 2005; Christiansen et al. 2004). Accurate estimates of the magnitude of these inter-linked responses are, however, proving to be a challenge due to the importance of small scale heterogeneity and a lack of long-term data: two issues that are addressed in the present study. The former include the formation of thermokarst features (Jorgenson et al. 2006), the possibility for increased water storage capacity, threats to the survival of wetlands by the opening of new subsurface flow connections (Mackay 1992; Woo et al. 1992) as well as increased flowpath depths (Keller et al. 2010). Collectively they represent a real challenge for modelling biogeochemical cycles because the regional models cannot yet encompass these small scale hydrologic feedbacks. For example, much uncertainty in the release of greenhouse gases from thawing permafrost is expressed in the recent research literature. A recent study by Gao et al. (2013) indicated that the common assumption of high microbial methane release from thawing permafrost, due to anaerobic decomposition of organic carbon, and its positive feedback to warming climate, was greatly overestimated and in fact can be responsible for an additional warming no greater than $0.1^{o}C$ by 2100. What is needed therefore, are detailed studies of the response of various watershed hydrological and biogeochemical cycles that include long term, accurate data for the next generation of Arctic biophysical models. These data are particularly lacking from the maritime Norwegian High Arctic (Svalbard), where it will be shown that there is a strategic need for us to consider climate change impacts in the following section.

1.1.2 Svalbard: a unique place in the High Arctic

Fig. 1.3 Topographic map of Svalbard archipelago in the Norwegian High Arctic. Map source: Räisänen 2008

Svalbard (74 - 81 N and 10 - 35 E; Fig. 1.3) is the northernmost land affected by the warm (6 - 8°C) waters of a branch of the North Atlantic Current (the West Spitsbergen Current) before its entry into the Arctic Ocean. The current is c. 100 km wide, steered by bathymetry and confined over the continental slope (Bourke et al. 1988; Saloranta & Haugan 2001). During transport it loses circa 0.5°C per 100 km (from 74.5 N to 81 N) and in winter, creates the northernmost area of open waters (Boyd & D'Asaro 1994; Førland at al. 1997a; Piechura et al. 2001). It is also responsible for the ice free conditions in Isfjorden (the largest fjord on the west coast of Svalbard) or Kongsfjorden, a typical broad fjord of Spitsbergen and the location of the present study. In contrasting to the west, the east coast of Svalbard often remains covered in pack ice, even during summer.

This is due to the southward flowing, cold waters of the East Spitsbergen Current (Sund 2008), see Fig 1.4.

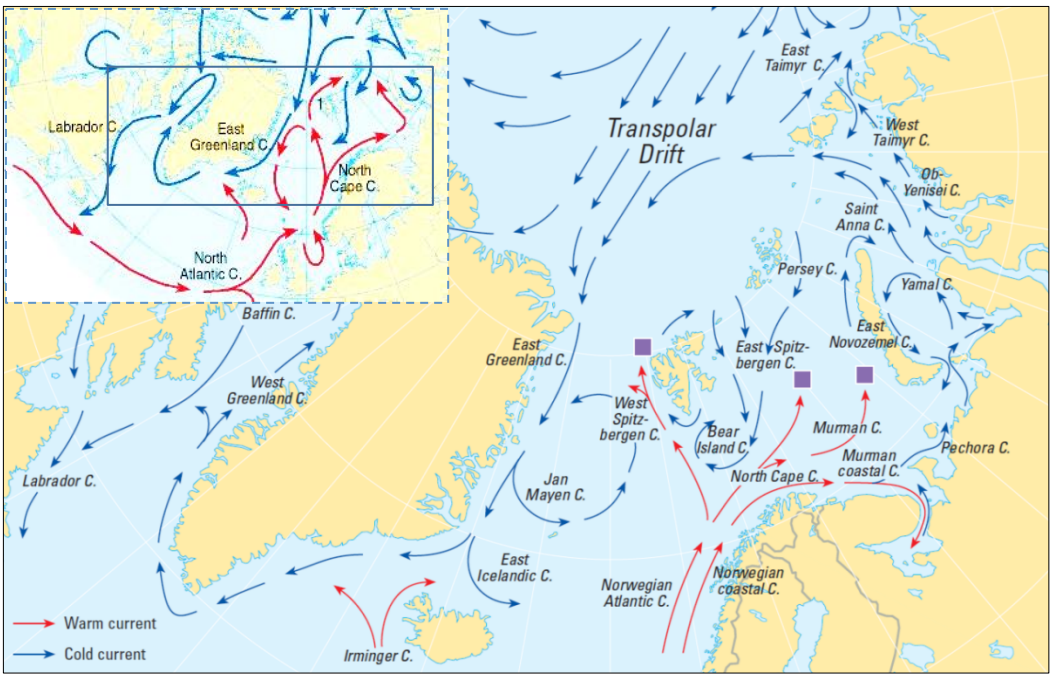

Fig. 1.4 Surface ocean currents in the Arctic. Squares indicate where denser Atlantic waters submerge under the Polar surface water. Modified from AMAP 1998

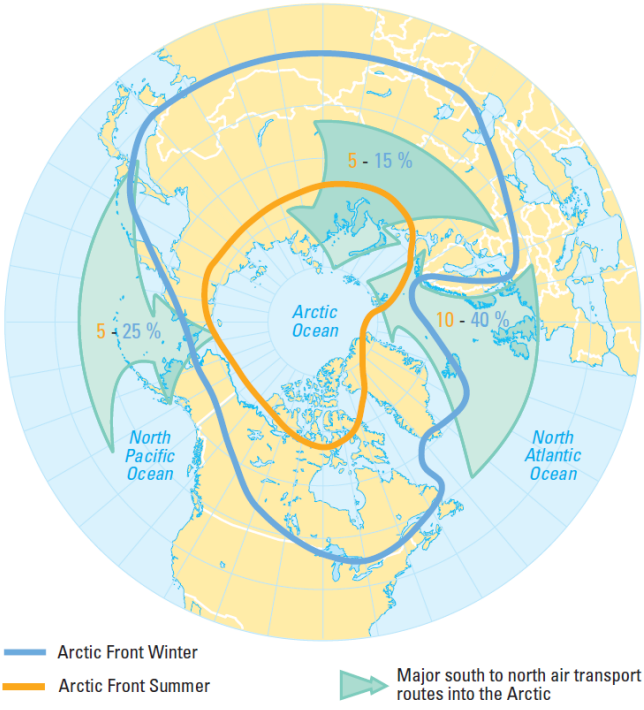

Fig. 1.5 Major air currents into the Arctic. Modified from Iversen 1996

Heat transported by ocean currents is the most important factor controlling Svalbard's climate (see Section 1.1.1 and Marsz 2010). However, inter-annual variations in T_a are influenced by the atmospheric circulation. Low pressure near Iceland and high pressure over Greenland determine the large scale air currents over North Atlantic. Prevailing westerly and south-westerly winds transport heat and moisture from the lower latitudes (Marsz 2010; Fig. 1.5). Such a coupling results in 5 - 10^{o}C warmer climate in Svalbard than in other land areas at the same latitude (Hansen-Bauer et al. 1990; Forsberg et al. 2000).

The latest observations show that recently more warm waters from the West Spitsbergen current have been entering Svalbard's fjords and influencing sea-ice conditions. It is apparent that in 2012 warm waters appeared higher than usual in the water column (at 60 – 70 m instead of 250 – 800 m). In addition, more frequent episodes of prevailing southerly, warm winds pushed freshly created sea-ice northwards and kept areas north of Svalbard warmer during winter. Those winds also contributed to mixing of the water column by bringing warm water into the surface and therefore restricting formation of sea-ice (Nilsen et al. www.unis.no). Such a delay in formation of sea-ice and an increased amount of warm water entering Svalbard's fjords are responsible for the warm moist air advection over a land surface that is 57% covered by glaciers. Furthermore, the ice free areas are covered by continuous permafrost that ranges in thickness from 100 m (coastal areas) to 400 - 500 m (in mountainous areas) (Liestøl 1976; Nuth et al. 2013). Therefore, a maritime location, a warm ocean current, numerous glaciers of various thermal regimes and continuous permafrost, make Svalbard a unique place that is especially vulnerable to the warming climate.

1.1.3 Trends in Svalbard glaciers related to the climate change

The above vulnerability makes Svalbard an early warning indicator of climatic change and its glaciers an early indicator of cryospheric change. Glaciers in Svalbard vary in size, type and thermal regime from cirque, valley glaciers, ice caps to ice fields and from land based to tidewater. Depending on their size, their thermal regime can differ from polythermal to polar (Fig. 1.6; Fig. 1.7; Hagen et al. 2003; Nuth et al. 2013).

Polythermal glaciers consist of two types of ice, temperate and cold. Temperate ice is at the pressure melting point, or in other words, is characterized by the occurrence of liquid water within the ice matrix (Lliboutry 1971). Paterson (1971) and Lliboutry (1976) indicated four different sources of origin of such water: water trapped in ice during

transition from firn to ice, melting as a result of strain heating, surface runoff and finally the adjustment of the pressure melting point as a result of a change in overburden pressure. Contrastingly, cold ice is below the pressure melting point and its ice matrix is virtually free of liquid water. In polythermal glaciers of a polar maritime climate, warm ice is created during spring in the accumulation zone (by refreezing of meltwater and release of latent heat) while in the ablation area, a near surface layer of cold ice is created in winter (Dowdeswell et al. 1984).

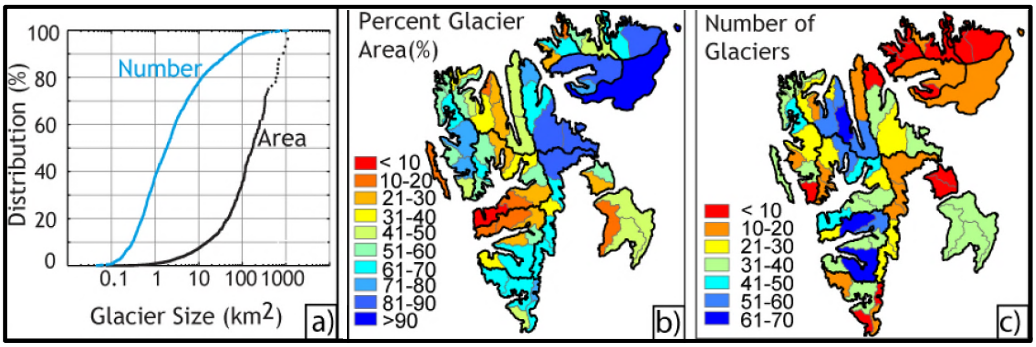

Fig. 1.6 (a) The distribution, number and area of glaciers in Svalbard; (b) the percentage of glacierized area; and (c) the number of glaciers recorded on Svalbard. Modified from Nuth et al. (2013)

(a) (b)

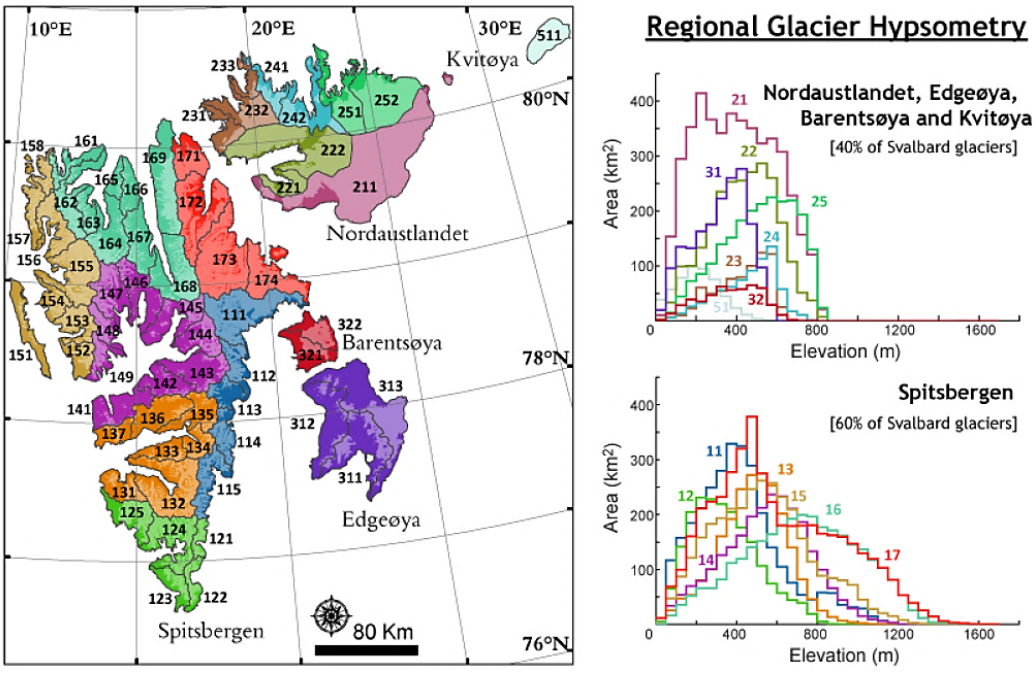

Fig. 1.7 (a) Drainage basins of Svalbard glaciers; and (b) regional glacier hypsometries shown in colour corresponding to the drainage basins. Modified from Nuth et al. (2013)

Generally, the thickness of polythermal glaciers is usually above 100m and their drainage system is well developed consisting of supraglacial, incised (or "*cut–and–closure*"), englacial and subglacial water flowpaths delivering meltwater to proglacial environments (see Fig. 1.8). Furthermore, water can be delivered to the bed via moulins that are formed by fracturing of the ice. The presence of warm ice also gives the possibility for basal sliding, bedrock erosion and water storage within the glacier, even throughout the winter (Irvine-Fynn et al. 2011). Such waters can also be discharged in winter and then freeze creating proglacial icings or naleds/aufeis, if the warm ice reaches the glacier margins (Wadham et al. 2000). However, caution needs to be taken in identifying the thermal regime of a glacier by the presence/absence of an icing since they can also be created by non-glacial water source such as a discharge of intra/subpermafrost groundwaters or the leakage of water from large englacial tunnels in cold ice (Hodgkins et al. 2004).

In contrast to polythermal glaciers, polar glaciers (also called *cold-based*) are, with the exception of the surface layer during summer, entirely made of ice at sub-freezing temperatures and they occur only in cold, arid environments (Fig. 1.9). Such a thermal regime is possible because in polar regions surface, englacial and subglacial heat sources are not sufficient enough to rise the ice temperature to the pressure melting point. Additionally, cold based glaciers are generally small and have thickness below 100 m (Fountain et al. 2006). Their thermal regime means that they are frozen to their beds and therefore lack subglacial drainage. However, in summer, surface melting allows for other hydrological flowpaths to develop upon and within the glacier. Therefore supraglacial, cut-and-closure and englacial channels are common and deliver meltwaters to proglacial environment during the ablation season.

A recent study by Nuth et al. (2013) indicated that since the end of the Little Ice Age (i.e. the 1920's), glacier surface mass balance has generally been negative. Furthermore, the glacierized area has decreased by 7% over the past 30 years (circa 80 km^2a^{-1}). At a regional scale, the timing of such a glacier response to changing climate is variable, proportional to ice thickness and inversely proportional to the ablation rate (Jóhannesson et al. 1989). In consequence, the response rate of glaciers to climate change varies from decades to centuries.

(a)

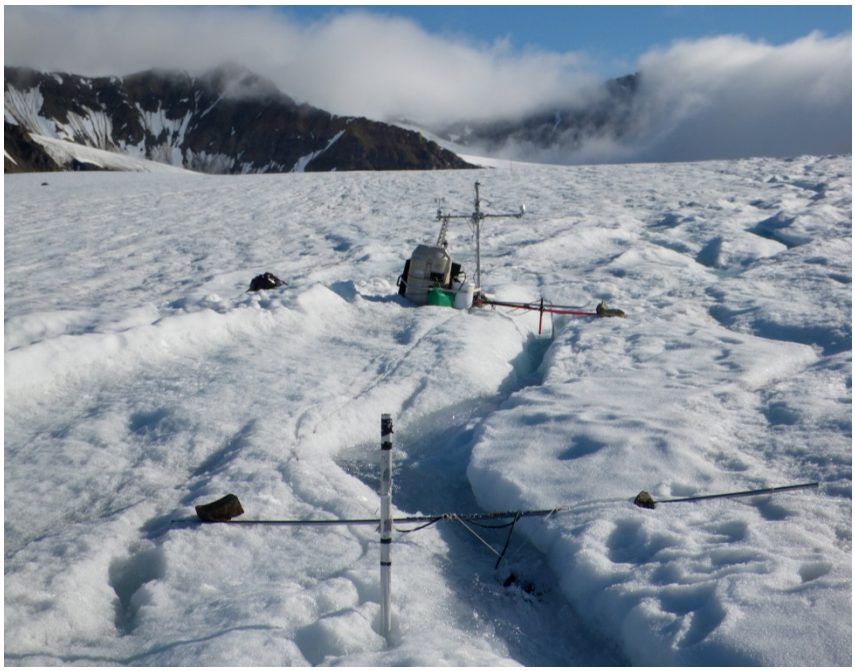

(b)

(c)

Fig. 1.8 An example of (a) supraglacial; (b) cut-and-closure; (c) englacial meltwater flowpath. Photo credit (a) A. Nowak, (b) A. Hodson, (c) modified from Gulley et al. (2009)

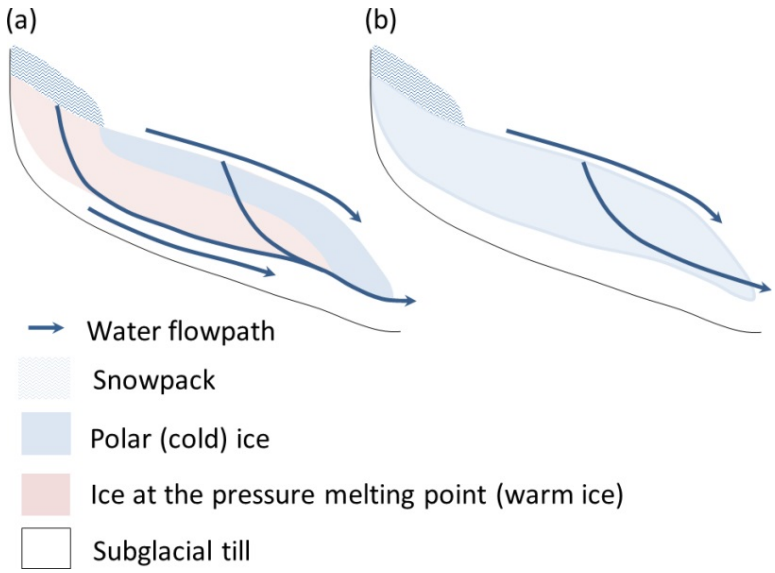

Fig. 1.9 Simplified diagram of: (a) polythermal glacier; (b) polar (cold based) glacier thermal regime and drainage system. Modified from Hodson et al. (2008) and Pettersson 2004

Small and thin glaciers such as those in the present study (see below) respond quicker to any T_a and precipitation changes than bigger and thicker glaciers. Although the temporal response of glaciers to climate change also varies between the polythermal and cold based glaciers, the drivers of the change and their influence upon glacier mass balance are the same. As a consequence, intense mass losses during Svalbard summers (ablation) and insufficient accumulation during winter, means the resident glaciers are getting smaller, thinner and their terminuses are retreating. Their thermal regime also changes, such that many polythermal glaciers become cold based (Hodgkins et al. 1999; Bælum & Benn 2011).

1.1.4 Hydrological and biogeochemical changes during deglaciation

Changes in glacier mass balance to climate forcing are likely to have a profound effect on the hydrology and biogeochemistry of Svalbard's glacierized catchments. However, these changes are yet to be fully understood and, in the case of biogeochemical processes, almost completely lacking in the research literature. For example, several important consequences of glacial thermal regime switch (from polythermal to cold-based) are implicit for meltwater flowpaths when Fig. 1.9a and 1.9b are compared. Impermeable cold ice prevents water from getting to the glacier bed, which becomes

frozen. As a result, subglacial weathering ceases and geochemical processes in other environments where rock-water contact is possible become dominant. For example, a study by Rutter et al. (2011) indicated that ion exchange and dissolution of secondary evaporates occurred in waters flowing thorough glacial moraines and some of the ions (such as Ca^{2+}, Mg^{2+} and SO_4^{2-}) might have been acquired via microbially mediated weathering reactions. The importance of glacial moraines in solute acquisition was also indicated in a study by Cooper et al. (2002). However, no detailed information on the chemical weathering processes in these and other environments in glacier forefields have been presented in the literature. Therefore close attention will be given to the above topic in this thesis (Chapter Three).

The retreat of a glacier terminus also uncovers reactive fine sediments (produced when the glacier was polythermal) and previously protected from intense physical and chemical erosion by overlying cold-based ice. Those former subglacial tills are then additionally subjected to seasonally variable atmospheric conditions (seasonal freeze-thaw, precipitation, wind) and begin to be influenced by terrestrial ecosystem development.

Studies show that physical and chemical erosion are intricately and proportionally linked (Anderson et al. 2002; Riebe et al. 2003). For example bedrock needs to be weakened to be susceptible to erosion. Moreover, chemical weathering fluxes depend on physical conditions such as water discharge (primary control), catchment lithology (secondary control; see Hodson et al. 2000) the importance of deep, long residence time flowpaths (Anderson 2007), the presence of acids (Moulton & Berner 1998) temperature (White & Blum 1995) and solution saturation state (Anderson 2007). Therefore, glacierized catchments, where rock formerly grinded by glaciers becomes increasingly subjected to freeze-thaw cycles and interaction with meltwater during deglaciation, are among the most effective weathering environments, restricted only by low temperatures. What's more, those weathering environments also have the ability to control atmospheric CO_2 levels via its consumption during the weathering of rock flour (Berner et al. 1983; Berner & Lasaga 1989; Kump et al. 2000; Hodson et al. 2002). The climatically driven, intensified thinning and retreat of glaciers that is described in the previous section therefore has the potential to influence physical and chemical weathering of freshly exposed subglacial tills, increase solute delivery to downstream ecosystems and take part in carbon burial by drawdown of atmospheric CO_2. Additionally, due to glacier retreat, an increase in water discharge may be observed in climatically affected glacierized watersheds, as a result of increased energy input, earlier snowmelt and lower albedo

(Milner et al. 2009). However, intensification of discharge is expected to be followed by its decline due to persistent negative glacier mass balance and a switch from meltwater dominated to a precipitation-driven water regime (Hannah et al. 1999; Barnett et al. 2005; Stahl et al. 2008).

Changes in hydrological regime caused by glacier retreat will most likely cause runoff timing and magnitude to be increasingly dependent upon variability in atmospheric circulation (see Sections 1.1.1 and 1.1.2; Lawler et al. 2003). Specifically, increased interannual variability in water discharge should be expected (Hannah et al. 2005a,b). Short term diurnal scale changes may also occur and reflect alterations in delayed drainage, predominantly from water stores that form base-flow (Hannah et al. 2000; Nowak & Hodson 2013). These include shallow groundwater flowpaths in the active layer, the debris mantle of ice cored moraines and the hyporheic zone. Such flowpaths modify physical and chemical properties of water and therefore become crucial when a glacier has transformed into a cold-based system that lacks water storage and long residence time flowpaths at its bed. The loss of subglacial runoff can also have a marked impact upon turbidity and temperature, thus changing the conditions for downstream flora and fauna. For example, some species of diatoms exhibit a significant negative relationship with water temperature whilst some algae and macroinvertebrates exhibit a positive relationship (Milner et al. 2009).

Increases in stream water temperature are one of the major long-term effects of deglaciation upon aquatic ecosystems. Ecological studies carried out in Alaska, as well as in Alpine catchments have indicated that due to landscape maturation, a switch from environments dominated by physical processes to those dominated by biological processes is taking place (Milner et al. 2007). Whilst river channels become more stable with warmer water temperatures, increased fungal biomass as well as a rise in heterotrophic activity can also occur. This enables more rapid decomposition of organic matter, further influencing river ecosystems (Milner & Petts 1994; Milner et al. 2009; Fig. 1.10). In addition to the changes observed in streams, lakes become more acidic as buffering by ions originating from glacial outflows as well as mineral soils decrease and levels of dissolved organic carbon rise (Engstrom et al. 2000). Another consequence of landscape maturation is the establishment of vegetation (Matthews 1992) that according to Anderson et al. (2000) is necessary to increase silicate weathering and its fluxes from glacierized watersheds.

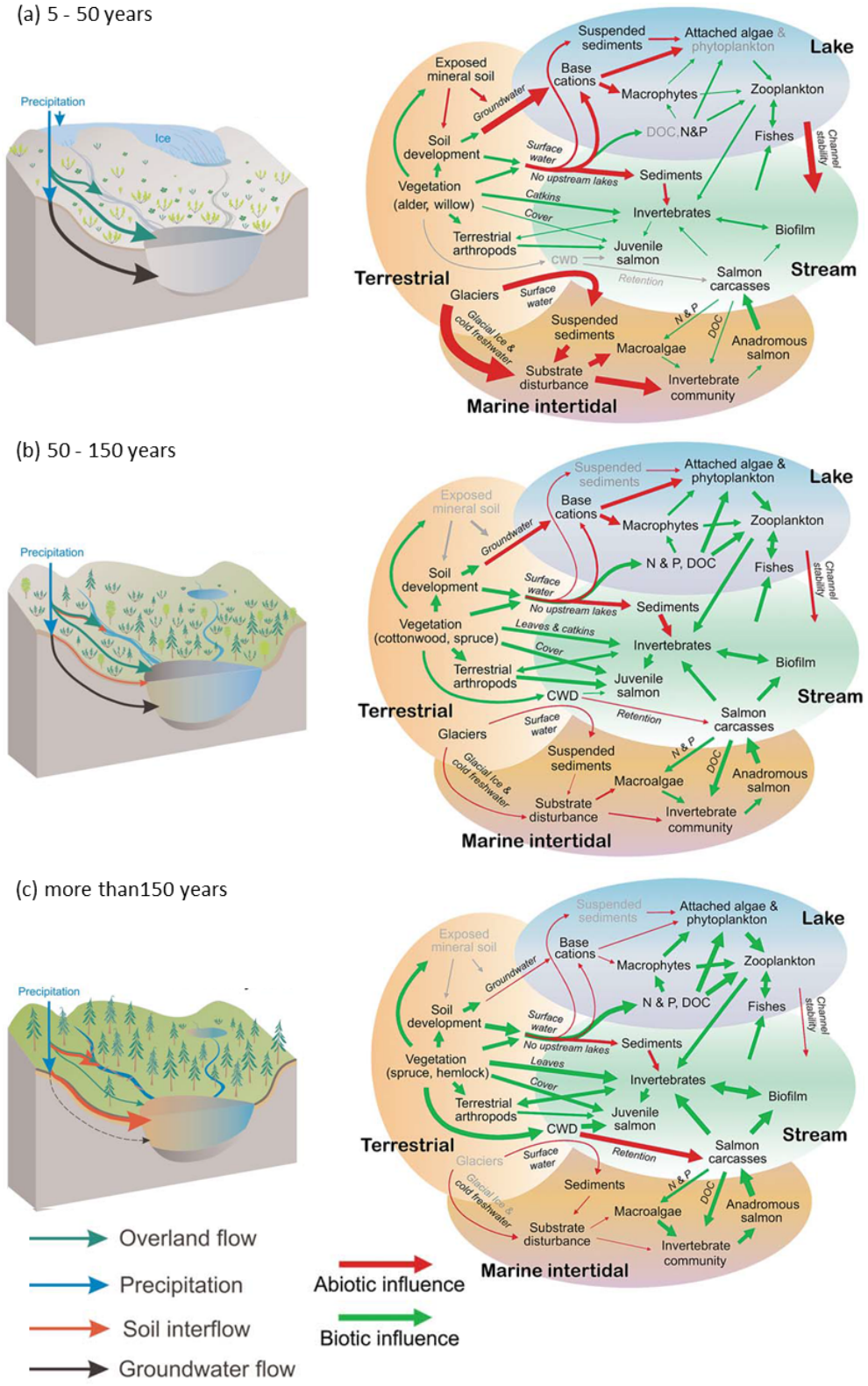

Fig. 1.10 Major features and interactions between terrestrial, lake, stream and marine ecosystems that follow deglaciation, based on a study from south-eastern Alaska. The landscape maturation is presented in three time periods: (a) 5 - 50 years; (b) 50 - 150 years; and (c) more than 150 years after glacier retreat. The thickness of abiotic and biotic influence arrows (red and green) indicates the strength of the influence. Processes that have little or no importance in the given time period are in greyscale. Modified from Milner et al. (2007)

Therefore, landscape maturation following glacial retreat most likely influences biogeochemical processes occurring in High Arctic catchments (Anderson 2005; 2007), but the processes have yet to be observed in detail. Furthermore, glacier retreat begins a phase of landscape evolution during which, over hundreds to thousands of years, isostatic rebound (or glacial isostatic adjustment) is also observed. In maritime Svalbard, this is responsible for the formation of raised beaches, benches and lowland environments prone to the development of wetlands. The importance of wetlands has been recognised thanks to their influence on local ecosystems. They are an important ecological niche, a source of ions to runoff, contribute to carbon cycling and provide major vegetated areas available for grazing (French 1996; Woo & Young 2006). In a High Arctic environment wetlands are confined by the AL depth and the presence of permafrost that prevents the downward percolation of rain and snowmelt (Woo & Young 2006). The first colonizers of such environments are *Nostoc*, nitrogen fixing algae (Chapin & Bledsoe 1992) followed by diatoms, mosses and vascular plants. Sedges and grasses in these areas include *Carex* species, while sedge hummocks are covered by *Salix* and *Dryas* species (Bliss & Matveyeva 1992; Edlund & Garneau 2000). Although the hydrology, ecology and biochemistry of coastal wetlands are being explored in the cold regions of Northern Hemisphere such as Alaska, Canada and Siberia (e.g., Rovansek et al. 1996; Christiansen et al. 2003; Woo & Young 2006; Zhu et al. 2013), little or no attention has been given to wetlands in Svalbard (e.g., Høj et al. 2005) where AL is relatively thin, the highest plants (usually below 10 cm) are dwarf shrubs and the availability of terrigenous organic matter is smaller in comparison with Alaskan, Canadian and Russian Arctic watersheds. In Svalbard, wetland hydrology (incl. temporal dynamics of water table and spatial dynamics), biogeochemistry, response to climate change, emission of greenhouse gasses and their potential to fertilize both local and more distal coastal ecosystems, are yet to be fully characterized.

Climatically driven changes in glacierized watersheds will not be restricted to glaciers, their immediate forefields and proglacial/paraglacial areas (see Fig. 1.10). Surface waters are exported to downstream ecosystems that often include coastal waters on continental shelves, where primary and secondary production is influenced by the changing delivery of freshwater, sediments, major ions and nutrients. For example, a study in western Canadian Arctic by Garneau et al. (2006) shows that coastal areas influenced by freshwater are, due to a change in salinity, characterized by enhanced microbial production. Higher concentration of Cyanobacteria and β-Proteobacteria such

as oxidizing ammonia *Nitrosomonas* and *Nitrosospira* can also be observed (Nold et al. 2000; Hollibaugh et al. 2002; Freitag & Prosser 2004; Sekar et al. 2004).

Increase in suspended sediments delivered by terrestrial surface water has significant, proportional relationship with the abundance of Archaea in the water column (Wells & Deming 2003). In fact, microbial production in turbid freshwater-influenced coastal environment is dominated by particle-based communities. Garneau et al. (2006) indicates that more than 65% of heterotrophic production of prokaryotes is associated with particles larger than 3 µm. Also, a proportional association exists between sedimentation rate and carbon preservation by organic matter burial (Keil et al. 1994) indicating that circa 30% of terrestrial organic carbon can be preserved that way (Hedges & Keil 1995).

Suspended sediments delivered to offshore marine environments are also subjected to inorganic chemical interactions with seawater. For example, reactions of ion exchange of Ca^{2+} for Na^{+} that occur when clays enter marine ecosystem, fuel formation and precipitation of carbonates and removal of circa 40% of total Ca^{2+} fluxes delivered from the terrestrial ecosystem (Gislason et al. 2006). Studies show that the processing of delivered terrestrial sediments can even exceed consumption of CO_2 observed in terrestrial weathering processes (Anderson 2007).

Further, Arctic riverine transport of organic matter to the Arctic Ocean is the greatest (by volume) compared to riverine transport to other world oceans (Lobbes et al. 2000) and the export of DOC compares to the Amazon River (Degens et al. 1991). Surface waters are also the source of nutrients such as inorganic phosphorus and dissolved inorganic nitrogen as shown in a study from Alaska by Hood & Scott (2008) or silica. The former is predicted to decrease following landscape maturation while the latter two increase. On the other hand, a study from Svalbard by Hodson et al. (2004) demonstrated that phosphorus export to the fjord is not only enhanced by glaciers but perhaps can be associated with iron III phases created by sulphide oxidation, therefore the prediction of the changes in phosphorus fluxes that follow deglaciation may be more complicated and require further research.

Although a motivation, the impact of deglaciation upon coastal biological productivity was not established as an objective for this study, because it instead addresses major uncertainties in the processes that control inputs to the coastal environment. Closer attention to the fertilisation of coastal ecosystems will be given in the 'Suggestions for Further Research' within Chapter Five.

1.1.5 Scope and motivation for research

Given the above, this research was motivated by a need to better understand the following consequences of climate change in glacierized Svalbard catchments:

1. What happens to the runoff quantity and quality as a glacier retreats, thins and switches to being cold-based?
2. What hydrological and biogeochemical signals are apparent as a result of permafrost change beyond the contemporary glacier margin?
3. What are the dominant signals from 1. and 2. that will drive terrestrial coupling to marine ecosystems during summer runoff?

1.1.6 Literature review

The relevant, broad literature has been reviewed above in the introduction and so more detailed literature specific to each individual objective are reviewed at the beginning of Chapters Two, Three and Four.

1.2 AIMS AND OBJECTIVES

1.2.1 Aims and objectives

This thesis aims to advance our understanding of the response of a glacierized High Arctic watershed to climate change. Therefore work presented here links meteorological, hydrological and biogeochemical measurements undertaken by the author and by other researchers in the Bayelva watershed on Svalbard. To fulfil the above aim, the specific objectives were constructed:

1. To explore the long term change in Bayelva's hydrology.
2. To explore the long term change in Bayelva's hydrochemistry.
3. To explore spatial and temporal changes in solute production and export from different parts of the catchment and assess their influence on solute fluxes from the whole watershed.

1.2.2 Experimental design

To achieve the above objectives it was necessary to perform a set of mathematical, statistical, hydrological and chemical analyses. Therefore,

Objective 1: A long term water balance time series based on respectively 35, 22 and 43 years of meteorological, hydrological and mass-balance monitoring in the Bayelva catchment had to be created. Therefore firstly, a sensitivity study of precipitation gradient with elevation change had to be explored, followed by creation of various statistical models for predicting annual river discharge. Secondly, water storage in the basin had to be estimated from annual water balance calculations. Lastly, traditional hydrological and statistical analyses of hourly and daily runoff data had to be used to complement the annual water balance analyses and indicate the dynamics of changing watershed hydrology.

Objective 2: A long term meltwater hydrochemistry time series incorporating solute concentrations and fluxes over the past 20 years had to be created using both existing and recently collected datasets. Secondly, a set of regression models had to be performed in order to explore the changes in chemical weathering processes between 1991 and 2010. Lastly, the change in the glaciers' thermal regime and also the retreat of the ice margins had to be considered in the interpretation of the above analyses.

Objective 3: A comparative study of various micro-environments existing in Bayelva watershed had to be performed. They included moraine, talus and soil micro-catchments in different stages of development following deglaciation and permafrost change. Regression models had to be used to indicate spatial and temporal changes in chemical weathering processes operating in various environments. Secondly, $\delta^{18}O\text{-}NO_3^-$ and $\delta^{15}N\text{-}NO_3^-$ isotope data had to be considered in order to better understand the links between hydrology, geochemistry and microbiology in the various micro-environments. Lastly, a comparison of solute fluxes between the sites and Bayelva had to be performed in order to establish the influence of micro-catchments on solute export from the watershed and consequently their influence on the downstream marine ecosystem.

1.2.3 Thesis structure

This thesis comprises of this extended summary (Chapter One), three self-contained pieces of research material written as manuscripts for peer-reviewed publications (Chapters Two to Four) and a concluding chapter (Chapter Five). Therefore, Chapter One introduces the research, key literature, presents the study's aims and objectives and outlines the methodology. Chapters Two to Four address each individual objective in full. Additionally, Chapters Two and Three were published in Polar Research, while

Chapter Four was submitted to Hydrological Processes. Chapter 5 concludes the thesis synthesising the results, drawing conclusions and identifying meaningful avenues for further research. Furthermore, in the cases of all jointly authored manuscripts (Chapters Two to Four), the author of this thesis conducted the research and prepared the documents while the co-author supervised with respect to the manuscripts' contents and structure.

1.3 GENERAL INTRODUCTION TO METHODOLOGY

In order to address the objectives, three types of dataset were used in this work: data available for download from a web portal, old datasets collected in the area of interest by other researchers and new primary datasets collected by the author over two consecutive ablations seasons. Therefore, to achieve Objective 1, analyses a secondary data analysis was undertaken using available data from Norwegian Meteorological Institute website (eKlima) which offers free access to weather and climate data from historical to real time observations. Objective 1 therefore required no field work. By contrast, to achieve Objectives 2 and 3 hydrological monitoring and geochemical sampling had to be designed and implemented in such a way that:

1) Integration of existing and new data sets could be undertaken (Objective 2)
2) New process data could be collected representing small sub-units or micro-catchments within Bayelva (Objective 3)

Therefore, since each of the Objectives required different sampling locations and sampling design, their specific description was presented in the methodology section of each individual thesis chapter corresponding to each Objective. However, a general overview of the study location and methodology of sampling procedure and laboratory analyses common for Objectives 2 and 3 are presented below.

1.3.1 Study location

The study was undertaken in the watershed of Bayelva on the Brøggerhalvøya in the western part of Oscar II Land in Svalbard (Fig. 1.11). The catchment has received considerable amount of research interest over the past 35 years and is one of the best described in Svalbard.

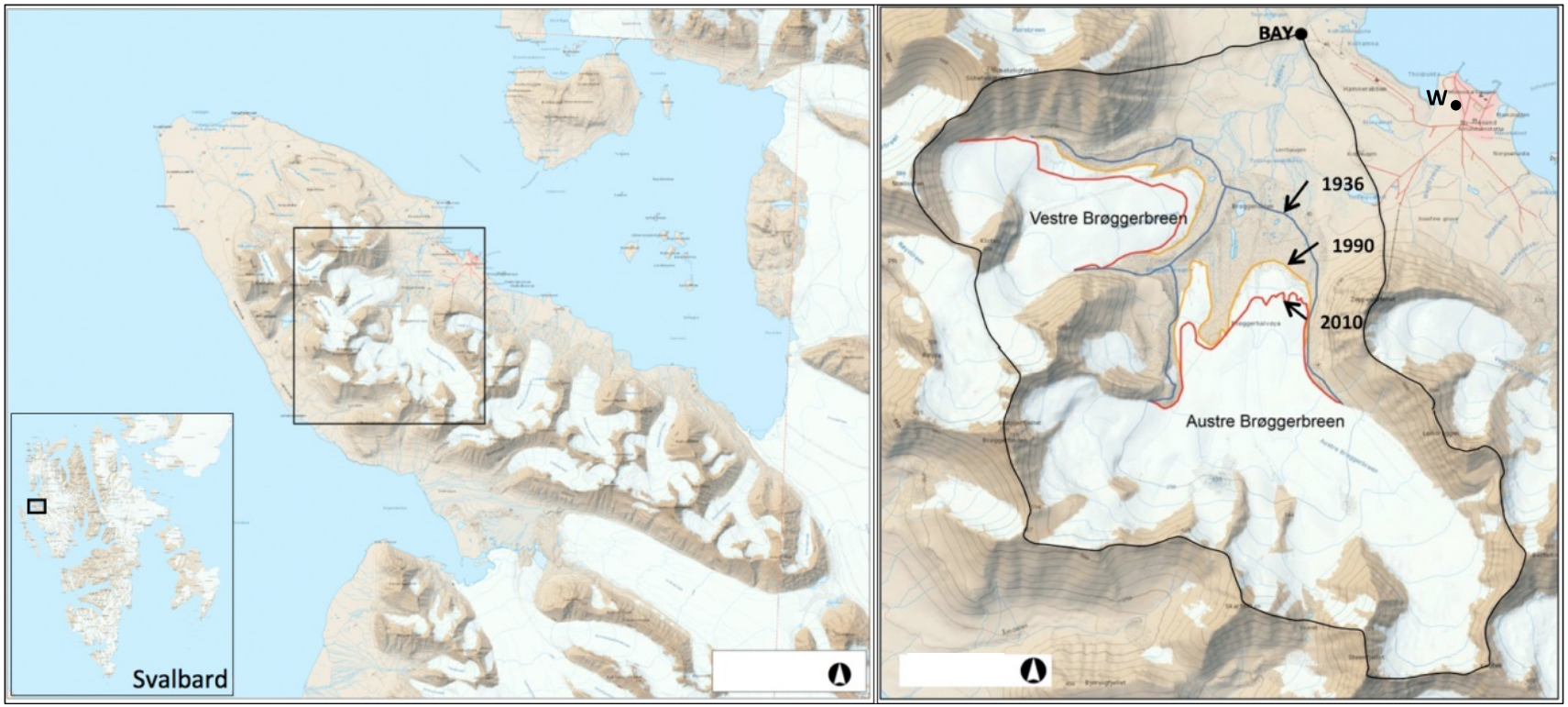

Fig. 1.11 Location of the study area on the Brøggerhalvøya, near Ny-Ålesund, Svalbard, with boundaries of Bayelva watershed (in black), glacier ice margins and the location of hydrological (BAY) and meteorological (W) monitoring stations. BAY is located at 78.9335 N, 11.838 E, and weather station W (99910) is at 78.923 N, 11.933 E. Maps modified from Norwegian Polar Institute's online map resource, www.toposvalbard.npolar.no

(a)

(b)

(c)

(d)

(e)

(f)

Plate 2 Panorama of Bayelva watershed on the (a) 27.06.2009; (b) 29.06.2009; (c) 06.07.2009; (d) 13.07.2009; (e) 21.07.2009; (f) 28.08.2009. Photo credit: A. Nowak

Plate 3 Austre and Vestre Brøggerbreen in 1911. Modified from Miethe & Hergesell (1911)

Plate 4 Austre and Vestre Brøggerbreen in 1930 (top). View from across Kongsfjorden. Modified from a postcard, author unknown; and in 2010 (bottom). View from Tvillingtvatnet. Photo credit: A. Nowak

The watershed covers 32 km^2, ranges in elevation from 4 to 742 m a.s.l. The catchment is located in the continuous permafrost zone reaching from 100 m (coastal region) to 500 m (mountainous region). During summer, its uppermost part thaws creating AL measuring from 0.5 to 1.5 m (Repp 1988; Killingtveit 2004). As a consequence of increasing air temperature over the past 35 years (Nowak & Hodson 2013), the AL in the Bayelva watershed deepened in the last decade by up to 50%. This corresponded with increases in AL depth and permafrost temperatures detected in other regions of Svalbard (Roth & Boike 2001; Hinkel & Nelson 2003; Åkerman, 2005; Isaksen et al. 2007; Westermann et al. 2009).

The watershed is circa 50% glacierized by two retreating, cold based, valley glaciers Austre and Vestre Brøggerbreen. Their retreat was documented by Norwegian Polar Institute and resulted in the loss of 1.86 km^2 (Austre) and 1.08 km^2 (Vestre) of ice at the glacier terminus between 1936 and 2010 (svalbardkartet.npolar.no; Fig. 1.11). Austre Brøggerbreen is by far the better known glacier. It extends from 50 to 600 m a.s.l and according to Lidar surveys performed in 2005, it covers an area of approximately 9.4 km^2 (Bruland & Hagen 2002; Porter et al. 2010). According to ground penetrating radar and thermistor data (Hagen & Sætrang 1991), its transition to cold-based thermal conditions most likely occurred just prior to the start of this study (i.e. 1990's). Beforehand, a thin, temperate ice was detectable at the bed of the upper accumulation area, but no hydrological connections between this ice and the proglacial streams was found during a number of investigations in the early 1990's (see Hodson et al. 1998a). Further, a high frequency radar profile described by Bjørnsson et al. (1996) found no evidence for temperate ice. By contrast, far greater ice thicknesses, a major subglacial channel and an artesian type discharge of glacier-fed groundwater are described at the site during the 1930's by Orvin (1934). These conditions therefore imply that the discharge of subglacial meltwaters from a temperate basal ice layer occurred whilst the glacier was still close to its Little Ice Age limit.

At present meltwaters from both glaciers are discharged through quaternary moraines onto a constrained sandur, consisting mostly of boulders and gravel with only patches of sand and silt (Bogen & Bønsnes 2003) to create Bayelva, and are then eventually conveyed through a well-defined rock channel into Kongsfjorden. No meltwater storage as proglacial icings (as in Hodgkins et al. 2004) occurs in the catchment. Unlike the glacierized part of the catchment, there have been few changes in the glacier forefield beyond the Little Ice Age moraine limit, although changes in the hydrology of the catchment's permafrost soils have been discussed as a consequence of the depth of the AL increasing (Chapter Two, Nowak & Hodson 2013; Westermann, Boike et al. 2011;

Westermann, Langer et al. 2011). The geology of the watershed consists of Carboniferous and Permian sedimentary deposits that show evidence of being deposited in shallow marine areas (calcareous and dolomitic beds). The catchment is composed of both carbonate and silicate minerals. Therefore, southern and eastern part consists of red sandstones, conglomerates, quartzite, phyllite, dolomite, limestone while northern and western part also includes Tertiary sandstone, shale and coal (Orvin 1934; Challinor 1967; Hjelle 1993; Bruland & Hagen 2002). Hence, a mixture of these sedimentary and metamorphosed sequences is being exposed by glacier retreat after advection and erosion by the glacier when it was polythermal at its base.

Average air temperature in the watershed measured at 8 m a.s.l. over 41 years between 1969 and 2010 were -4.9^{o}C. The annual mean (catch corrected) precipitation in the catchment during the last 35 years was just under 540 mm a^{-1} with the mean July-October rainfall of about 157 mm (Nowak & Hodson 2013).

1.3.2 Sampling procedure

To address Objective 2 new water samples were collected during two consecutive ablation season of 2009 and 2010 in the same location as samples collected in 1991, 1992 and 2000 ablation season. To address Objective 3 water sampling was carried out only during 2009 and 2010 ablation seasons.

In order to be able to integrate newly collected data with already existing datasets the author carried out the same sampling procedure. Therefore, water samples were collected using a polyethylene bottle prerinsed three times with meltwater before sampling. The samples were then filtered within 12 hrs. of collection through a 0.45 µm Whatmann cellulose nitrate filter paper using a Nalgene filtration unit. Filtered samples were then placed in 60 ml sterile polypropylene bottles with no air and stored in +4^{o}C for up to three months until the analyses (see below). Contamination of samples by the filtration process was examined by the use of deionized water blanks. No contaminants were detected.

1.3.3 Laboratory analyses

Water samples collected in 2009 and 2010 were determined as follows. Sample pH was measured directly after collection with the use of VWR handheld pH meter. Calibration of the electrode was carried out daily with fresh buffers 4 and 7 at the beginning of the ablation season and 7 and 10 after initial snowmelt phase. The precision of the pH meter

was ± 0.01 pH unit and the electrode efficiency was always above 95%. Total alkalinity (HCO_3^-) was determined directly after sample collection by acidimetric titration with 10 mmol HCl to the end point pH of 4.5 (APHA 2005) and used to validate charge balance calculations of HCO_3^- (Wolf-Gladrow et al. 2007) when all the ions were analysed (see below). Additionally, charge balance calculations were also used to determine HCO_3^- concentrations in samples collected in years 1991, 1992 and 2000. Concentrations of major ions (Ca^{2+}, Mg^{2+}, Na^+, K^+, Cl^-, SO_4^{2-}) and nutrients (NO_3^-, NH_4^+, PO_4^{3-}) were determined using Dionex ICS90 ion chromatography. The detection limit was 0.001 mg L^{-1} and precision errors of all analyses were below 5%, no PO_4^{3-} was detected. A Skalar, wet chemistry nutrient analyser, was used to determine concentration of dissolved silica (Si) using the same colourimetric principle as the manual molybdenum blue method. The precision error of all analysis was also below 5%.

Analytical methods for samples collected in 1991, 1992 and 2000 were described in Hodson et al. (2002) and Hodson et al. (2005). pH was determined post-filtration using a 60 mL sample stored in the dark at +4°C with no air present and within ten days from collection using Orion or WPA portable pH meters with low ionic strength electrode calibrated with pH buffers 4 and 7. The precision of the measurements was ± 0.1 pH unit. NO_3^-, Cl^- and SO_4^{2+} were determined by Dionex DX-100 ion chromatography. Lastly, major cations such as Ca^{2+}, Mg^{2+}, Na^+ and K^+ were determined by atomic absorption spectrometry and silica was determined using a manual molybdenum blue method (APHA 1995). The precision errors of all methods were below 5%.

Therefore, the above analyses allowed for direct comparison of all data collected between 1991 and 2010, with the exception of pH. The consequences of the pH measurement routine used in 1991, 1992 and 2000 being different to that used in 2009 and 2010 are explored in the Results section of Chapter Three.

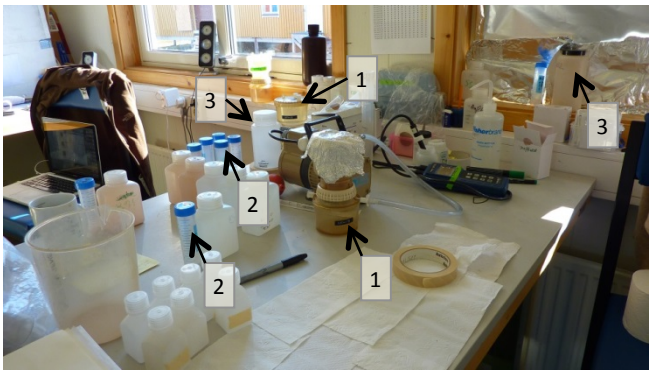

Plate 5 Laboratory setup for filtration of collected samples during 2009 and 2010 ablation seasons. 1 – Nalgene filtration unit, 2 – 60 ml polypropylene sample tubes, 3 – sampling bottles

CHAPTER TWO:

HYDROLOGICAL RESPONSE OF A HIGH ARCTIC CATCHMENT TO CHANGING CLIMATE OVER THE PAST 35 YEARS; A CASE STUDY OF BAYELVA WATERSHED, SVALBARD

Published as: Aga Nowak & Andy Hodson, 2013. Hydrological response of a High Arctic catchment to changing climate over the past 35 years: A case study of Bayelva watershed, Svalbard. Polar Research 32: 19691.

2.1 INTRODUCTION

It is widely acknowledged that the climate has been warming and the High Arctic is particularly vulnerable to changes in air temperature and moisture (Symon et al. 2005; Anisimov et al. 2007). The scientific community is beginning to realize that the hydrological response of glacierized catchments to this climate change is far more complex than it was originally believed, especially, when the relationships between air temperature, precipitation and glacial mass balance are considered. Increasing air temperature and precipitation have already been affecting the High-Arctic environment of Svalbard (Hanssen-Bauer 2002) and it is now known that winter months have been influenced the most (Beldring 2009; Førland et al. 2009). Downscaled and regional climate models for the High Arctic predict further increases in annual air temperature by 2-8^{o}C and in precipitation by up to 40% (Benestad 2008; Førland et al. 2009). Such changes will have various consequences for our understanding of the water budget and hydrological processes in the High Arctic. They can: (1) prolong the melt season (Sharp & Wolken 2010), (2) deepen the AL (Åkerman 2005), and (3) warm the permafrost (Boike 2009; Christiansen et al. 2010). They can also cause: (4) rain on snow, thaw-refreeze events, slush avalanches (Eckerstorfer & Christiansen 2012), and (5) the formation of ground icings. In a hydrological year (1 October - 30 September), (1) - (3) may act as a water source by producing more meltwater from glacial ice and ground ice. Additionally, (2) and (5) may act as a water store and therefore prolong the transfer of meltwaters over a range of time scales. Furthermore, (4) may influence glacier mass balance by redistributing snow across the landscape and also by changing the type of accumulation that is occurring (i.e., the creation of superimposed ice layers vs. firn densification). Measurement of these local changes in the quantity, distribution and form of precipitation can provide real challenges for glacier mass-balance monitoring (e.g., Jansson 1999; Østrem & Haakensen 1999; Zemp et al. 2009). Predicting the hydrological response of Svalbard's glacierized catchments to the above climate change scenario is therefore complicated and depends on many variables. Additionally, collecting and processing precipitation data is very demanding and not without errors associated with catch efficiency and the altitude gradient (see Killingtveit et al. 2003). Furthermore, existing water budget studies (such as Hodgkins et al. 2009; Cooper et al. 2011; Rutter et

al. 2011) are based on short-term (one or two ablation seasons) observations, and although they describe hydrological processes in detail, they do not enable predictions of the long-term hydrological response of High-Arctic catchments to climate change to be made. Therefore, here an updated water-balance study is therefore presented that is based on meteorological, hydrological and mass balance monitoring for, respectively, 35, 22 and 43 years in the important Bayelva watershed that lies in the immediate vicinity of the international research facility at Ny-Ålesund in the Norwegian High Arctic. The research represents part of a wider study of biogeochemical response of a High-Arctic catchment to climate change, and places particular emphasis upon temperature and precipitation change during the winter and so-called shoulder seasons (spring and fall). Mass-balance records of glaciers within the catchment are examined and incorporated into water-balance calculations. Furthermore, various models for predicting river annual discharge are considered after establishing their sensitivity to the various precipitation correction procedures that are in the literature. Finally, the investigation includes traditional hydrological and statistical analyses of hourly and daily runoff data to complement the annual water balance analysis by trying to reveal the response of this cold-based glacial basin to changing climate.

2.2 METHODS

Temperature and precipitation change within the watershed Meteorological data in the Ny-Ålesund area have been collected since 1967 by the Norwegian Meteorological Institute and are available for free download from the eklima.met.no web portal. Here, air temperature and precipitation data from weather station 99910 were used (Fig. 1.11; Fig. 2.1).

The station is located at 78.923N, 11.933E, at 8 m a.s.l and has operated since 1974. Mean air temperature (T_a) data that were filtered using a Gauss filter 3.0 with a gliding slope of 10 years were also downloaded to depict trends in climate change at this site. Precipitation types were deduced from air temperature and classified as snow or rain (when $T_a<0^oC$ or $T_a>0^oC$, accordingly). Measured precipitation data were then corrected for catch (P_c) by the value of 1.15 (rain) and 1.65 (snow), after Killingtveit (2004). Finally, several different elevation gradients were applied that have been employed in the past (see Table 2.1). The different elevation gradients exist on account of uncertainty and variability in orographic effects upon precipitation and a full discussion is presented by Killingtveit (2004).

Fig. 2.1 Meteorological station (99910) in Ny-Ålesund, Svalbard. Photo credit: E. Bjørtvedt

Table 2.1 Precipitation gradients used in the literature for calculating true precipitation in the Norwegian High Arctic. Corrections producing optimum results (here marked by *) were selected for the final discharge models

Type of precipitation	Elevation correction per 100 m (%)	Reference
rain & snow	15*	Killingtveit 2004
	19*	
	20 up to 300m	Førland et al. 1997b
	25*	Hagen& Lefauconnier 1995
	16	Sand et al. 2003
	12	Mercier 2001
rain	15*	Killingtveit 2004
snow	25*	Hodson et al. 2005
snow	14	Tveit & Killingtveit 1994

2.2.1 Austre Brøggerbreen's mass-balance change

The Norwegian Polar Research Institute has conducted the mass-balance measurements of Austre Brøggerbreen since 1966. Stake measurements, snow depth and density observations and the collection of shallow superimposed ice-cores are conducted in May and September/October at the end of accumulation and ablation periods, respectively. All mass balance data used in this article have been acquired from Jack Kohler (pers. comm. 2011). Further details are available in Kohler et al. (2002) and Kohler (2010).

2.2.2 Bayelva runoff

Hydrological monitoring of Bayelva has been carried out continuously since 1989 by the Norwegian Water Resources and Energy Administration (NVE). The position of the gauging station (Fig. 1.11 see also Fig. 3.1 in Chapter Three) allows for the determination of runoff from the whole Bayelva catchment area. Early discharge records for the period 1975/78 were acquired from Hagen & Lefauconnier (1995). Errors associated with the discharge rating curves used to calibrate the records are thought to be 5% or less, according to Skretteberg (1991).

2.2.3 Water balance for the Bayelva catchment

Surface water runoff from the catchment was calculated from the water-balance equation (Eqn. 1) modified from Hagen & Lefauconnier (1995) and Killingtveit et al. (2003).

$$P_a+B_s+C-Q_s-O_g-E_a\pm\Delta S=\epsilon \quad (2.1)$$

Where:
P_a - Areal precipitation with both catch and elevation gradient corrections applied (mm a^{-1})
B_s - Summer mass balance loss from the glaciers (mm a^{-1})
C - Condensation (mm a^{-1})
Q_s and Q_g - Respectively surface and groundwater runoff from the watershed (mm a^{-1})
E_a - Evaporation (mm a^{-1})
ΔS - Changes in catchment's water storage (mm a^{-1})
ϵ – Residual balance (mm a^{-1})

Various models for predicting surface water runoff (hereafter Q_s) in the Bayelva watershed were explored under the assumption that $\varepsilon=0$. The predicted discharge (hereafter Q_p) was derived from estimates of ice-, firn and snowmelt, winter and summer precipitation, evaporation and condensation. In keeping with the earlier studies conducted here (i.e., Hagen & Lefauconnier 1995; Killingtveit et al. 2003), the storage term was assumed to be negligible in the first instance: an assumption based on the glaciers' cold-based thermal regime, the presence of permafrost in the watershed and, as suggested by Killingtveit et al. (2003), the long time period of analyses. Ice-, firn- and glacial snowmelt in the watershed were calculated from summer mass balance of Austre Brøggerbreen extrapolated over both glaciers in the catchment (50% of the total area) on account of their near-identical hypsometry. Winter precipitation on non-glacierized areas below 100 m elevation was calculated from winter P_c at the monitoring station (summed for all intervals when discharge was not recorded). Winter precipitation on

mountainsides (i.e., above 100 m elevation) was estimated as 26% of winter mass balance on the glacier surface, based on the areal extent of this terrain in the catchment. It was then assumed that all precipitation, which fell as snow outside the glacier, melted during the summer. Summer P_c was corrected for elevation according to different gradients presented in Table 2.1. In so doing, we maintained the use of 50 m elevation zones that has been traditionally used with respect to the glacier mass-balance monitoring (Kohler et al. 2002; Kohler 2010) and geochemical flux studies (Hodson et al. 2005) conducted in this basin over the last 35 years. Additionally, three different summer periods were considered: (1) June, July, August (hereafter JJA) employed by Hagen & Lefauconnier (1995); (2) June, July, August, September (hereafter JJAS); and (3) JJAS+P_Q which included all precipitation events that occurred when discharge of Bayelva was observed. Precipitation causing discharge that occurred during months other than JJAS was assigned to the appropriate hydrological year. Precipitation in JJA in 2000 was not included in the analyses due to the lack of daily precipitation records in the eKlima data. Finally, evaporation and condensation were assumed to be constant after Hagen & Lefauconnier (1995) at 46.88 and 9.38 mm a^{-1}, respectively, as derived from the sparse measurements in the area (Killingtveit et al. 2003).

The full range of water-balance models employed to estimate Q_p is described in Table 2.2. Error analyses were performed to indicate the best model for reconstructing Q_s. Therefore, the mean error (ME) was calculated to examine whether the Q_p models over- or under-estimated measured discharge and the root mean-square error (RMSE) used to indicate the standardized mean error of each model. The Nash-Sutcliffe efficiency criterion (E) and coefficient of determination (R^2) were then used to indicate which model fitted best (E and $R^2 \approx 1$) to the measured discharge data series (Krause et al. 2005). Finally, two years: 1999 and 2008, were excluded from data series. These years represented very significant outliers for which the quality of one or more of the water-balance terms (defined above) was questionable. Optimum estimates of Q_p were then used to fill gaps in the Q_s time series to create a complete water balance in the Bayelva watershed for the hydrological years 1974/75 - 2009/10.

Table 2.2 Models for estimating predicted runoff (Q_p) of Bayelva River. The best model for calculating Q_p resulting in smallest errors and the best fit to the measured discharge is presented in bold. Models 1.0 - 1.2 were based upon Hagen and Lefauconnier (1995)

Model no.	Models for estimating predicted runoff (Q_p)	Precipitation gradient correction	R^2	ME	RMSE	E
1.0	16.253*Bs+0.057*P_JJA+5.498	25 % rain and snow	0.37	96.9	163.3	0.16
1.1	16.253*Bs+0.057*(P_JJA+P_Q)+5.498	25 % rain and snow	0.60	21.8	122.3	0.62
1.2	16.253*Bs+0.057*(P_JJAS + P_Q)+5.498	25 % rain and snow	0.66	-101.0	144.4	0.62
2.0	Pwinter(ngs)+P_JJA+B_s+C-E_a	15 % rain and snow	0.27	221.5	249.2	-0.06
2.1	Pwinter(ngs)+P_JJAS+B_s+C-E_a	15 % rain and snow	0.41	126.5	175.1	0.11
2.2	Pwinter(ngs)+(P_JJAS+P_Q)+B_s+C-E_a	15 % rain and snow	0.65	68.6	121.8	0.56
3.0	Pwinter(ngs)+P_JJA+B_s+C-E_a	25 % rain and snow	0.28	213.0	242.7	-0.05
3.1	Pwinter(ngs)+P_JJAS+B_s+C-E_a	25 % rain and snow	0.43	112.9	166.9	0.15
3.2	Pwinter(ngs)+(P_JJAS+P_Q)+B_s+C-E_a	25 % rain and snow	0.66	51.7	115.1	0.61
4.0	Pwinter(ngs)+P_JJA+B_s+C-E_a	19 % rain and snow	0.29	208.1	239.0	-0.04
4.1	Pwinter(ngs)+P_JJAS+B_s+C-E_a	19 % rain and snow	0.43	105.0	162.4	0.17
4.2	**Pwinter(ngs)+(P_JJAS+P_Q)+B_s+C-E_a**	**19 % rain and snow**	**0.66**	**42.0**	**112.2**	**0.63**
5.0	Pwinter(ngs)+P_JJA+B_s+C-E_a	15 % rain and 25% snow	0.28	213.1	242.7	-0.05
5.1	Pwinter(ngs)+P_JJAS+B_s+C-E_a	15 % rain and 25% snow	0.38	103.5	165.6	0.12
5.2	Pwinter(ngs)+(P_JJAS+P_Q)+B_s+C-E_a	15 % rain and 25% snow	0.62	42.5	117.8	0.59

Where:

P_JJA - Areal precipitation during June-August (mm)
P_JJAS -Areal precipitation during June-September (mm)
P_Q - Daily winter precipitation causing discharge (mm)
Pwinter(ngs) –Areal winter snowfall on non glacierized areas (mm)
B_s - Summer mass balance (mm a^{-1})
C - Condensation (mm a^{-1})
E_a - Evaporation (mm a^{-1})
R^2 – Correlation coefficient
ME – Mean error (mm a^{-1})
RMSE – Root mean square error (mm a^{-1})
E – Nash-Sutcliffe efficiency criterion

2.2.4 Hydrological analyses

Hourly and daily discharge data sets acquired from NVE were used to perform various analyses for the 22 years of flow records. Therefore, flow duration curves (FDC) were used to study the variability of Bayelva's flow regime and flow recession analysis was undertaken to uncover seasonal changes in the catchment's flow routing characteristics. Various FDCs were created from mean daily discharge using Oregon State University's streamflow analysis techniques (www.streamflow.engr.oregonstate.edu) for: (1) the whole period of record (1989-2010); (2) 1989-1999, 2000-10; and (3) individual years of Bayelva flow. Flow recession analyses were also performed according to Gurnell (1993) for three selected years-1991, 2000 and 2009 representing the beginning, middle and the end of the data records. Furthermore, the years were also chosen on the basis of their similarity. Therefore, they were not subjected to extreme rainfall events, unusually high or low discharge duration, magnitude and mean air temperatures. For each year, linear segments of individual diurnal recession curves were identified visually from breaks in the slope of semi-logarithmic plots of discharge against time (Gurnell 1993; Sujono et al. 2004; Rutter et al. 2011). Storage constants (K) for each recession segment were then estimated using the following equation:

$$K = \frac{-t}{\ln\left(\frac{Q_t}{Q_0}\right)} \tag{2.2}$$

Where:

t - Time (hours) since the start of the recession segment of the hydrograph

Q_0 - Reservoir's initial discharge ($m^3\ s^{-1}$)

Q_t - Discharge at time t ($m^3\ s^{-1}$)

After log-transformation of the discharge data, the K values were calculated using linear regression best-fit lines applied to each recession segment, thus allowing for some compensation for errors in Q_s. Each diurnal hydrograph was examined independently. Days that either failed to exhibit a clear, diurnal melt discharge signal (i.e., the significance level of the slope of the regression models was <95%), or days when precipitation influenced the discharge recession were excluded from the analysis. Storage constants for up to three consecutive reservoirs (K1, K2, K3) were identified in the data set.

2.3 RESULTS

2.3.1 Temperature and precipitation change within the watershed

Mean T_a and P_c data for the hydrological year of the Bayelva catchment show distinct decadal and seasonal increases within the last 30 years (Fig. 2.2).

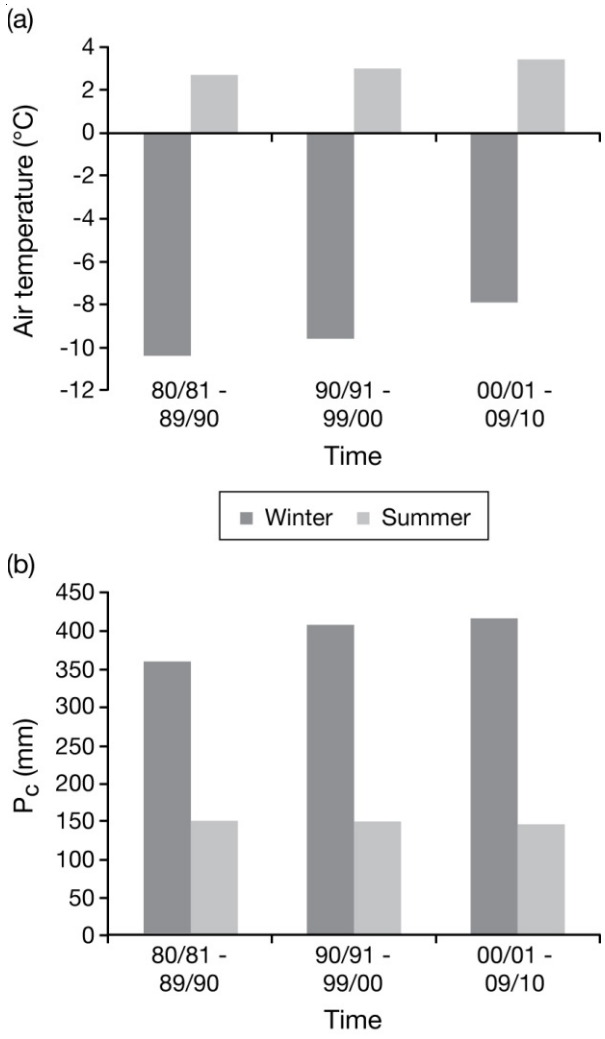

Fig. 2.2 Average seasonal changes by decade in (a) air temperatures and (b) P_c measured precipitation corrected for catch errors, after Killingtveit et al. (2003). Winter is defined as 1 October until 31 May, while summer is 1 June until 30 September

It is noticeable from the separate decadal seasonal series that mean T_a has been increasing during both winter and summer, with the highest rise within the last 10 years (winter: 1.7°C and summer: 0.4°C), while P_c has been increasing, only during winter. Spearman's rank correlation coefficients between T_a, rain and snow (corrected for gauge catch), showed significant positive correlation between winter T_a and rainfall and significant negative correlation between April, May, June and September T_a and snowfall (Table 2.3). Closer investigation of T_a changes during the winter months showed that

mean T_a in the ‘‘shoulder months’’ (March, April, May and September, October) increased most significantly during April and May, with just a slight increase in September and October (Fig. 2.3).

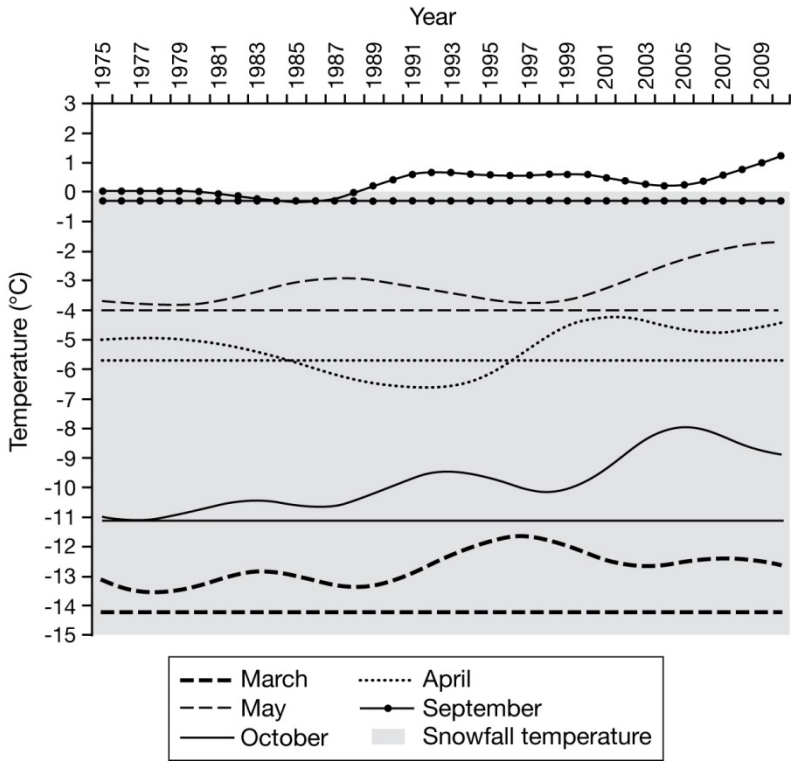

Fig. 2.3 Mean air temperature trends of shoulder months with their long-term averages recorded at the 99910 weather station. Data downloaded on 15 December 2011 from www.eklima.met.no

The examination of precipitation types during shoulder months indicated that although March, April and October were dominated by snowfall, rain events in those months were not uncommon during the last 35 years of records. In contrast, May and September were dominated by rainfall with a sporadic appearance of snowfall. It was noticeable that during eight of the last 10 years of records, rainfall has been the more dominant form of precipitation during May, September and October. For the remaining shoulder months, March and April, the dominance has not occurred although the incidence of rainfall in April has increased (Fig. 2.4).

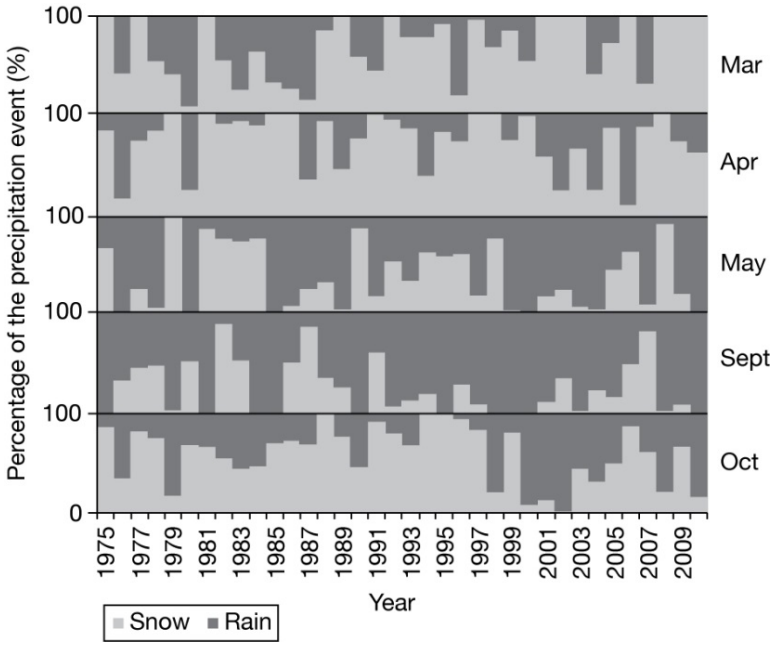

Fig. 2.4 The percentage of snowfall and rainfall during precipitation events recorded throughout shoulder months. Precipitation was corrected for catch errors. Precipitation in May and September in 2000 was deleted due to lack of daily precipitation records in the eKlima data set

Table 2.3 The results of the correlation between monthly mean air temperature (T_a) and precipitation in the Bayelva catchment

Month	**Pearson Correlation**	
	T_a vs Rain	**T_a vs Snow**
January	0.538**	-0.059
February	0.280	-0.001
March	0.503**	0.189
April	0.473**	-0.294
May	0.252	-0.409*
June	-0.069	-0.536*
July	-0.010	-0.111
August	0.087	-0.238
September	0.681**	-0.291
October	0.606**	-0.160
November	0.472*	0.011
December	0.353*	-0.032

Where:

T_a – Air temperature (^{0}C)

*- Correlation is significant at the 0.05 level (2-tailed)

**- Correlation is significant at the 0.01 level (2-tailed)

2.3.2 Austre Brøggerbreen's mass-balance change

Despite yearly variations in the glaciers' winter and summer mass balance (Fig. 2.5), Austre Brøggerbreen has been almost constantly retreating between 1966 and 2010, with a total mass loss of 21.1 m water equivalent (Fig. 2.6).

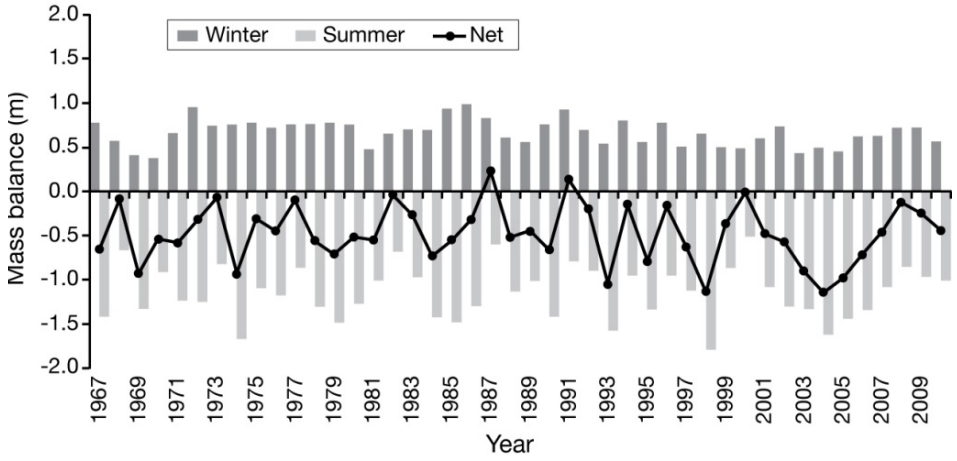

Fig. 2.5 Winter, summer and net mass-balance record of Austre Brøggerbreen glacier. Net balance is the sum of winter and summer mass balance (data from Kohler, pers. comm. 2011)

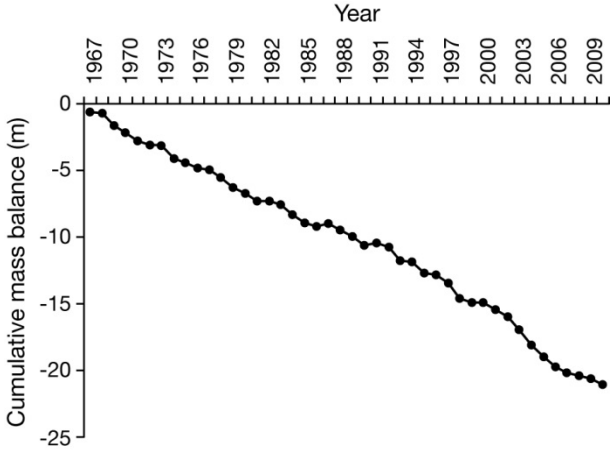

Fig. 2.6 Cumulative mass balance of Austre Brøggerbreen (data from Kohler, pers. comm. 2011)

There have been just two years with small positive net mass balance gains (1987 and 1991). Average winter, summer and net mass balances over the observation period

were 0.66 ± 0.15, -1.14 ± 0.30 and -0.48 ± 0.33 m a^{-1}, respectively. Spearman's rank correlation performed on glaciers' mass-balance and meteorological data revealed significant negative correlation of summer mass balance with T_a in July (r=-0.620, P=0.01) and events of temperature below 0^oC in September (r=-0.683, P=0.01). Events of temperature below 0^oC refers to every record of T_a below 0^oC (in the thrice daily monitoring interval of 6:00, 12:00 and 18:00). Winter mass balance correlated well only with snowfall in May (r=0.562, P=0.01). Spectral analysis performed using SPSS Statistics software did not show any significant cycles in the winter, summer or net mass-balance series.

2.3.3 Bayelva runoff

The number of days each year with observed discharge (Fig. 2.7) varied throughout the whole period of records from 61 to 155 days with neither any significant trend nor any correlation with summer mean T_a or P_c. The start of discharge was relatively constant and only showed a negative correlation with mean T_a in April and June (r=-0.426, P=0.05 and r=-0.431, P=0.05, respectively). The end of flow, although more variable than the beginning, also did not show any correlation with either summer T_a or summer P_c, but correlated well with rain in September and October (r=0.453, P=0.05; r=0.489, P=0.05). The magnitude of mean daily discharge depended more upon mean daily air temperature (r= 0.559 - 0.838, P=0.01) than precipitation (r=0.072 - 0.574, P=0.01). Annual minimum Q_s did not correlate with summer T_a nor P_c while annual maximum Qs correlated significantly with September rain (r=0.502, P=0.05). No statistically significant correlations between discharge and the North Atlantic Oscillation index were found (r= -0.006 - 0.295, P<0.05). The majority of discharge occurred between 1 June and 30 August, with very variable discharge magnitude during September - October and only a sporadic appearance of flow during January - May and November - December (Fig. 2.8). During 1989 - 1999, the average duration of the flow was 108 days, which was nine days shorter than the second half of the observation record (2000 - 2010). The difference in flow duration in those two periods was entirely the result of the occurrence of flow before 1 June and after 30 September (hereafter early and late flows). For example, early flows were recorded on six and 46 days during 1989 - 1999 and 2000 - 2010, respectively, while late flows were recorded on 20 and 80 days accordingly. The sum of Q_s for 1989 - 1999 and 2000 - 2010 was 10.5 and 11.9 m, respectively. Mean Q_s from 1989 until 2010 was 1.08±0.21m a^{-1} with a minimum of 0.56 m a^{-1} (2010) and a maximum 1.42 m a^{-1} (2008).

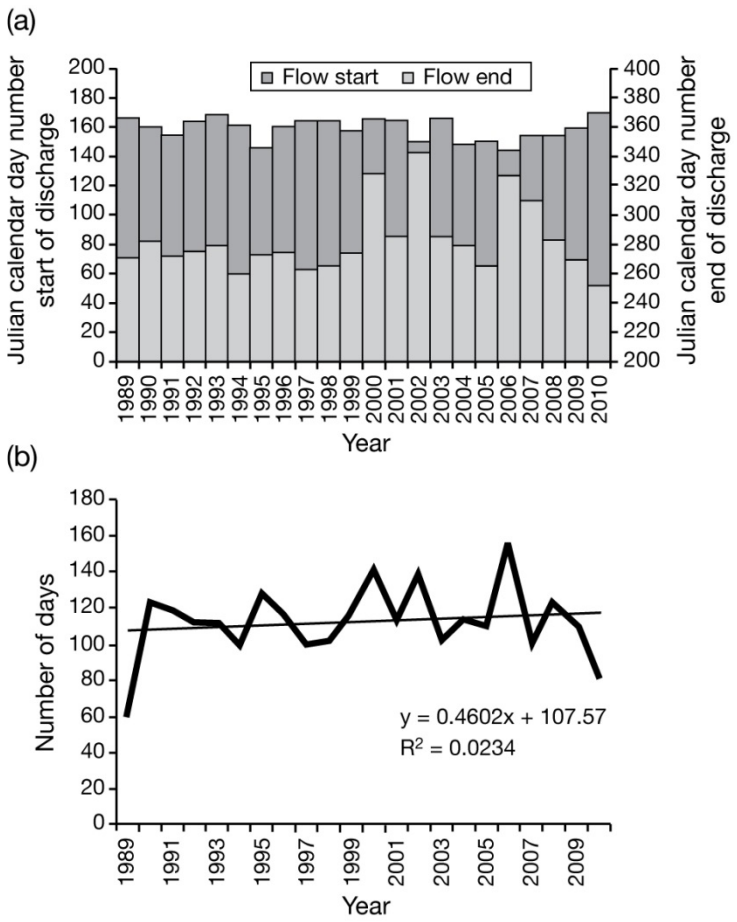

Fig. 2.7 Records of days with discharge of Bayelva from 1989 until 2010: (a) commencement and cessation of runoff; (b) The duration of discharge (in days) with linear regression line showing no significant trend

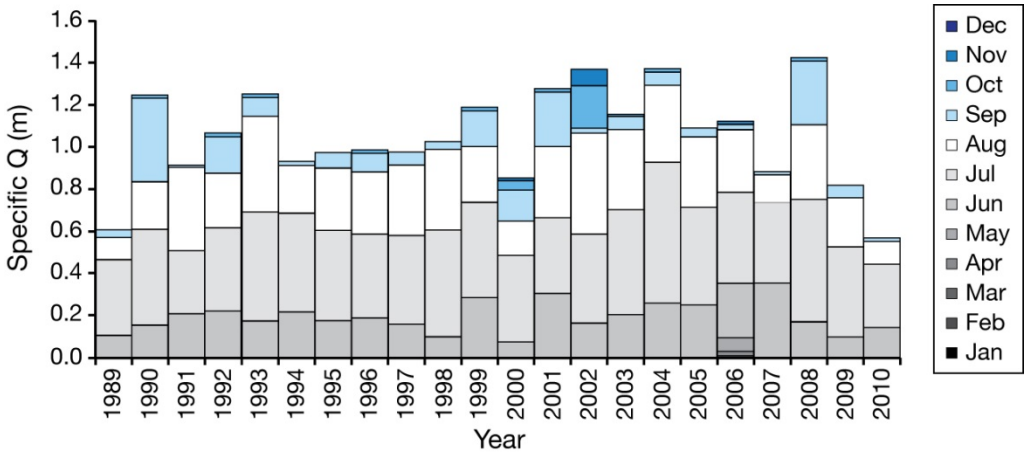

Fig. 2.8 Monthly specific discharge of Bayelva. Data source: Norwegian Water Resources and Energy Administration

2.3.4 Water balance for the Bayelva catchment

The results of the predicted runoff models, their fit to the observed time series and total errors are presented in Table 2.2. Model 4.2 was selected as the best predictor of measured discharge. It included summer P_c derived from JJAS, winter rain events causing river discharge and a 19% precipitation gradient (for rain and snow). The model underestimated Q_s with an ME of 42.0 mm a^{-1} and had a Nash-Sutcliffe E value of 0.63. The water-balance calculations performed for the years 1974/75 - 1977/78 and 1989/90 - 2009/10 for which Q_s rather than Q_p was used had a mean residual value (e in Eqn. 1) of 44 mm a^{-1} (standard deviation 161 mm a^{-1}). The water balance calculated for the period 1974/75 - 2009/10 with the use of predicted runoff, produced a mean e of 31 mm a^{-1} (standard deviation of 138 mm a^{-1}). The values of e are presented in Fig. 2.9. Even though the mean and standard deviation of e for the whole period of records were relatively small, there were some years with more extreme values in the range -250 to 386 mm a^{-1} (the positive values being indicative of storage). A variable, sometimes a significant source of error, was therefore present in the calculations that require a discussion below.

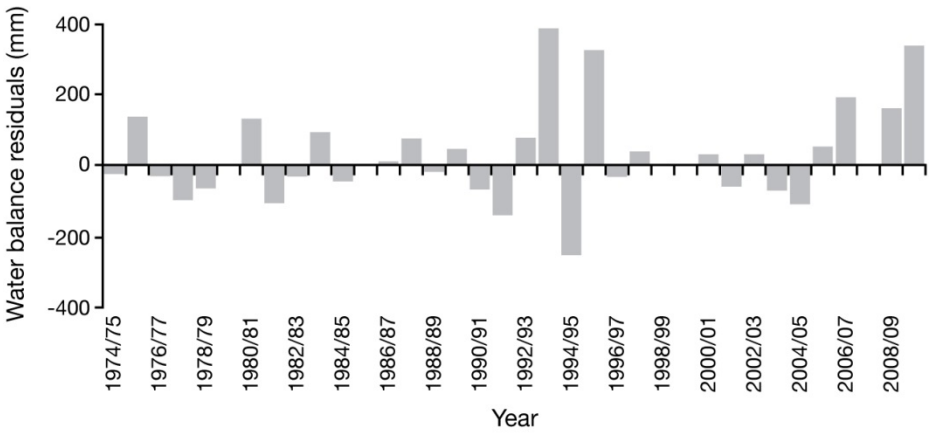

Fig. 2.9 The residual term in the water balance of Bayelva derived from measured and predicted runoff data

2.3.5 Hydrological analyses

The FDC analyses performed for measured runoff (Fig. 2.10) showed that the 25th, 50th and 75th percentiles corresponding to high, median and low flows of the entire record were 5.11, 3.22, and 0.85 m^3 s^{-1} accordingly. Values in years 1989-1999 and 2000 - 2010 differed only slightly and were 5.13, 3.16, 1.00 m^3 s^{-1} and 5.04, 3.26, 0.75 m^3 s^{-1},

respectively (Fig. 2.11). FDC analysis performed for every year of record revealed that flows during 2000 - 2010 were much more variable than during 1989 - 1999. The variability of the flows is presented in Fig. 2.10b and c where the outstanding FDCs are compared to the FDC of the entire period of records. Higher flow years were mainly recorded during 1989 - 1999 while years with lower flow were mainly recorded during 2000 - 2010. Flow recession analysis performed for three selected years representing the beginning, middle and the end of the period of measurement (1991, 2000 and 2009), showed significant changes of K1 and K2 reservoirs (Fig. 2.12, Table 2.4). It is therefore apparent that the K1 reservoir values decreased both over the entire period of record, and during each season. Furthermore, the seasonal decrease became more distinct at the end of the observational period than at the beginning. The appearance of the K2 reservoir became more frequent with time and its values, although more variable than K1, also decreased as the season progressed. The K3 reservoir was only recorded a few times during 2000 - 2010 (Table 2.4) and therefore it was not possible to notice any trends.

Table 2.4 The results of flow recession analyses of Bayelva for years representing the beginning, middle and the end of data records. K1 - K3 represent different storage reservoirs

	1991	**2000**	**2009**
	Average (hours)		
K1	29	25	16
K2	95	64	32
K3	0	14	25
	Count		
K1	43	31	45
K2	7	11	24
K3	0	2	2
	Minimum (hours)		
K1	14	9	1
K2	47	7	3
K3	0	12	14
	Maximum (hours)		
K1	57	47	43
K2	160	174	192
K3	0	16	36

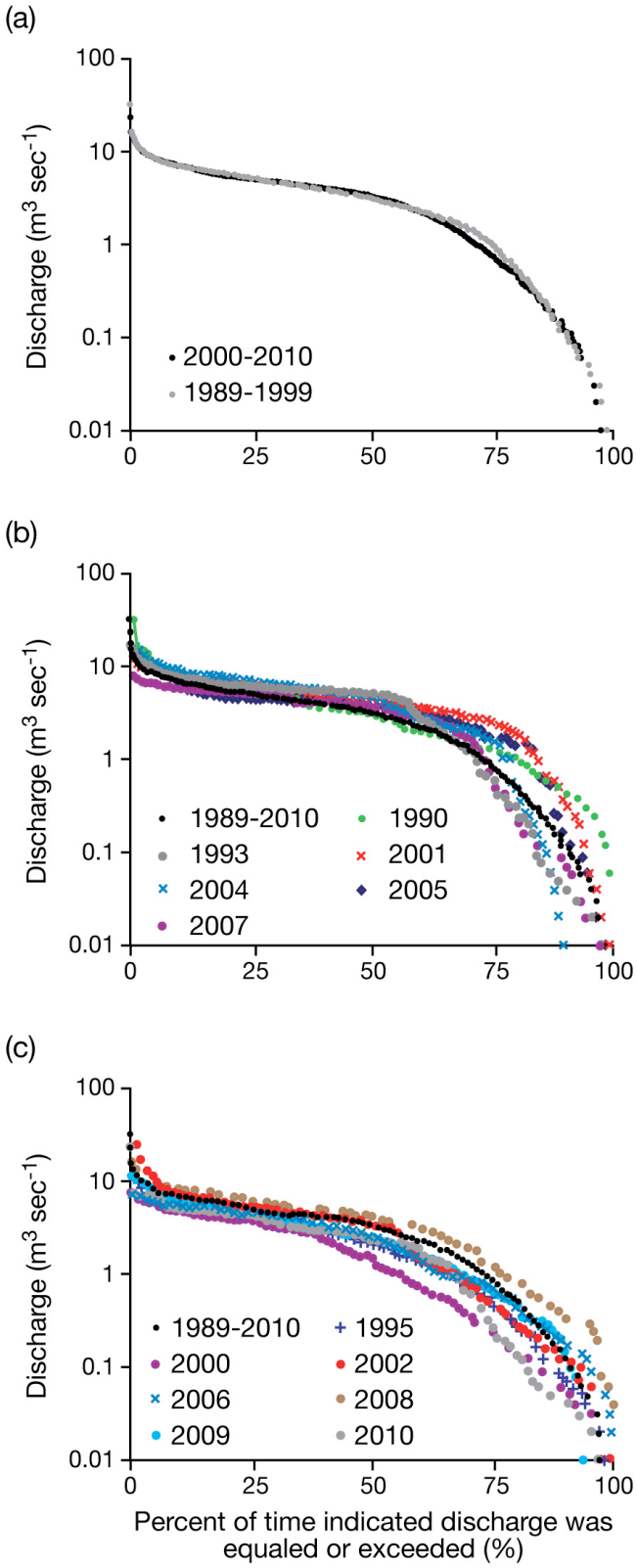

Fig. 2.10 Flow duration curves for Bayelva showing: (a) two periods of records 1989 - 1999 and 2000 - 2010; (b) outstanding years with steeper curves of low flows than the whole period of records; and c) outstanding years with shallower curves than the whole period of records

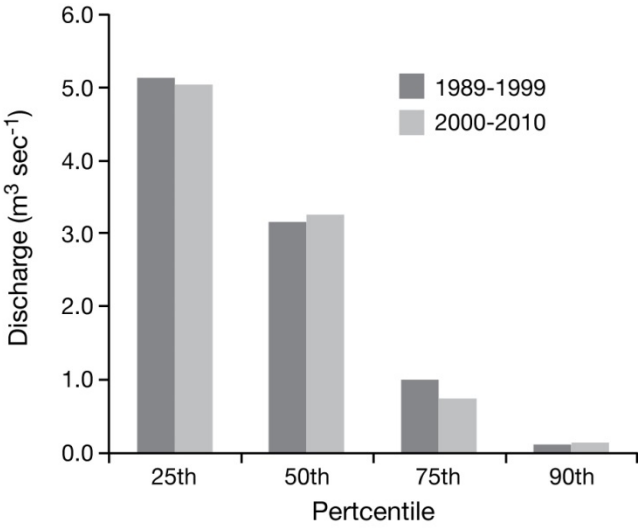

Fig. 2.11 Flow duration values of Bayelva during 1989 - 1999 and 2000 - 2010

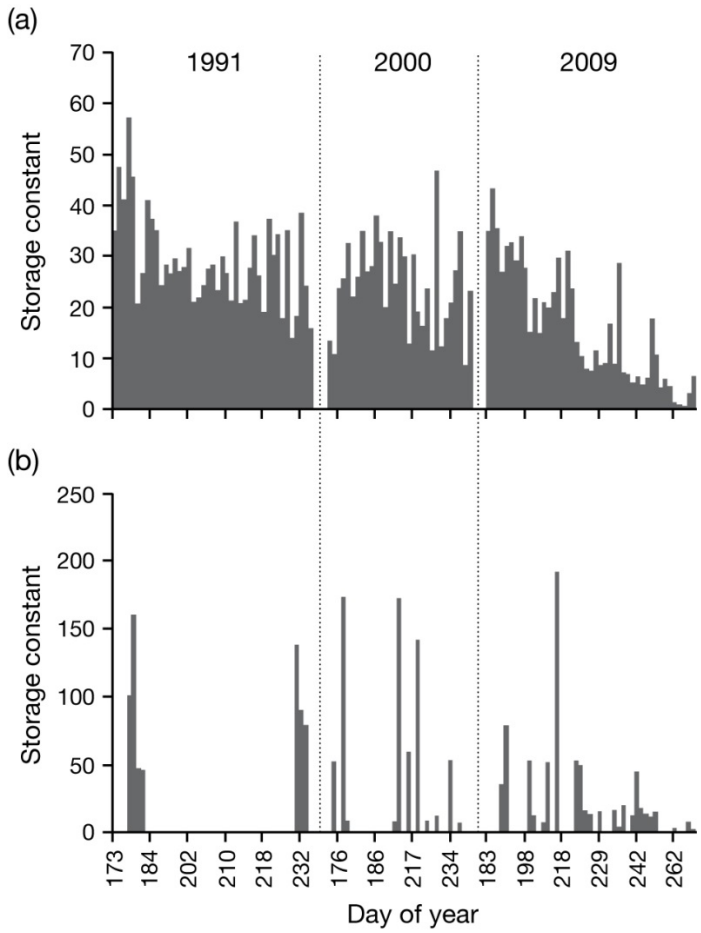

Fig. 2.12 Flow recession analysis of Bayelva for 1991, 2000 and 2009: (a) K1 constant values (hours) represent fast water flowpaths; (b) K2 constant values (hours) represent delayed water flowpaths

2.4 DISCUSSION

2.4.1 Temperature and precipitation change and their influence on catchment's hydrology

The results of statistical analysis of T_a and P_c performed for the period 1975 - 2010 indicate that the biggest changes in the catchment's climate were recorded during the winter, as indicated by Førland et al. (2009) and Beldring (2009). Furthermore, those changes are more intense during the last 10 years. The increase in winter air temperatures had a direct connection to the increase in winter rainfall. Rainfall during shoulder months, although not unusual, also became more frequent within the last 10 years. It is significant that although April and May were the two months most affected by the increase in air temperature, and September was affected the least, it is the change during the latter that had the biggest influence on hydrology of the catchment. The reason is that September's mean air temperature lies close to 0^{o}C and so the changes influence precipitation type (from snow to rain). Air temperature changes in September also had a direct effect upon the timing of the transition from ablation to accumulation and therefore influenced the mass balance of the glaciers existing within the catchment. The beginning of the ablation season was also influenced by temperature changes in April and June. Therefore, a near-constant, steady retreat of at least one glacier existing within the catchment has been documented (Kohler 2010).
Changes in air temperature and precipitation were also reflected in the Bayelva runoff. During summer months, melt-driven river flow depended more on air temperatures than precipitation. However, during winter, rainfall events were directly responsible for the early and late flows of the river. Changes in the discharge before 1 June and after 30 September distinguished years 1989 - 1999 and 2000 - 2010. Of particular importance is the fact that flows that occurred outside the main summer months were more apparent during 2000 - 2010 (3.8% of total discharge in that period as opposed to 0.3% in 1989 - 1999). For example, those early and late rainfalls and their subsequent flow events were responsible for as much as 0.28 m of additional discharge in 2002 (26% of total Q_s in that year). Importantly, such flows have not been traditionally included in the reconstruction of runoff yields in Svalbard (e.g., Hodson et al. 2000).

Another interesting result of the statistical analyses was that while total glacier ablation was correlated to July and September temperature indices, the beginning and end of river discharge correlated with air temperatures in the spring/summer transition (i.e., early snowmelt) and precipitation in September and October (i.e., rainfall runoff). This shows the relationship between climate change, glaciers and river discharge. Although

change in temperature is responsible for the timing of snowmelt and the magnitude of icemelt, precipitation is the driving force for river flows at the end of summer when almost all the snow has melted and glacier icemelt is greatly reduced by low solar radiation and air temperature.

Therefore, it seems justifiable to use both precipitation and glacier mass balance for water-balance calculation and runoff predictions in the Bayelva watershed and presumably other High-Arctic catchments as well. Furthermore, the statistical analyses performed on different water-balance models and comparison of the many precipitation elevation corrections available in the literature, clearly show that 19% precipitation gradient (for rain and snow) should be applied in addition to catch correction (1.15 for rain and 1.65 for snow).

Finally, when reconstructing river runoff, winter rainfall responsible for early and late flows of catchment rivers must be included in the calculations. This will then allow for minimal residuals in the water-balance computation.

2.4.2 Water-balance error or water storage?

Reconstructed water balance for 1974/75 - 2009/10 also revealed that in some years there were large positive (1994, 1996 and 2010) or negative (1995) residuals in the water-balance calculations (Fig. 2.9), which may be due to error and/or storage. The water-balance calculation was based on the assumptions made by previous researchers in this catchment, whereby the presence of permafrost, the glaciers' cold-based thermal regime and the long duration of monitoring mean that change in storage can be neglected (Killingtveit et al. 2003). However, due to increased winter rainfall as shown in this article, and also warming of the permafrost which has resulted in a deepening of the AL (as shown by Boike 2009 and Westermann, Boike et al. 2011), we believe that storage now needs to be considered. Both 1994 and 1996 were characterized by air temperatures that were lower than average, while precipitation, when flow was recorded, was higher than average by 40 and 17%, respectively. These years were also characterized by occasional summer snowfalls that caused flow recessions. In contrast, the summer of 1995 was warmer than average and precipitation reached only about 50% of the average value for the whole period of records. Despite these differences, Q_s was very similar in all three years, while the ablation was higher by 40% in 1995. After careful analyses of P_c, T_a and Q_s records, it is clear that those water-balance years with large positive residuals experienced exceptionally high (above 240 mm) winter rain on

snow (hereafter ROS) that did not contribute to the early and/or late Q_s. Moreover, those high rainfalls were extreme events resulting in more than 100 mm of rain (catch corrected) within a month (e.g., 1993/94: 239 mm in November; 1995/96: 114 mm in December, 107 mm in January and 124 mm in March). Years where such extreme rainfalls did not occur, produced water-balance residuals within 100 mm that are more indicative of error rather than storage. Therefore, we believe that in 1994 storage of the ROS (318 mm in November and December) occurred after percolation through snow and refreezing, creating a ground icing. Upon freezing, the latent heat release will have warmed the ground and helped maintain the temperature closer to 0^{o}C, as described in instrumented plots within the study area by Westermann, Boike et al. (2011). Importantly, such large rainfall events could have penetrated the upper part of the AL and frozen later on during winter. Furthermore, with colder than average air temperatures the following summer, thick ground icings could not only prevail through part of summer (insulated by the overlying sediments and soil) but also actually persist through to the next hydrological year. An example of such ground icing after winter rain can be seen in Fig. 2.13. This icing persisted in the watershed until the middle of August of 2010, even though the summer of 2010 was warmer than average by 0.8^{o}C.

Fig. 2.13 Example of ground icing after winter rainfall in the Bayelva catchment in July 2010. Photo credit: A. Hodson

Given the above, it follows that the warmer than average summer of 1995 could have melted out the previous year's icing, and also result in the possible release of water already stored in the active layer. Additionally, glacier ablation compensated for low precipitation, resulting in an unusually low (negative) water-balance residual term (-250 mm). We also believe that similar processes to 1994 also occurred in 1996, with the only

difference being the magnitude of winter and summer rainfall.

In an attempt to quantitatively test the above hypothesis, the correlation between ROS events that did not cause runoff at the Bayelva station and the magnitude of the water-balance residuals was examined. In so doing, a statistically significant correlation was found (Fig. 2.14a), which improved markedly when years with extreme ROS events (as defined above) were considered alone (Fig. 2.14b). As the slope of both graphs is close to unity, the storage of the ROS events is therefore sufficient to explain the magnitude of the residuals in the original water-balance calculation.

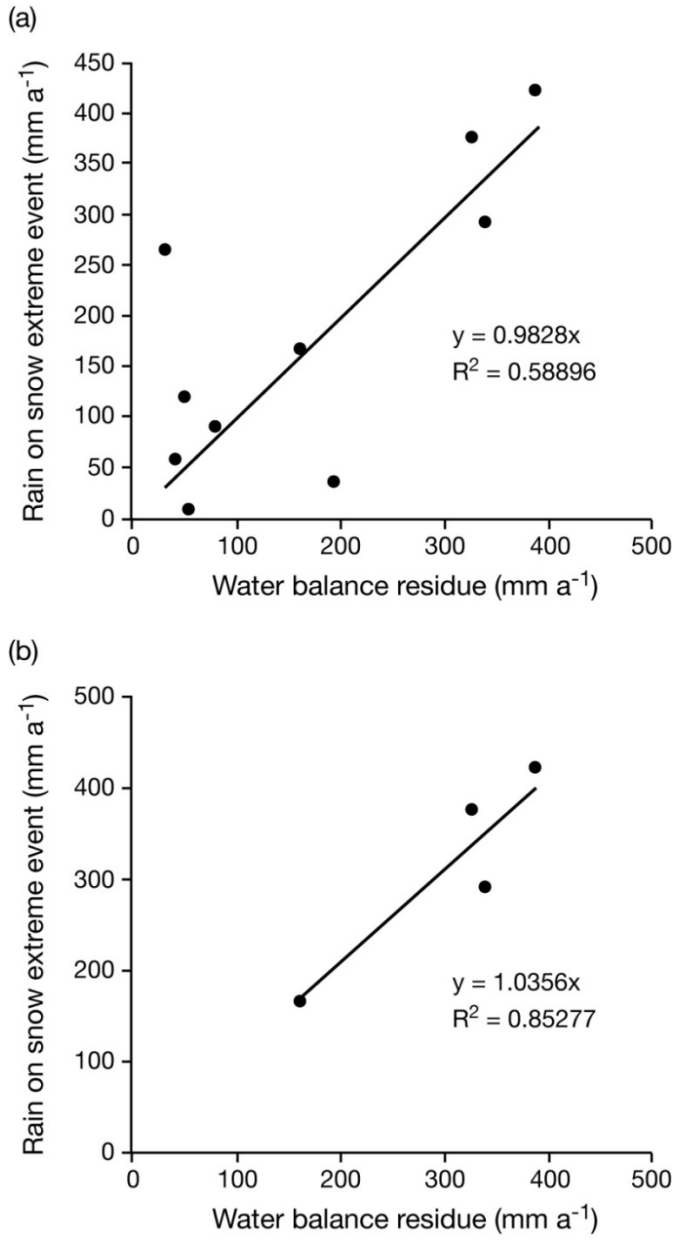

Fig. 2.14 The correlation between water-balance residuals (e) and winter rain on snow events in the Bayelva catchment: (a) all hydrological years when ϵ was positive; (b) hydrological years when large recorded winter rain on snow events coincided with high water-balance residuals

2.4.3 Hydraulic changes as revealed by flow recession curves

Given above argument, it is intuitive to expect to see changes in the flow recession curve characteristics (K1 and/or K2, K3 values) as the influence of the AL water store changes. However, the dominant reservoir, K1, is rapid and most likely governed by channelized flows through the glacier and the sandur. Therefore, changes in the K1 reflect changes in the hydraulic characteristics of the channel network in the Bayelva catchment and not storage in the active layer. The decrease in the K1 coefficients showed by Fig. 2.12a reveals a seasonal decline in storage capacity and/or recharge characteristics (Covington et al. 2012) that is indicative of increasingly efficient icemelt transfer through the channel network (e.g., Hodson et al. 1998; Rutter et al. 2011). Additionally, the 2009 summer was associated with a major reorganization of the flowpath along the eastern flank of the glacier. This was observed as the abandonment of a long existing lateral channel (more than 1 km long) and the formation of a new channel delivering meltwaters more directly to the proglacial river. This coincided with a marked decrease in the K1 values on DOY 224 in Fig. 2.12a. Other characteristics of channel migration have been reported further upstream in the glacierized part of the catchment. For instance, Vatne (2001) reports knick point development and up-glacier migration in a large englacial channel at an average rate of 30 m a^{-1} that could also influence K1 reservoir characteristics. These changes are typical of the tendency for channels to incise into cold-based glaciers such as Austre Brøggerbreen, since they offer little or no opportunity for drainage along the glacier bed. The increasing dominance of such channels could be a key feature of the hydraulic response of cold-based glacier basins to climate change.

Long-term storage phenomena like those described in the preceding section (i.e., ground icings), could therefore only be reflected in either the K2 or the K3 reservoir recession curves. Although, as Table 2.4 reveals, these apparent reservoirs are less pronounced in the data set than K1 and in some cases (K3) rather rare in occurrence. However, the K2 reservoir is more prevalent during years 2000 - 2010. Additionally, the flow recession analysis was also performed for 2010 (data not shown) and, similarly to 2009, it revealed a seasonal decline in K2 values and an even more frequent appearance of K3.

This could be an indication of a new delayed water flowpath developing within the Bayelva watershed, showing that changes in the flow recession curve characteristics could indeed be linked to hydrological changes as a consequence of the permafrost/AL warming.

2.5 CONCLUSIONS

This study has shown that climate change has already begun affecting Bayelva watershed hydrology and the changes have been most noticeable within the last 10 years. Long-term monitoring, statistical analyses and water-balance modelling of the important records collected at this site have revealed the following key features of this change.

Catchment hydrology was influenced the most by temperature and precipitation changes occurring in the winter period, especially the so-called shoulder months (MAM and SO). Furthermore, amongst the shoulder months, climate-driven changes during September had the biggest influence on hydrology of the catchment, influencing precipitation form and the timing of the transition from glacier ablation to accumulation. The changes in river discharge were driven by higher temperatures at the beginning of the ablation season and by rainfall at the end.

Warmer and wetter winters led to extreme winter rainfall events responsible for the creation of ground icings and the occurrence of early/late runoff. In 2000 - 2010, winter rainfalls accounted for 3.8% of the bulk runoff comparing to 0.3% in 1989/1999. If the rate of the warming persists, more rain on snow events are expected, therefore more frequent icing formation and early/late river Q events will be recorded.

The above processes have a direct influence upon major terms in the water balance. The storage can no longer be assumed negligible even when the watershed is underlain by permafrost and accommodates cold-based glaciers. Moreover, short-term river discharge events caused by winter rainfalls should be included in the calculations and if not accounted correctly to appropriate hydrological year, can be the source of significant error.

Therefore, when calculating water-balance the following should be considered: (1) precipitation in JJAS and rainfall events responsible for early or late flow and their assignment to the correct hydrological year; (2) precipitation gradient correction of 19% per 100 m (for rain and snow) in addition to the catch correction (1.15 for rain and 1.65 for snow); (3) the use of glacier mass balance for both snow accumulation and icemelt runoff; and (4) water storage/release from ground icings in the AL as a result of extreme winter rainfalls.

Even though the duration and magnitude of Bayelva discharge did not show any significant trends in the last 35 years, a subtle increase in the volume of discharge was

recorded during the last decade. Furthermore, the flow was also more variable and prolonged. These key features are due to winter rainfall, which has the capacity to offset any reduction in flow that might be caused by continued glacier shrinkage.

Finally, longer term and seasonal changes in the flow recession characteristics revealed that the transfer of meltwaters through the watershed is becoming more and more efficient as the glacier retreats. This is due to the large supraglacial, englacial and proglacial channels conveying most of the runoff. Furthermore, the retreat of the Austre Brøggerbreen glacier has enabled proglacial channels to become more efficient following the reorganization of meltwater flowpaths in the glacier forefield. The recession flow characteristics have also revealed an increase in the occurrence of flow transfer through a longer residence time reservoir (K2), indicating the development of a new delayed water flowpath that is becoming more important as the glaciers retreat.

CHAPTER THREE:

CHANGES IN MELTWATER CHEMISTRY OVER A 20 YEAR PERIOD FOLLOWING A THERMAL REGIME SWITCH FROM POLYTHERMAL TO COLD-BASED GLACIATION AT AUSTRE BRØGGERBREEN, SVALBARD

In Press as: Aga Nowak & Andy Hodson. Changes in meltwater chemistry over a 20 year period following a thermal regime switch from polythermal to cold-based glaciation at Austre Brøggerbreen, Svalbard. *Polar Research*

3.1 INTRODUCTION

Changes in the thermal regime of many high Arctic glaciers are occurring in response to climate forcing (see ACIA 2005). In Svalbard, this has caused a loss of temperate basal ice and a shift toward cold-based conditions since the early 1900s (e.g. Hodgkins et al. 1999; Bælum & Benn 2011). The long term biogeochemical response of such glacier thermal regime change has yet to be documented, which is a surprising oversight given the attention that is being given to the response of the high Arctic to changes in air temperature, precipitation (e.g. Førland et al. 2009), glacier retreat (IPCC 2007), and permafrost degradation (e.g. Westermann et al. 2011). One can argue that there is no need for a long term hydrochemistry study since modelled hydrological change due to warming climate could be potentially integrated with existing data from various glacial environments (e.g. Tranter, Huybrechts et al. 2002). This might then result in a prediction of watershed response to climatic changes if weathering environments remain similar throughout. However, it is becoming apparent that the weathering environments change drastically during the transition from polythermal to cold-based thermal conditions at the bed of Arctic glaciers, because subglacial sediments become inaccessible to dilute, chemically aggressive surface meltwaters (e.g. Rutter et al. 2011). Therefore subglacial weathering environments, wherein a range of microbially-mediated and inorganic reactions typically cause significant solute acquisition by meltwaters (e.g. Mitchell et al. 2013; Skidmore et al. 2002, 2005; Tranter et al. 2005, Wadham et al. 2004), are effectively removed from the watershed biogeochemical cycle. Paired catchment studies of a cold-based and an adjacent polythermal-based glacier (Austre Brøggerbreen and Midtre Lovénbreen respectively) clearly demonstrated these differences in Svalbard. In short, greater solute export and more evidence of microbially-mediated nutrient cycling were apparent at Midtre Lovénbreen (see Irvine-Fynn and Hodson 2010 and Wynn et al. 2006) yet apparently absent at Austre Brøggerbreen, at least during the peak of the runoff season (Hodson et al. 2002; Krawczyk et al. 2003).

Studies that also include inorganic weathering processes within High Arctic watersheds provide knowledge about chemical denudation and give estimates of solute yields entering High Arctic fiords (see e.g., Hodson et al. 2000; Krawczyk et al. 2003; Krawczyk

& Pettersson 2007; Krawczyk & Bartoszewski 2008). The matter whether such research, based upon one or at most two consecutive ablation seasons, is sufficient and representative of a long-term changes has been somehow overlooked. Clearly, if the mass balance changes of glaciers will cause a shift toward cold-based conditions, then the timing, magnitude and composition of solute transfer into fjords will also change. Furthermore, a recent study by Nowak & Hodson (2013; Chapter Two) on 35 years of hydrology in the watershed occupied by Austre Brøggerbreen showed that the simple concept wherein warming means more glacial melt and therefore more meltwater discharge into fjords simply does not apply. Instead the relationship between glacier retreat and runoff flux turned out to be more complicated, dependent upon many variables and did not result in a direct, significant increase in water discharge. The role of rainfall and its storage in the geochemically reactive AL of the glacier forefield was one of the most important reasons for masking the impact of glacial retreat upon watershed hydrology. The question therefore remains – what is the real and measured hydrochemical response (if any) of cold-based systems as they undergo further response to climate-driven deglaciation?

Therefore here a case study of biogeochemistry in the Bayelva watershed, incorporating solute concentrations and fluxes over the past 20 years is presented. Such a dataset gives a unique insight into hydrochemistry of a glaciated catchment where, due to glacier retreat, its thermal regime switched from polythermal (Orvin 1934, Hagen & Sætrang 1991) to predominantly cold based (Hodson et al. 1998b). Furthermore, datasets covering more than two ablation seasons allow investigation of whether cold based glaciers in the High Arctic are relatively inactive in terms of chemical weathering due to the lack of subglacial weathering environments and short water residence times of surface runoff.

3.2 METHODS

3.2.1 Hydrological and mass balance monitoring

Hydrological monitoring of Bayelva has been carried out continuously since 1989 by NVE at the gauging station described in Chapter One, Section 1.7.1 (see also Fig. 3.1). Errors in the discharge calculations were estimated by Skretteberg (1991) and are thought to be less than 5%. The position of the station circa 2.5 km from both glaciers allows determination of runoff from the whole Bayelva catchment area. Additionally, meteorological conditions as well as the hydrology of the Bayelva during the last 35

years was explored in detail in Chapter Two (Nowak & Hodson 2013).

The mass balance measurements of Austre Brøggerbreen have been conducted by The Norwegian Polar Research Institute since 1966 and they are described in detail in Kohler et al. (2002) and Kohler (2010).

3.2.2 Runoff sampling

The meltwater sampling for water chemistry during ablation seasons of 1991, 1992, 2000, 2009 and 2010 (Table 3.1) was carried out at the BAY station located at 78.9335 N, 11.838 E (Fig. 1.11 and Fig. 3.1) next to a crump weir established by Norwegian Water Resources and Energy Administration (NVE) in 1989. Detail description of the site is provided in Chapter One.

Hodson et al. (1998b) and Tranter et al. (1996) showed that variations in electrical conductivity in meltwater are muted in the Bayelva catchment due to 24 hours of daylight and the lack of concentrated runoff from a subglacial drainage system. Hence twice daily samples were not necessary for describing the seasonal evolution of the streamwater chemistry. Daily sampling was therefore used for the beginning of the runoff season, and a two day interval thereafter (following the initial snowmelt phase).

Table 3.1 Sampling periods and the length of Bayelva discharge including early and late flows. Early and late flows were defined as the days of river discharge recorded outside summer season (1 June – 30 September). [1]Sum of days of river discharge accounted for in the solute yields calculations

Year	Sampling period		Bayelva discharge period	
	Dates	Days	Dates	[1]Days
1991	25 June – 12 August	49	3 June – 29 September	119
1992	12 June – 3 August	53	12 June – 2 October	113
2000	16 June – 10 August	56	14 June – 8 November	136
2009	13 June – 9 September	89	8 June – 26 September	111
2010	29 June – 23 August	56	18 June – 9 September	84

(a)

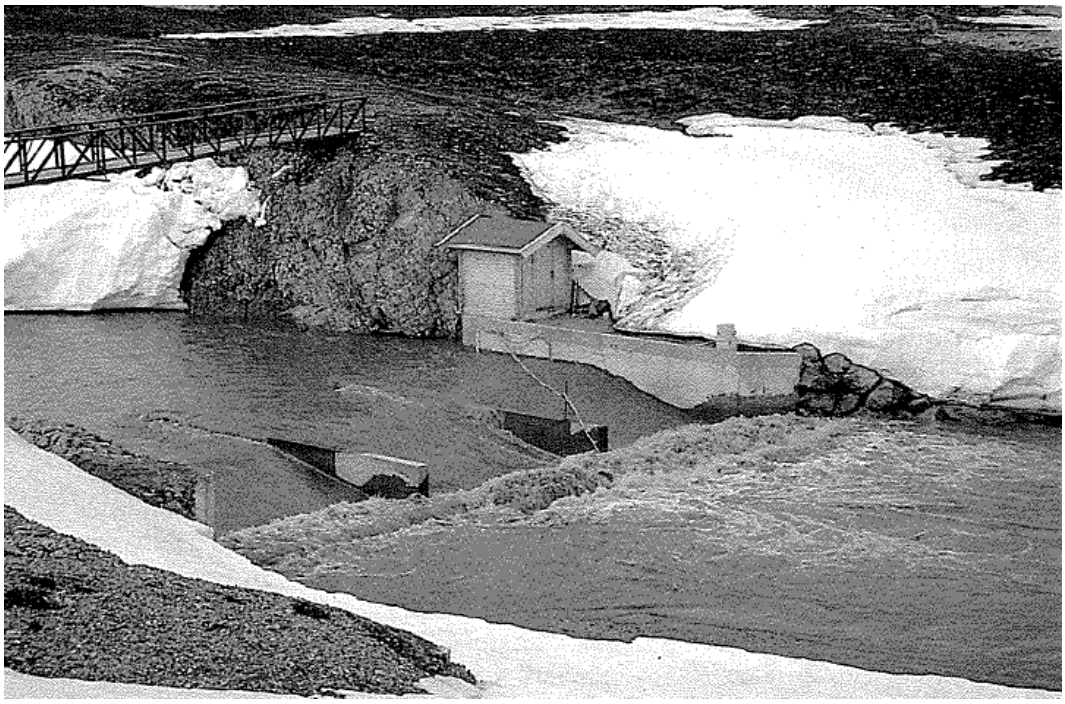

(b)

Fig. 3.1 Sampling location at BAY station in: (a) 1992 Photo credit: J. Bogen; and (b) 2010 Photo credit: A Nowak

3.2.3 Solute provenance

Solutes were separated into sea-salt (hereafter ssX) and crustal (hereafter *X) derived components. Firstly, the assumption was made that due to the watershed geology all Cl^- ions were of sea-salt provenance. Therefore, the sea-salt components of the ions were calculated from standard marine ratios of ions to Cl^- in seawater (see Holland 1978). Secondly, the crustal derived component was calculated by the subtraction of sea-salt derived ion from its total concentration. Additionally, the proportion of SO_4^{2-} derived from atmospheric aerosols was calculated after Hodson et al. (2000) and deduced along with the $ssSO_4^{2-}$ from the total SO_4^{2-} concentrations to create rock and microbially derived sulphate ($*SO_4^{2-}$).

3.2.4 Speciation of Ions

In order to better explore the weathering processes undergoing in the proglacial environment of Brøggerbreen glaciers, WEB-PHREEQ programme was used to simulate chemical reactions (www.ndsu.nodak.edu/webphreeq), ions speciation and saturation indices of pCO_2 and various rock types present in the catchment.

3.2.5 Solute yields and fluxes

Ions fluxes (g day^{-1}) and yields (kg $km^{-2}a^{-1}$) were calculated according to Hodson et al. (2005). Therefore, ion fluxes were calculated following the Eqn. 3.1 as the sum of daily river discharge and ion concentration, whereas yields were determined as fluxes corrected for the area of the catchment (32 km^2) and the entire duration of river discharge.

$$F_{tot} = \sum_{i=1}^{n} (Qd \cdot C_i) \quad (3.1)$$

Where:

F_{tot} – Total flux of species of interests (g day^{-1})

Qd – Total daily discharge of Bayelva River (m^3 day^{-1})

C_i – Concentration of a single daily sample (mg L^{-1})

The daily concentrations of ions in days when the sample was not collected were estimated by linear interpolation. Furthermore, missing solute fluxes at the very beginning and the end of each ablation season were calculated from daily river

discharge volumes and the volume weighted mean (hereafter VWM) concentration of each ion of interest. The VWM concentrations were estimated from either the first or the last ten days of the observation period and calculated according to Eqn. 3.2.

$$\text{VWM} = \frac{\sum_{i=1}^{n}(Q_i \cdot C_i)}{\sum_{i=1}^{n} Q_i} \quad (3.2)$$

Where:

VWM – Concentration of species of interest (mg L^{-1})

Qi – Bayelva discharge at the time of sampling (m^3 s^{-1})

C_i – Concentration of a single daily sample (mg L^{-1})

Lastly, Bayelva discharge data collected by NVE at BAY site were used to estimate the length of ablation season during each year of interest and calculate the runoff flux.

3.3 RESULTS

3.3.1 Hydrological and mass balance monitoring

Specific annual discharge varied between 1989 and 2010 from 0.56 m a^{-1} (2010) to 1.42 m a^{-1} (2008) with the mean of 1.08 ± 0.21 m a^{-1}. The years under study, namely 1991, 1992, 2000, 2009 and 2010, were characterized by a similar, moderate discharge close to the 1989 - 2010 mean value. The exception was 2010 when the discharge magnitude was smaller by circa 50% (see above). The daily discharge data (Fig. 3.2) revealed temporal variability in Bayelva flows. Therefore, the shortest runoff season and the lowest mean flows were recorded during 2010. The end of season discharge was caused by rainfall events. Detailed analyses of Bayelva hydrographs can be found in Chapter Two (Nowak & Hodson 2013).

The retreat of Austre Brøggerbreen was almost continuous since the beginning of mass balance monitoring in 1966. The exceptions were two years of positive mass balance, namely 1987 and 1991. A total mass loss of 21.1 m of water equivalent was recorded since the start of the measurements in 1966.

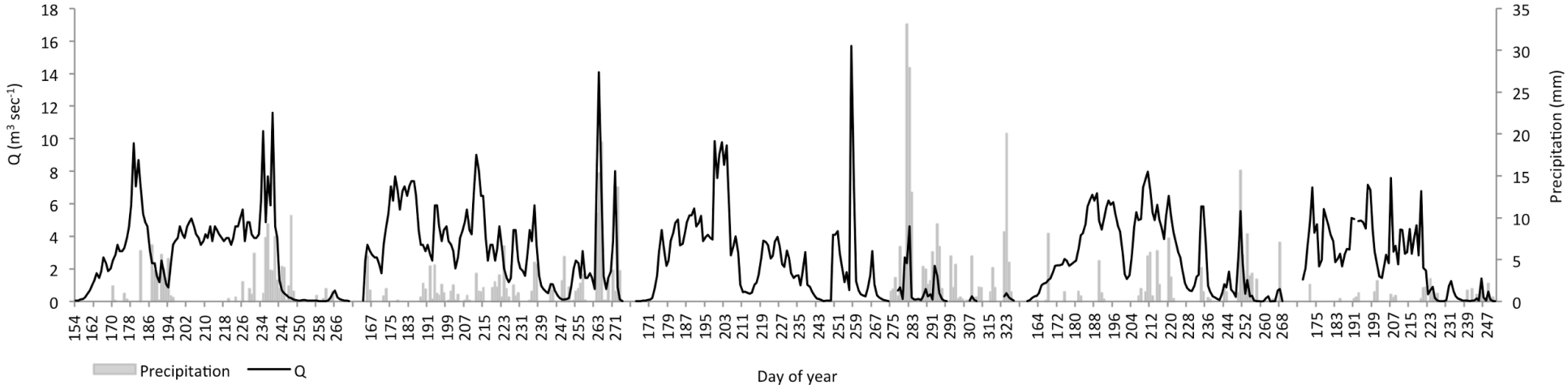

Fig. 3.2 Mean daily discharge and total daily precipitation in 1991, 1992, 2000, 2009 and 2010. Data source: NVE and eklima.met.no

3.3.2 Meltwater characteristics

A summary of statistical comparison between sea salt and crustal ions in the Bayelva is presented in Table 3.2. While the mean concentrations of sea-salt derived ions remained relatively constant, with the exception of Cl^-, the crustal ions differed between the years. An increase in the mean concentration of all crustal species and HCO_3^- was recorded with an exception of Si, where a slight decrease was noted. The change was also observed in the minimum and maximum values of the concentrations. However, the increases of the former were not as significant as the latter and were noticeable only for HCO_3^- and $*Ca^{2+}$. The differences in the maximum values were more evident and included all non sea-salt derived species, with the most pronounced increases observed for HCO_3^-, $*Ca^{2+}$, $*K^+$ and $*SO_4^{2-}$. Furthermore, the above changes were recorded during the later years of monitoring, namely late 2000 - 2010 when, for example, mean concentrations of the above ions were up to twice higher than in 1991, 1992 and early to mid 2000. Detailed time series of crustal ion concentrations are presented in Fig. 3.3.
Although the highest and most pronounced increases in concentrations concerned HCO_3^- and $*Ca^{2+}$ species, the rise in concentrations of $*Mg^{2+}$ and $*K^+$ was also noticeable. Furthermore, it became apparent that the increase in mean and maximum values of $*SO_4^{2-}$ recorded in 2000 - 2010 was more of a result of the end of season maxima rather than a steady marked rise in concentrations throughout the years (as observed with other crustal ions mentioned above). The end of season maximum was also noticeable with Si concentrations even though the general trend was decreasing. Lastly, a mid-season peak in all crustal ions was detected in 1991 and 2009. Values of pH ranged from 6.5 (2009) to 8.7 (2010) with the 1991-2010 mean 7.4 (Fig. 3.4). A general increase in pH was recorded over the whole period of monitoring with the marked increases during 2000 - 2009 when the mean yearly values increased from 7.0 in 1991- 1992 to 7.5 in 2000, 7.8 in 2009 and 7.9 in 2010. This increase cannot be explained by the methodological differences in pH measurement described earlier, because high pCO_2 conditions were estimated from the filtered samples in 1991, 1992 and 2000 (see below). Post-filtration pH measurement is likely to result in higher values than those estimated during the immediate pH measurements of 2009 and 2010 due to likely degassing of CO_2. Therefore, the observed changes are in the opposite direction to any filtration effects upon pH and CO_2.

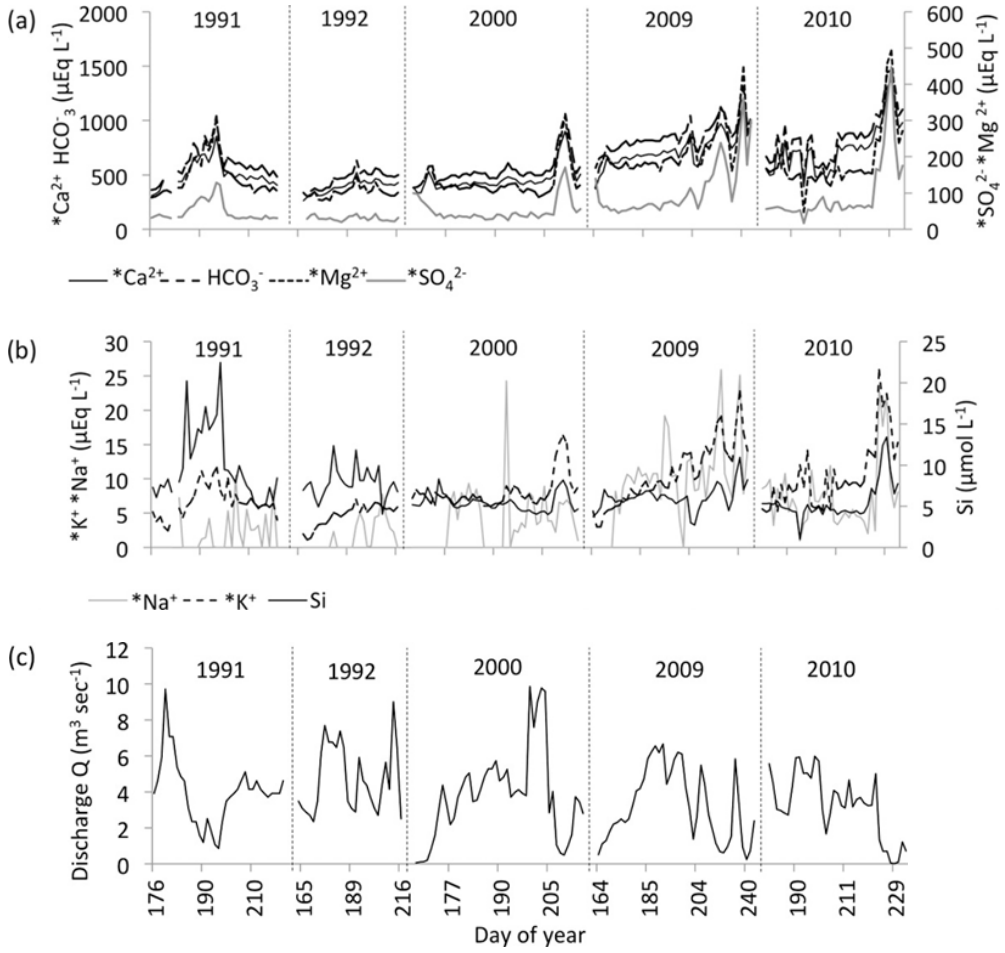

Fig. 3.3 The timeseries of crustal ion concentrations in the Bayelva between 1991 and 2010: (a) concentrations of ions associated with carbonate rocks; (b) concentration of ions associated with silicate rocks; (c) discharge of Bayelva at the time of sampling

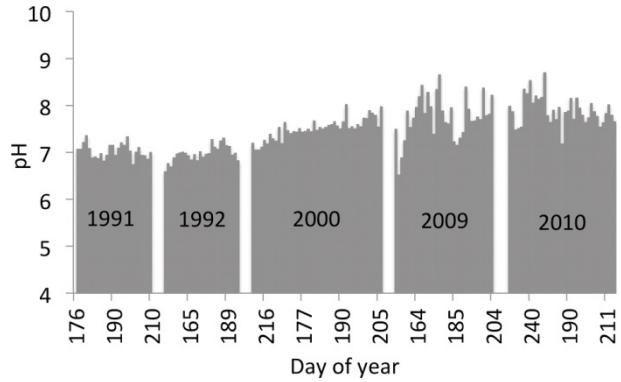

Fig. 3.4 pH changes in Bayelva meltwater between 1991 and 2010

Table 3.2 Basic statistics for ion concentrations in Bayelva between 1991 and 2010

Year		HCO_3^-	Cl^-	NO_3^-	$*Ca^{2+}$	$*Mg^{2+}$	$*Na^+$	$*K^+$	$*SO_4^{2-}$	$ssCa^{2+}$	$ssMg^{2+}$	$ssNa^+$	ssK^+	$ssSO_4^{2-}$	Si
		($\mu Eq\ L^{-1}$)													($\mu mol\ L^{-1}$)
	1991	601	119	1.66	510	144	1.81	6.69	49.4	4.19	21.6	93.8	2.22	12.3	9.92
	1992	474	129	2.08	384	102	1.53	4.61	31.8	4.86	25.2	103	2.42	12.6	7.71
Mean	2000	556	234	4.41	462	130	3.79	8.07	51.6	8.79	45.5	180	4.38	29.0	5.43
	2009	852	103	1.97	729	216	9.64	10.7	108	3.84	20.2	86.4	1.97	12.4	6.08
	2010	854	32.6	0.82	745	189	7.41	10.5	97.9	1.21	6.37	27.9	0.62	14.2	5.50
	1991	362	31.3	0.00	309	87.4	0	2.41	27.8	1.18	6.09	26.9	0.59	3.24	4.70
	1992	353	25.7	0.00	222	79.9	0	1.12	19.3	0.96	4.99	22.0	0.48	2.65	4.04
Minimum	2000	433	27.2	0.81	335	88.9	0	6.06	24.5	1.02	5.29	23.3	0.51	3.37	4.02
	2009	379	30.7	0.00	373	160	0	3.00	44.8	1.14	6.00	26.3	0.58	3.70	2.75
	2010	434	16.7	0.00	391	47.1	0.94	5.16	16.5	0.62	3.26	14.3	0.32	2.56	1.02
	1991	1040	368	8.79	854	307	10.5	11.6	129	13.8	71.6	265	6.89	38.1	22.5
	1992	633	589	11.3	522	145	7.75	7.00	77.2	22.1	115	456	11.0	60.9	12.4
Maximum	2000	1062	1695	18.1	900	314	24.2	16.3	171	63.7	330	1160	31.7	210	8.32
	2009	1312	396	10.3	1181	447	25.9	22.8	362	14.7	77.5	318	7.55	47.7	11.0
	2010	1465	70.6	3.59	1379	493	23.2	25.9	448	2.62	13.8	60.6	1.35	63.8	13.4
	1991	150	90.5	2.07	120	53.5	2.84	2.29	27.8	9.36	16.0	67.0	1.69	9.36	4.46
	1992	72.6	145	2.37	67.9	15.0	2.22	1.65	11.3	14.8	28.2	111	2.71	14.8	1.87
SD	2000	135	352	4.67	115	43.5	4.48	2.36	31.8	43.6	68.5	248	6.59	43.6	1.06
	2009	156	89.4	2.93	148	60.6	6.24	4.49	73.2	10.8	17.5	72.0	1.70	10.8	1.44
	2010	239	13.2	0.94	230	89.9	4.93	5.00	90.8	12.9	2.59	11.4	0.25	12.9	2.31

3.4.3 Speciation of ions and pCO_2

The results of ion speciation, saturation indices and pCO_2 are presented in Fig. 3.5. The pCO_2 was decreasing steadily towards $10^{-3.5}$ bar equilibration with the atmosphere (solid black line on Fig. 3.5a) until the end of ablation season in 2000. However, equilibration with the atmosphere in that period was not reached and the minimum value of saturation index was -3.48. The most variable values were recorded in 2009 ranging from -1.78 at the beginning of the ablation season (day 178) to -3.89 at the middle (day 194). Values below equilibration (i.e. low pCO_2) were also recorded at the end of 2009 ablation season (days 226 and 234). Such variability in pCO_2 was absent in 2010. After the start of the ablation season values remained below equilibration (-3.55 day 187) until the day 197 (-3.95), after which they began increasing to reach a final value of -2.77 (day 235).

The saturation indices of carbonate minerals such as calcite ($CaCO_3$) and dolomite ($CaMg(CO_3)_2$) increased throughout the period of records (Fig. 3.5b). It has been evident that although saturation index of dolomite changed the most, it was calcite that reached saturation on a few occasions in the 2009 and 2010 ablation seasons. Saturation indices of sulphate minerals such as gypsum ($CaSO_4*2H_2O$) and anhydrite ($CaSO_4$) increased only slightly throughout the monitoring period (Fig. 3.5c). The maximum values were recorded at the end of each ablation season with the exception of 1991, when the maximum values were recorded in the middle (day 184 - 197). The saturation indices of silicates were the most variable throughout the years (Fig. 3.5d), although the saturation of SiO_2 was relatively constant with just minor variation in 1991 and at the end of each ablation season. The general trend in magnesium silicates was an increase. The most variability was recorded during the middle of 2009 and 2010 seasons, ranging from -17.52 (day 178) to -4.76 (day 194) in 2009 and -14.08 (day 208) to -4.91 (day 197) in 2010.

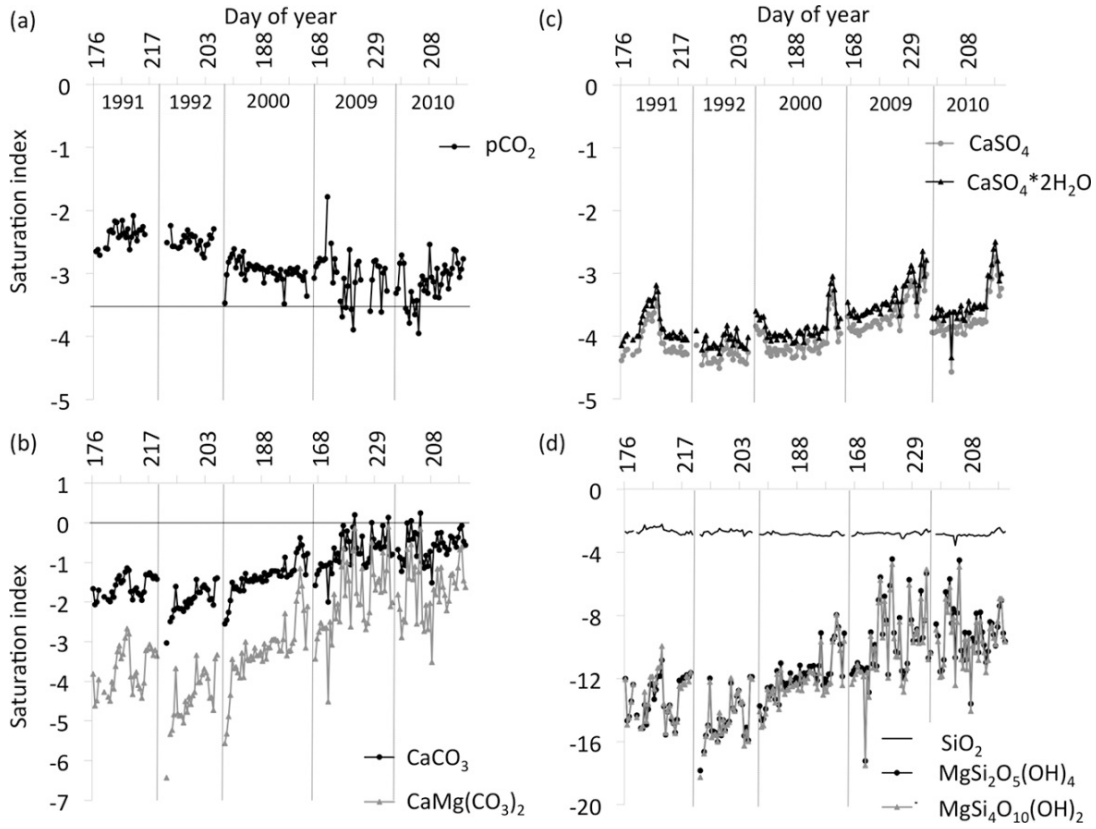

Fig. 3.5 Timeseries of saturation indices of (a) pCO_2; (b) carbonate; (c) sulphate; and (d) silicate minerals in Bayelva between 1991 and 2010

3.3.4 Solute yields

A comparison of marine (Cl^-, ssK^+, $ssNa^+$, $ssMg^{2+}$, $ssCa^{2+}$, $ssSO_4^{2-}$), crustal ions ($*K^+$, $*Na^+$, $*Mg^{2+}$, $*Ca^{2+}$) and Si yields from the Bayelva catchment over the entire period of records is presented in Fig. 3.6. A decrease in marine ion yields has been recorded since 1991. In comparison, although crustal ions were also decreasing between 1991 and 2000, a peak in their yields in 2009 was followed by a decrease in the subsequent year. The comparison between individual ion yields and their proportion in the non sea-salt derived component is presented in Table 3.3. The yields varied with time and no marked trends were recorded. The exception was Si whose yields were decreasing since 1992. In comparison, the proportion of ions in the total yields revealed more $*Ca^{2+}$ since 2000.

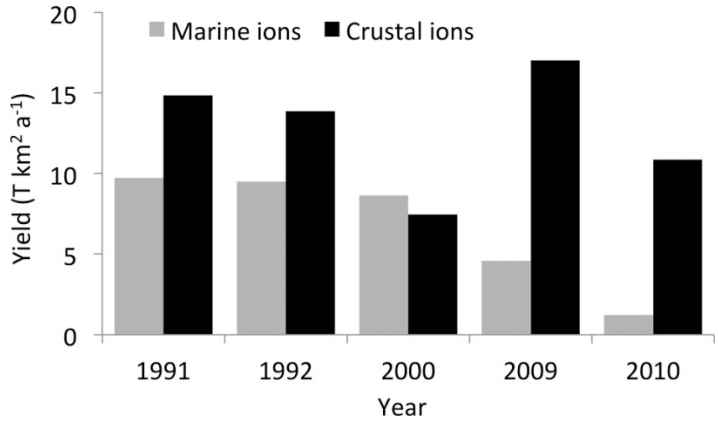

Fig. 3.6 The comparison of marine (Cl^-, ssK^+, $ssNa^+$, $ssMg^{2+}$, $ssCa^{2+}$, $ssSO_4^{2-}$) and crustal (Si, $*K^+$, $*Na^+$, $*Mg^{2+}$, $*Ca^{2+}$) ion yields from Bayelva catchment between 1991 and 2010

Table 3.3 Ion yields from the Bayelva catchment with their proportion in the non sea-salt derived component. The catchment area used in the calculations was 32km^2. Italic values in parentheses of the top row show Bayelva's specific annual discharge (mm)

Ion species	**1991** *(914)*	**1992** *(1062)*	**2000** *(849)*	**2009** *(813)*	**2010** *(562)*	**1991**	**1992**	**2000**	**2009**	**2010**
	(kg km^{2}a^{-1})					**(%)**				
$*Ca^{2+}$	12191	11300	5953	13867	9108	19.4	18.3	16.9	19.2	20.2
$*Mg^{2+}$	1976	1794	787	2387	1309	3.15	2.90	2.24	3.30	2.90
HCO_3^-	45566	45792	24887	50931	31981	72.6	74.1	70.8	70.5	70.9
$*SO_4^{2-}$	2395	2139	2814	4321	2285	3.81	3.46	8.00	5.98	5.07
$*Na^+$	83	171	131	210	105	0.13	0.28	0.37	0.29	0.23
$*K^+$	297	277	394	404	239	0.47	0.45	1.12	0.56	0.53
Si	289	312	188	149	91.1	0.46	0.50	0.53	0.21	0.20

*3.*4 DISCUSSION

The literature on solute acquisition by glacial meltwaters is extensive and covers glaciers of various thermal regimes as well as their proglacial environments (see e.g., Raiswell 1984; Tranter et al. 1993; Sharp et al. 1995; Tranter et al. 1996; Anderson et al. 1997; Hodgkins et al. 1997; Brown et al. 1998; Hodgkins et al. 1998; Brown 2002; Hodson et al. 2002; Tranter, Sharp et al. 2002; Hodson et al. 2005). In brief, solutes are supplied from two primary sources, atmospheric and crustal. The former is the source of gases, aerosols and sea salt species (such as CO_2, O_2, NO_2, SO_2, HNO_3, H_2SO_4, Cl^-) while the latter delivers products of chemical weathering of glacial flour, moraines and snow dust (such as Ca^{2+}, Mg^{2+}, Na^+, K^+, HCO_3^-, SO_4^{2-}, Si) (Tranter et al. 1993). The relationships

between the above in glacial environments are complicated and governed by many variables. These are bedrock lithology, the supply of hydrogen protons (H^+) (therefore pH) and gases such as CO_2 and O_2, sediment surface area, ratio and duration of rock-water contact, microbial processes, and lastly the rate of runoff production (Raiswell 1984; Brown et al. 1994; Sharp et al. 1995; Anderson 1997; Brown 2002). Biogeochemical studies of the above dependencies and the mechanisms driving reactions in glacial environments were explored well in the publications given above, while others, such as Anderson (2007), Fairchild et al. (1999) and Cooper et al. (2002) provided insights into the same processes in glacier forefields. Therefore in the discussion below the focus is upon characterizing the variations in Bayelva's hydrochemistry between 1991 and 2010 and how they reflect changing weathering processes during glacier retreat.

3.4.1 Inter annual change in solute transport

Carbonates

The dominance of HCO_3^-, $*Ca^{2+}$ and $*Mg^{2+}$ in the Bayelva waters was not unexpected considering the geology of the catchment (limestone and dolomite). Furthermore, it is widely accepted that highly reactive minerals such as carbonates, evaporates or sulphides can dominate meltwater chemistry from glacially eroded bedrock, even when they occur only in trace amounts (Raiswell & Thomas 1984; Tranter et al. 1996). The order of magnitude lower dissolution rates of dolomite compared to calcite (Chou et al. 1989; Fairchild et al. 1994a,b) can also be responsible for much lower concentrations of $*Mg^{2+}$ than $*Ca^{2+}$. Dissolution of carbonates (see Eq. 3.3a) takes place in open, well oxygenated channels where meltwater transfer is rapid and results in 2:1 ratios of $*Mg^{2+}$ and $*Ca^{2+}$ to HCO_3^- (in $\mu Eq\ L^{-1}$) (Tranter et al. 1993). Since the Bayelva catchment is characterised by rapid drainage through well-aerated supraglacial, englacial and proglacial channels (Nowak & Hodson 2013; Chapter Two), the hydrological system should provide a good environment for this reaction. Despite that, a 2:1 ratio was not reached during the entire period of records (see Fig. 3.7).

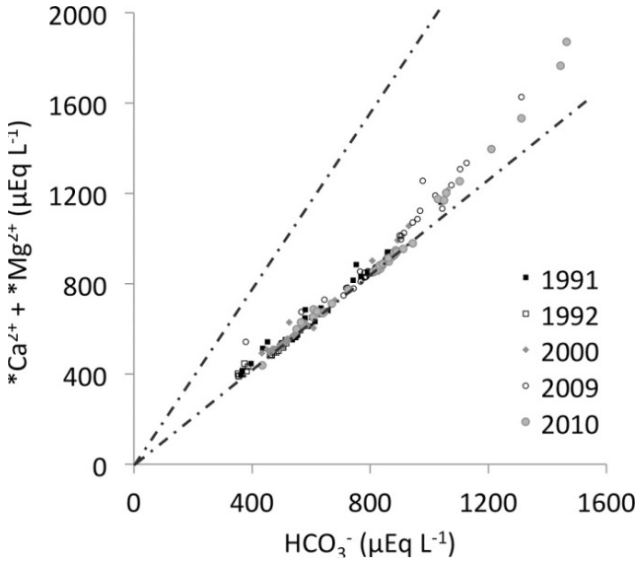

Fig. 3.7 The relationship between carbonate derived ions in Bayelva during 1991 - 2010 period of records. Dashed lines indicate 1:1 ratio (lower) indicating carbonation and 2:1 ratio (upper) indicating dissolution

Instead, a linear association between the above ions with a slope close to 1 (0.9 ± 0.01 in $*Ca^{2+}/HCO_3^-$ and 1.2 ± 0.01 in $*Ca^{2+}+*Mg^{2+}/HCO_3^-$) in equivalent units was recorded, explaining 98% of the 1991 - 2010 data. These ratios indicate that carbonate (namely calcite) carbonation was the major reaction in the system (Eqn. 3.3b). Additionally, the fact that the $*Ca^{2+}/HCO_3^-$ ratio was marginally less than unity indicates uptake of $*Ca^{2+}$ by cation exchange, which is a well known early reaction following the wetting of freshly exposed glacial sediments (see Hodson et al. 2002). Dolomite carbonation (resulting in a $*Ca^{2+}$**:**$*Mg^{2+}$ ratio close to 1, see Eqn. 3.3c) was discarded as a main weathering process since the Ca^{2+}**:**Mg^{2+} ratio was 2.6.

$$CaCO_3 + H^+ \leftrightarrow Ca^{2+} + HCO_3^- \quad (3.3a)$$

$$CaCO_3 + CO_2 + H_2O \leftrightarrow Ca^{2+} + 2HCO_3^- \quad (3.3b)$$

$$CaMg(CO_3)_2 + 2CO_2 + 2H_2O \leftrightarrow Ca^{2+} + Mg^{2+} + 4HCO_3^- \quad (3.3c)$$

However, Fig. 3.7 shows that a minor shift towards 2:1 ratios for $*Ca^{2+}+*Mg^{2+}/HCO_3^-$ did in fact occur. Those data points represent samples collected at the end of the ablation season, and indicate an increase in chemical weathering that also involved silicate minerals as a source of $*Mg^{2+}$. This period receives closer attention in the following section. Carbonation was also reflected in the pCO_2 time series (Fig. 3.5a) on account of the slower kinetics of atmospheric CO_2 dissolution (Eqn. 3.4) in comparison with the kinetics of H_2CO_3 dissociation (Eqn. 3.5; Raiswell 1984).

$$CO_2 + H_2O \leftrightarrow H_2CO_3 \quad (3.4)$$

$$H_2CO_3 \leftrightarrow H^+ + HCO_3^- \quad (3.5)$$

A steady decline of pCO_2 from 1991 to 2000 was followed by the high variability and even periods of under-saturation in 2009 and 2010, although the change in the latter year was less pronounced. The above pCO_2 reduction can therefore be linked to enhanced weathering following the steady retreat of glaciers and the subsequent uncovering of fine, reactive subglacial tills produced when the glacier had polythermal regime. These sediments were, until recently, frozen under a cold ice margin. The increased weathering is supported by a steady increase in 1991 - 2010 concentrations of ions derived from carbonate weathering (see Fig. 3.3), pH (see Fig. 3.4) and an increase in the saturation indices of calcite, dolomite, sulphate and silicate minerals (see Fig. 3.5b,c,d). The most pronounced changes in saturation indices, pH and ion concentrations were, however, recorded in 2009 and 2010. This coincided with a major reorganization of the flowpath in 2009, which was a result of Austre Brøggerbreen's retreat. In that year, a long-existing portal on the eastern margin of the glacier remained frozen and meltwater burst through thin glacier ice circa 50 m to the West (Fig. 3.8).

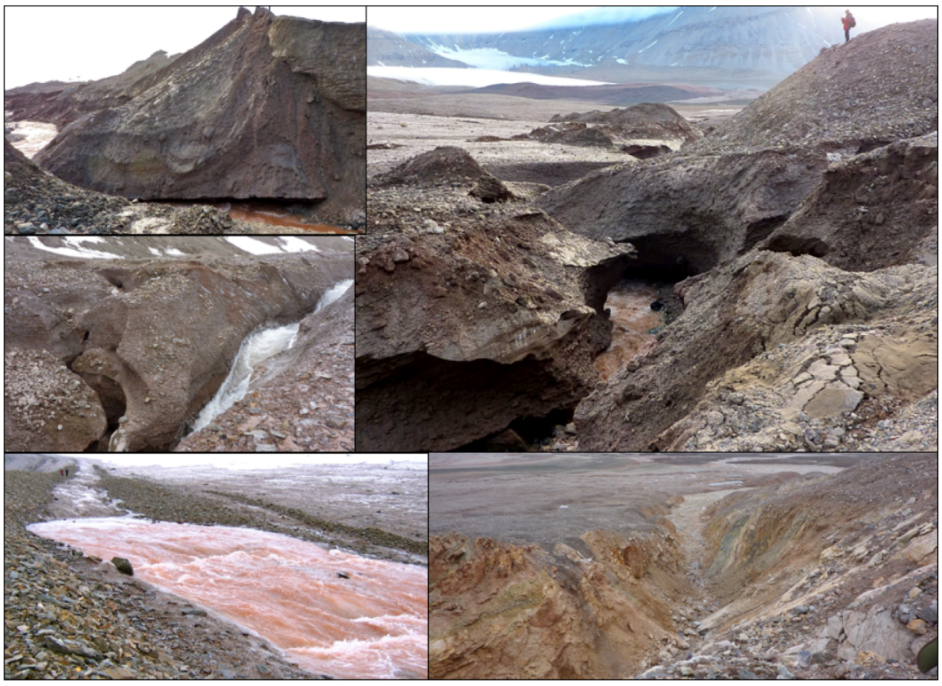

Fig. 3.8 Meltwater transit along Austre Brøggerbreen terminus after the reorganization of a major flowpath in 2009. Upper right, middle and left: new flowpath through sediments at the glacier terminus with a person for scale; bottom right: abandoned rock-wall channel; bottom left: new portal created in 2009. Photo credit: A. Nowak

The portal was draining supra and englacial meltwaters from about 7 km^2 of the eastern part of the glacier, which represents circa 74% of the total glacier area (Hodson et al. 1998a; Stuart et al. 2003). Consequently, a long-existing, more than 1 km long, proglacial channel in a rock-walled valley was abandoned and a new flowpath was eroded through recently exposed sediments (see Fig. 3.8). This reorganization of the major flowpath was responsible for routing of meltwaters through melting moraines along the glacier terminus, which supplied fresh fine sediments that enhanced chemical weathering to such an extent that long established high pCO_2 conditions transformed temporarily into low pCO_2. Therefore, the chemical weathering was so great that the demand of hydrogen protons exceeded the supply of CO_2 from the atmosphere and microbial respiration, and undersaturation of pCO_2 was recorded for the first time. It has to be noted that the sampling was undertaken circa 2.5 km from the glacier terminus. Therefore, turbulent meltwater had time to acquire some CO_2 from the atmosphere, increasing final levels of pCO_2 (a process that can have an observable effect after 20 - 30 min: Raiswell 1984). The change in flowpath was also reflected in the crustal ion yield (see Fig. 3.6, Table 3.3), which in 2009 exceeded 17 T km^{-2} in comparison with 14.8 in 1991, and only 7.5 T km^{-2} in 2000.

Silicates

The changes in carbonate-derived solutes were accompanied by changes in solutes derived from silicate weathering such as $*K^+$, $*Na^+$ and Si (see Fig. 3.3). However, unlike the ions linked to carbonates, the relationship between Si and $*K^+ + *Na^+$, varied between the years (Fig. 3.9a), indicating a change in meltwater chemistry and therefore chemical weathering. Two groups were distinguishable and they consisted of years 1991, 1992, 2000 (June only) and 2000 (July, August), 2009, 2010. The former was characterized by low Si, low $*K^+$, $*Na^+$, while the latter by low Si and high $*K^+$, $*Na^+$. The same pattern was also observed in the ratios of $*SO_4^{2-}$, $*Ca^{2+} + *Mg^{2+}$ and HCO_3^- to Si (Fig. 3.9b, c, d). The year 2000 seemed to mark a transition between 1991, 1992 and 2009, 2010. This agrees with the results presented by Nowak & Hodson (2013) (Chapter Two), where changes in Bayelva hydrology, that followed changes in air temperature and precipitation, also became apparent in the same year.

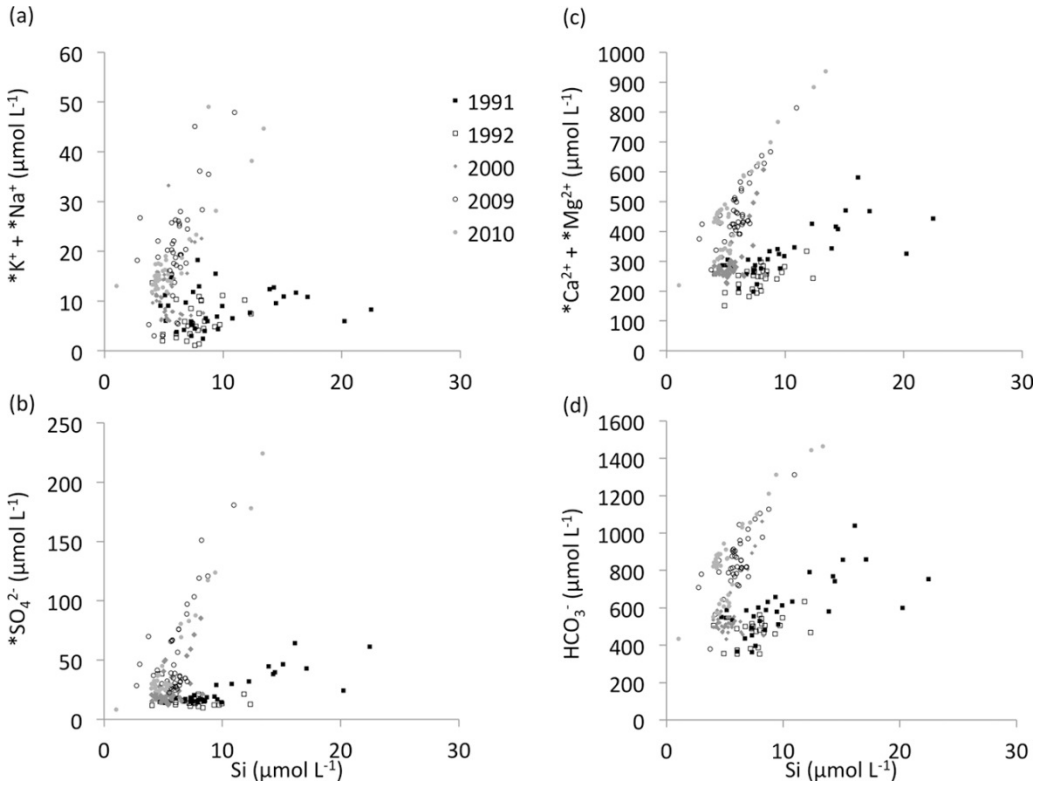

Fig. 3.9 Correlations between ions taking part in silicate weathering in Bayelva during 1991-2010 period of records: (a) associations between $*K^+$, $*Na^+$ and Si; (b) associations between $*SO_4^{2-}$ and Si; (c) associations between $*Ca^{2+}$, $*Mg^{2+}$ and Si; (d) associations between HCO_3^- and Si

Based on the above results, it can be assumed that silicate weathering in Bayelva increased during 2000 (July, August), 2009 and 2010. Despite that, the general 1991 - 2010 trend in dissolved Si concentrations showed a slight decrease followed by the decrease in Si yields (Tables 3.3 and 3.4). The exceptions were short term, end of season Si maxima (Fig. 3.3) that will be discussed below along with the end of season concentration maxima of other crustally derived ions. The phenomenon of increased silicate weathering throughout the entire period of records and a slight decreasing trend of dissolved Si concentrations also require explanation. This is offered below.

Firstly, as suggested by Hodson et al. (2002) and Anderson (1997; 2005) among others, the weathering of silicates in glacial environments is incongruent and non-stoichiometric. The study by Hoch et al. (1999) showed that $*K^+$ can be released rapidly from glacially eroded material without the same increase in Si concentrations. This was also recorded in our dataset and presented in Fig. 3.10. The steady increase in $*K^+$ relative to Si can be achieved by rapid reactions of surface exchange (Eqn. 3.6), reversible cation exchange (Eqn. 3.7) (Tranter et al. 1993) as well as leaching from

biotite, mica and k-feldspar (Newman & Brown 1969; Stallard 1995; Anderson et al. 1997, Anderson 2007) that are present in the catchment.

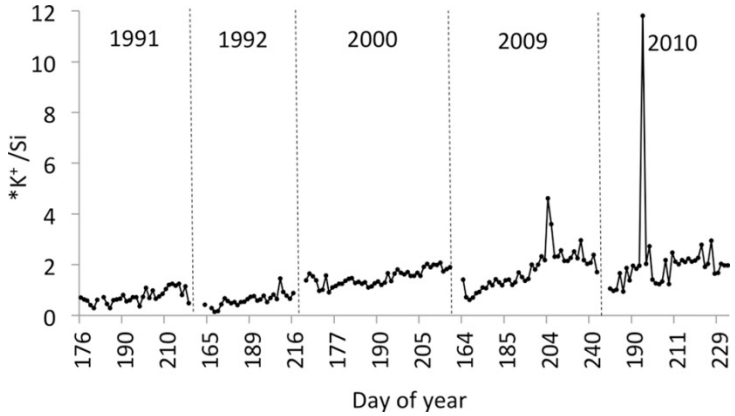

Fig. 3.10 The change in ratio of rock derived potassium (*K^+) to dissolved silica (Si) during 1991 - 2010 period of records in the Bayelva

$$K - clay + H^+ \rightarrow H - clay + K^+ \quad (3.6)$$

$$2K - clay + Ca^{2+} \rightarrow Ca - clay + 2K^+ \quad (3.7)$$

To explore the above reactions, various associations between ions were investigated. Although no correlation between *K^+ and pH was recorded, it was difficult to discard surface exchange entirely, due to H^+ also being used in other weathering reactions. Similarly, positive significant correlations (R^2= 0.74 – 0.88, P=0.05) and small intercepts (0.59 ± 0.06 – 9.04 ± 1.62) between *Ca^{2+} and *K^+ (Fig. 3.11) would suggest that cation exchange had little effect in the period of records. However, the concentrations of *Ca^{2+} in the pool of ions were roughly fifty times higher than *K^+. Therefore, a clear signal from cation exchange (i.e. a negative correlation between *Ca^{2+} and *K^+) could have been masked. Cation exchange was also supported by *Ca^{2+}/HCO_3^- ratios lower than 1 indicating calcium uptake (Tranter, Sharp et al. 2002) as discussed above.

The uptake of *Ca^{2+} to create secondary gypsum was discarded on the account of low saturation indices of gypsum presented in Fig. 3.5c and high slopes in correlations between *Ca^{2+} and *SO_4^{2-}. What's more, the study by Fairchild et al. (1994) showed that *Ca^{2+} - 2*K^+ ion exchange is largely responsible for *K^+ concentrations in meltwaters, with much less *Ca^{2+} - 2*Na^+ exchange.

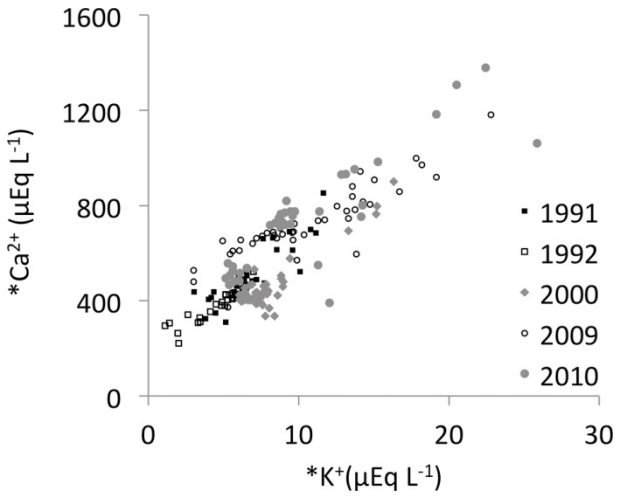

Fig. 3.11 The correlation between crustally derived calcium ($*Ca^{2+}$) and potassium ($*K^{+}$) in the Bayelva meltwaters between 1991 and 2010

The second means of explaining the increased silicate weathering and decreasing trend in Si concentrations is based on the study of Dove (1994), indicating that silicate weathering is slow due to the low temperature and slow kinetics. Therefore, it seems natural that increased weathering can take place in the presence of acids such as H_2SO_4 or H_2CO_3 that can enhance the process. Those acids can be produced by two types of reactions, namely carbonation and sulphide oxidation (see Eqn. 3.8 and 3.9). Both of them occur in the watershed, however, according to the data, the latter is constrained to the end of season hydrochemistry. The carbonation of silicates was identified only in 1991 and 1992 when the positive correlations between $*K^{+}$ and HCO_3^{-} reached respectively 0.75 and 0.87 (P=0.05).

$$CaAl_2Si_2O_8 + 2CO_2 + 2H_2O \rightarrow Ca^{2+} + 2HCO_3^{-} + H_2Al_2Si_2O_8 \quad (3.8)$$

$$4FeS_2 + 16NaKAlSi_3O_8 + 15O_2 + 86H_2O \rightarrow \quad (3.9)$$

$$4Fe(OH)_3 + 16Na^{+} + 16K^{+} + 8{SO_4}^{2-} + 32H_4SiO_4 + 4Al_4Si_4O_{10}(OH)_8$$

Based on the Eqn. 3.8 and Eqn. 3.9 it is clear that chemical weathering of silicates and aluminosilicates via reactions such as sulphide oxidation coupled to silicate dissolution (hereafter SO/SD) and silicate carbonation results in different products. Depending on the water residence time the above reactions can create new silicate minerals, weathered feldspar surfaces (e.g., kaolinite) and/or highly soluble silicic acid (see Eqn. 3.8 and 3.9). Further, Wollast (1967) indicated that there are reactions that can remove Si from the solution to form an amorphous alumina silicate, a hydrated kaolinite-like material ($H_4Al_2Si_2O_9 \cdot nH_2O$). Lastly, when trying to explain the behaviour of dissolved Si

concentrations in meltwaters one must also remember that turbulent and turbid waters of Bayelva preclude any biogenic uptake of dissolved Si.

Therefore we suggest that, during the period of early-mid ablation season, when the water contact with freshly available, glacially disintegrated minerals is high and relatively short, ion exchange takes place along with the carbonation of carbonates and carbonation of silicates (1991, 1992). Thus, since new secondary minerals are created by carbonation and surface exchange, there is no additional release of easily dissolved Si forms into the system (Eqn. 3.8) and Si concentrations remain relatively steady. Some of those minerals created during periods of high turbidity could also have been deposited on the proglacial sandur since the area was proved to be a net sink for suspended sediments by Hodson et al. (1998). Then, later in the season, when discharge falls, the duration of rock-water contact increases while contact with suspended sediment is maintained, the waters from AL and hyporheic zone are no longer hugely diluted, an increased contribution from SO/SD becomes apparent. Enhanced silicate weathering is recorded and in consequence, an increase in the release of silicic acid (therefore dissolved Si) is observed. The end of season meltwater characteristics will therefore be discussed in the next section.

3.4.2 End of season changes in solute acquisition

The seasonal changes in meltwater chemistry are usually marked by two events, the high solute concentrations early in the ablation season and the end of season maxima. The former are heavily influenced by snowpack elution which was explored in detail for the Bayelva watershed by Tranter et al. (1996) and Hodson et al. (2002). Therefore here, we focus only on the end of season changes. It is apparent that the concentrations of all crustal ions increased at the end of summer (August, September) during each year of record. The exceptions were 1991 and 1992 when the sampling was undertaken only until the beginning of August before significant fall in meltwater discharge and late summer rainfalls occurred (see Krawczyk et al. 2003). Additionally, data from the end of 2000 field campaign comprised of samples from between 30th July and 5th August, therefore, they were used to provide an indication of late summer hydrochemistry rather than represent the true end of season period for that year.

As mentioned in the previous section, at the end of summer delayed flowpaths are no longer masked by the large amount of glacial meltwaters and it is possible to record the signal from the melting active layer (that has reached its maximum depth), from solutes

washed out by heavy rains, and from the water exchange within the hyporheic zone of the river channels. Furthermore, as the season progresses the water table in the immediate glacier forefield drops following channelization, allowing the outflow of more concentrated waters from melting moraines and areas near the glacier terminus (see Cooper et al. 2011). Additionally, as the studies by Bogen (1991) and Hodson et al. (1998) show, suspended sediment concentration in the Bayelva does not decrease with time but rather remains relatively high, delivering sediments from lateral and marginal moraines and slopes throughout the season. We believe that the processes presented above and the significant reduction in discharge serve to increase water residence time in the watershed and provide the conditions for reactions other than carbonation and much more commonly observed in subglacial environments. The best examples are microbially mediated sulphide oxidation coupled to carbonate dissolution (hereafter SO/CD, see Eqn. 3.10a and 3.10b) and the already mentioned SO/SD (Eqn. 3.9).

$$4FeS_2 + 8CaCO_3 + O_2 + 14H_2O \rightarrow 4Fe(OH)_3 + 8Ca^{2+} + 8HCO_3^- + 8{SO_4}^{2-} \quad (3.10a)$$

$$4FeS_2 + 16CaMg(CO_3)_2 + 11O_2 + 22H_2O \rightarrow 4Fe(OH)_3 + 16Ca^{2+} + 16Mg^{2+} + 8{SO_4}^{2-} + 32HCO_3^- \quad (3.10b)$$

As a result, waters with high solute concentrations such as those recorded at the end of 2000, 2009 and 2010 ablation seasons are observed. The end of season meltwaters were also characterised by higher concentrations of $*SO_4^{2-}$ that exceed 100 µEq L^{-1} (see Fig. 3.3a and Fig. 3.12).

Additionally, during that time, the relationships between crustally derived ions and $*SO_4^{2-}$ as well as Si (see Table 3.4) revealed significant linear correlations that were not recorded earlier in the ablation season, when the $*SO_4^{2-}$ concentrations were below 100 µEq L^{-1}. Therefore, to better explore the reactions occurring at the end of ablation season a comparison of regression models was performed according to the scheme presented by Tranter, Sharp et al. (2002), Wadham et al. (2001) and Wadham et al. (2010). Following this, the primary reaction occurring during the end of season was again carbonate carbonation. What's more, the significant (R^2=1, P=0.05) correlation between $*Ca^{2+}+*Mg^{2+}$ vs $*SO_4^{2-}$ and HCO_3^- vs $*SO_4^{2-}$ intercepts in August - September 2000, 2009 and 2010 and 0.99 ± 0.01 gradient (see Fig. 3.13) indicated that about 99% of H_2CO_3 dissolved carbonates and the remaining dissolved silicates.

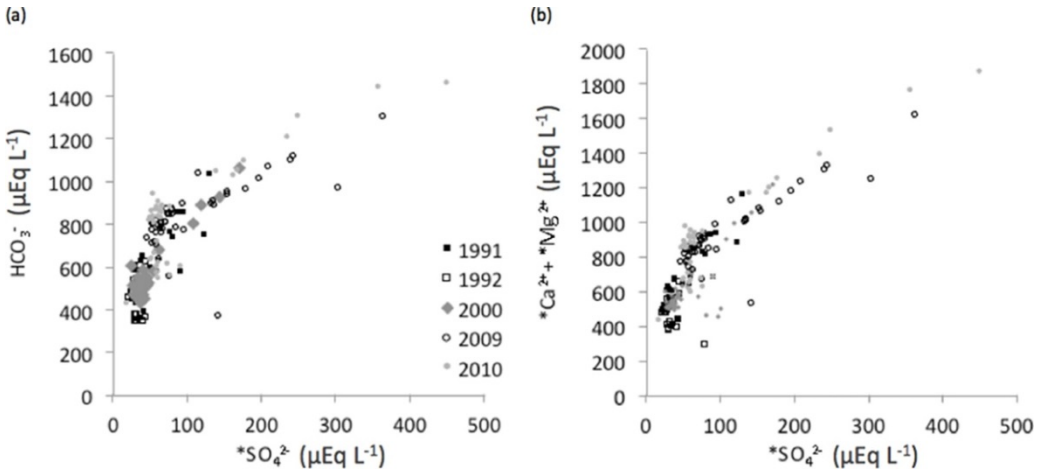

Fig. 3.12 The relationship between carbonate derived ions and sulphates in the meltwaters of Bayelva during 1991-2010; (a) relationship between HCO_3^- and $*SO_4^{2-}$; (b) relationship between the sum of $*Ca^{2+}$and $*Mg^{2+}$ versus $*SO_4^{2-}$

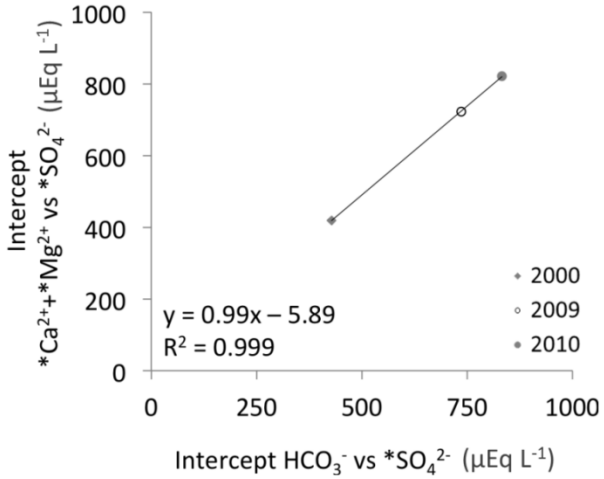

Fig. 3.13 Association between intercepts of $*Ca^{2+}$+$*Mg^{2+}$ and $*SO_4^{2-}$ versus HCO_3^- and SO_4^2

What's interesting is that the amount of carbonate acid hydrolysis nearly doubled between 2000 and 2010, which according to Wadham et al. (2010a) could be an indication of increased proportion of fine sediments in the meltwaters. This also placed Bayelva runoff between subglacial waters of polythermal glaciers such as Midre Lovénbreen (years 1991, 1992 and 2000) and Finterwalderbreen (years 2009, 2010) presented as well by Wadham et al. (2010). Furthermore, mean ratios of

Table 3.4 The relationships between carbonate and silicate derived ions at the end of ablation season when concentrations of $*SO_4^{2-}$ exceeded 100 µEq L^{-1}. The confidence level (P) of all correlations was 0.05

Year	$*Mg^{2+}$ vs Si	$*Ca^{2+}+*Mg^{2+}$ vs Si	$*K^{+}$ vs Si	$*SO_4^{2-}$ vs Si	$*Ca^{2+}+*Mg^{2+}$ vs $*SO_4^{2-}$	$*Ca^{2+}+*Mg^{2+}$ vs HCO_3^{-}	$*Mg^{2+}$ vs $*SO_4^{2-}$	$*Ca^{2+}$ vs $*SO_4^{2-}$	$*K^{+}$ vs $*SO_4^{2-}$	HCO_3^{-} vs $*SO_4^{2-}$	$*Ca^{2+}+*Mg^{2+}$ vs $*K^{+}+*Na^{+}$
	(µmol L^{-1})				(µEq L^{-1})						
1991	n/a	n/a	n/a	n/a	n/a	n/a	n/a	n/a	n/a	n/a	n/a
1992	n/a	n/a	n/a	n/a	n/a	n/a	n/a	n/a	n/a	n/a	n/a
2000											
Slope	31 ± 1.9	117 ± 3.5	3.2 ± 0.6	20.9 ± 2.5	4.6 ± 0.5	1.2 ± 0.01	1.6 ± 0.1	2.9 ± 0.4	0.1 ± 0.01	3.6 ± 0.6	38.4 ± 18.4
Intercept	111 ± 14	358 ± 26.3	8.9 ± 4.8	19.5 ± 19.4	418 ± 74.6	-103 ± 47.5	29.6 ± 17.4	389 ± 61.5	1.5 ± 2.0	427 ± 80.3	248 ± 281
R^2	0.99	0.99	0.97	0.68	0.97	0.99	0.99	0.96	0.54	0.95	0.91
2009											
Slope	20 ± 1.1	55.8 ± 2.8	1.7 ± 0.3	37.8 ± 2.2	2.3 ± 0.6	1.1 ± 0.1	0.79 ± 0.1	1.5 ± 0.2	0.03 ± 0.01	1.4 ± 0.3	20.5 ± 3.0
Intercept	3.3 ± 7.2	191 ±20.7	3.7 ± 2.1	71.6 ± 16.2	722 ± 123	37.9 ± 84.9	131 ± 20.2	603 ± 39.3	9.9 ± 1.6	735 ± 68.0	565 ± 93.3
R^2	0.97	0.97	0.75	0.81	0.89	0.94	0.81	0.89	0.57	0.72	0.84
2010											
Slope	18 ± 0.7	51.9 ± 2.5	1.3 ± 0.5	40.7 ± 1.3	2.5 ± 0.2	1.5 ± 0.1	0.9 ± 0.1	1.6 ± 0.1	0.03 ± 0.01	1.5 ± 0.2	16.5 ± 6.0
Intercept	3.8 ± 6.6	243 ± 23.5	4.7 ± 4.9	125 ± 12.6	821 ± 52.4	-435 ± 91.5	112 ± 16.2	708 ± 39.2	9.0 ± 3.4	832 ± 53.1	926 ± 195
R^2	0.99	0.99	0.95	0.97	0.96	0.99	0.97	0.95	0.91	0.91	0.55

$*Ca^{2+}$,$*Mg^{2+}$ versus HCO_3^- (above 1) and $*Ca^{2+}$ versus HCO_3^- (below 1) indicated that $*Mg^{2+}$ and $*Ca^{2+}$ were also acquired from/involved in other reactions. Hence, to explain the ratio above 1 additional regression models were developed. For example, high R^2 values for associations between $*Mg^{2+}$ and Si (0.99 in 2000; 0.97 in 2009 and 0.99 in 2010; P=0.05) and low intercepts (3.35 ± 7.2 in 2009, 3.80 ± 6.6 in 2010) suggested silicate weathering was one of the additional and most likely sources of $*Mg^{2+}$. Regression models performed on other crustally derived ions (see Table 3.4) indicated that SO/SD was more responsible for the end of season solute acquisition than SO/CD. This would also explain the increase in dissolved Si during that time, since one of the products of SO/SD is highly soluble silicic acid. Additionally, mean ratios of $*Ca^{2+}$ versus HCO_3^- lower than 1, as indicated above, were thought to be caused by uptake of $*Ca^{2+}$ released during carbonate carbonation and liberation of $*K^+$. This would account for and high R^2 values in regression models between $*K^+$ and $*Ca^{2+}$ (0.90 in 2000, 0.74 in 2009 and 0.97 in 2010, P=0.05). Therefore, in addition to carbonate carbonation, SO/SD and SO/SD supplying ions to Bayelva meltwaters at the end of ablation season, quick cation exchange reactions were also taking place.

3.4.3 Ion yields

Despite the marked and constant increases in ion concentrations since 2000, those changes were not entirely reflected in ion yields. For example 2000 and 2010 were characterized by smaller ion yields than 1991 and 1992 (Fig. 3.6; Table 3.3) even though concentrations of ions during the former years were much higher (see Table 3.2). This was not unexpected considering that ion yields were calculated from ion concentrations and river discharge. The control of water flux on chemical erosion was already explored by Anderson et al. (1997) and Hodson et al. (2000). However, the interesting outcome of our multiannual study is the impact of a cold based-glacier retreat on ion yields. The flowpath change that rerouted meltwaters through new, freshly exposed, fine sediments produced at the glacier terminus was the direct result of glacier retreat and it connected previously isolated environments such as melting ice cored moraines, to the main water channel. This nearly doubled $*SO_4^{2-}$ yields. This process also led to a marked increase in most of the ion yields presented in Fig. 3.6 and Table 3.3. What's more, the flowpath change also affected meltwater chemistry in the subsequent year, maintaining high solute yields even though the river discharge in 2010 was smaller than in 2000 by

38%. Discrete events such as the one described above occurring during the retreat of cold-based glaciers can therefore have a marked impact on ion delivery to downstream terrestrial and marine ecosystems.

*3.*5 CONCLUSIONS

A multiannual study like this one gives a rare opportunity for insights into meltwater hydrochemistry during the retreat of a cold-based glacier. During our study two periods were identified based on the solute concentrations, pH and the chemical weathering processes. They consisted of samples collected before and after July/August 2000. During the latter period mean ion concentrations were from 1.6 to 3.4 times greater due to changes in carbonate (1.6) and silicate (3.4) derived ions. The same pattern was also observed in the mean pH values which increased by 1 unit between 1991 and 2010. This was the result of increased chemical weathering during which the main process of ion acquisition, namely carbonate carbonation, nearly doubled between 2000 and 2010 placing Bayelva runoff between subglacial waters of polythermal glaciers such as Midre Lovénbreen (for years 1991, 1992 and 2000) and Finterwalderbreen (for years 2009, 2010) presented by Wadham et al. (2010). However, the change in chemical weathering was not constrained to just carbonate rocks. The increase in rapid weathering of silicate minerals via surface exchange and leaching was also marked. Furthermore, additional reactions such as SO/SD and SO/CD were responsible for clear increases in ion concentrations during the end of the 2000, 2009 and 2010 ablation seasons. Since the same processes were responsible for ion acquisition throughout the entire period of record, the change in ion concentrations was associated with the increased proportion of fine sediments available for weathering. This could only be linked to the glacier retreat, which consequently uncovered fresh, fine, reactive sediments. Furthermore, the retreat also resulted in the meltwater flowpath through these newly uncovered sediments and also through melting moraines at the glacier terminus. As a consequence, crustal ion yields in 2009 doubled even though the specific discharge in that year was similar to 2000. The release of sediments from the immediate glacier terminus and further deposition of these fine sediments downstream from glaciers and in their forefields also means that the chemical weathering characteristics can be influenced for some time. This was the most likely reason why crustal ion yields in 2010 although smaller than in the previous year, were still relatively high.

In the light of the above, this study has shown that:

1. The predictions of chemical denudation rates from catchments glacierized by cold-based glaciers should not be estimated with the use of old meltwater chemistry data and contemporary discharge data. Long term/multiannual measurements are necessary for the accurate predictions of the hydrochemical response of a glacierized catchment to climate change.

2. During glacier retreat, the immediate vicinity of a cold-based glacier is the most chemically reactive part of the watershed.

3. The end of season chemical weathering makes an important contribution to solute concentrations, since more concentrated waters from the active layer, melting moraines and hyporheic zone are less diluted by glacial meltwaters. Therefore, microbially mediated sulphide oxidation weathering carbonates and silicates and microbial production will contribute to the total ion yields. Those concentrated waters can be flushed out by the end of season rainfalls or stay within the active layer until the next ablation season (see Nowak & Hodson 2013).

4. Although it is believed that due to the primary control of water fluxes on chemical erosion rates (Anderson et al. 1997; Hodson et al. 2000), climate warming will increase chemical denudation rates in glacierized catchments (Førland et al. 2009; Krawczyk & Bartoszewski 2008), it has to be taken into account that the long term study of Bayelva's hydrology by Nowak & Hodson (2013) did not record significant increase in water flux over the last 35 years. What's more, the present study indicated that the marked increase in ion yields during 1991 - 2010 was only the result of a change in water flowpath in response to glacier retreat that connected fresh, fine reactive sediments to the main water channel.

5. Our study shows that major reorganisation of the drainage system caused by glacier retreat can occur suddenly and result in an "annual flush" of crustally-derived ions. Furthermore, carbonation reactions occurring during these events cause significant pCO_2 depletion incidents in an otherwise high pCO_2 system. Lastly, although this enhanced geochemical weathering appears to be short-lived, its impact on the annual solute flux shows that it can be significant for downstream terrestrial and marine ecosystems.

CHAPTER FOUR:

ON THE BIOGEOCHEMICAL RESPONSE OF A GLACIERIZED HIGH ARCTIC WATERSHED TO CLIMATE CHANGE: WHAT CAN WE LEARN FROM A STUDY OF MICRO-CATCHMENTS?

Submitted to Hydrological Processes on 4th Nov 2013 as: Nowak A. & Hodson A. On the biogeochemical response of a glacierized High Arctic watershed to climate change: What can we learn from a study of micro-catchments?

4.1 INTRODUCTION

It is expected that the change in permafrost thickness that is following climate warming will have an effect on the hydrology and biogeochemistry of Arctic tundra streams (e.g. Rouse et al. 1997; Hobbie et al. 1999; Smith et al. 2005; Prowse et al. 2006; Zarnetske et al. 2007; Schuur et al. 2009). Furthermore, an increase in export of organic matter, major ions and inorganic nutrients in response to the permafrost thinning is also expected to affect the productivity of the Arctic Ocean (Tye & Heaton 2007; Frey & McClelland 2009), although the magnitude of this influence is unclear (Le Fouest et al. 2013; Tank et al. 2012). Therefore, numerous studies have been devoted to the dynamics of the permafrost table and seasonally thawing active layer (hereafter AL), which is especially susceptible to any changes in air temperatures (T_a). Although annual variations in the AL thickness strongly depend on the regional setting and seasonal weather conditions (Rachlewicz & Szczuciński, 2008), interannual variations respond to long term climatic changes that have already been observed in many parts of the Arctic (ACIA 2005; Etzelmüller et al. 2011). For example, studies from the Bayelva watershed in Svalbard (the location of the present study) have documented up to a 50% increase in AL depth over the last decade (e.g. Roth & Boike 2001; Boike 2009). This coincided with an increase in the AL thickness in other locations in Svalbard as well as in the Alaskan, Canadian and Russian Arctic (IPCC 2007), demonstrating the near-global trend in AL deepening and permafrost warming. Thus, one could expect an extensive research literature investigating the changes in physical, hydrological and biogeochemical processes in High Arctic environments that follow such AL/permafrost transformation. However, although research on soil-water interactions in Svalbard's tundra and AL have received some attention (Pecher 1994; Stutter & Billet 2003; Tye & Heaton 2007), little or no attention has been given to other important permafrost sediments, namely talus slopes and moraines (e.g. Cooper et al. 2002). This is surprising considering that most of these reactive stores of physically comminuted rock debris are commonplace in Svalbard's mountainous land surface. Therefore understanding landscape biogeochemical change here requires the integration of process studies from a range of smaller micro-catchments in glacial and proglacial environments where these sedimentary habitats are present. Such micro-catchments are most likely very

chemically productive and can therefore influence the downstream evolution of glacial runoff. For example, work from Alpine or temperate glacier forefields has already shown us that the high rock-water contact and longer water residence times they afford, provide an ideal environment for microbially mediated chemical weathering reactions (e.g. Williams et al. 2006; von Rohr 2007). Additionally, young and unstable sediments in the High Arctic often lack the plants that might otherwise assimilate nutrients produced by chemical weathering. Hence, it can be expected that the sediments nearer changing glaciers might be far more capable of driving changes in solute acquisition and export from the landscape than the stable, vegetated and up to 10^4 year old tundra surfaces that lie beyond Little Ice Age moraines. However, the prediction of changes in solute export to downstream aquatic and marine ecosystems can be challenging when we consider the lack of studies characterizing spatial and temporal patterns in hydro-biogeochemical coupling across the High Arctic landscape. For example, no studies in Svalbard have yet been devoted to the comparison of ion yields exported separately from tundra, talus and moraine environments. Nor have their ion yields been compared to those exported from whole catchments. This potentially important oversight prevents the early detection of change, because landscape signals might be masked in the first instance by dilution from the large volumes of glacial meltwater produced in the early stages of deglaciation (see Chapter Three).

Hence, here, we focus firstly on the spatial and temporal signal of ion production from various micro-catchments that represent young moraines, talus and soils within a High Arctic, partially glacierized watershed. Most emphasis is given to the biogeochemical processes at end of ablation season which, we think, are especially interesting in the light of the recent findings by Nowak & Hodson (2013) in the same study site. There, it was shown that despite climate warming and sustained glacier retreat over the last 35 years, one of the important changes in glacial watershed hydrology was mostly caused by an increasing occurrence of rainfall during the so called shoulder months. These represent times when the AL is either frozen (March, April, May) and can only be influenced by a latent heat transfer from freezing rain and creation of icings; or when the AL is at its deepest (August, September), when plants have passed their senescence and water infiltration into subsurface environments are intensified by rain. Delayed water flowpaths through the AL are therefore an increasingly conspicuous feature of the entire watershed's hydrograph during the last decade (Nowak & Hodson 2013). Secondly, we compare the productivity of the micro-catchments, defined as solute yields, to the solute delivery into an Arctic fjord (Kongsfjorden) by Bayelva (hereafter

BAY), which drains the entire watershed. Therefore, we link the hydrology and biogeochemistry of various micro-catchments to the potential impact of landscape solute fluxes upon the downstream marine ecosystem. In so doing, our work complements two other publications describing the long term hydrological (Chapter Two) and biogeochemical (Chapter Three) responses of the High Arctic Bayelva catchment to changing climate.

4.2 STUDY LOCATION

The study was carried out in the Bayelva watershed described in detail in Chapter One (see also Fig. 1.11).

The Micro-catchments

Table 4.1 describes four study sites selected to represent young moraine (MM), talus (TM) and two soil micro-catchments (SM1 and SM2) monitored during 2009 and 2010 ablation seasons. The study location is also presented in Fig. 4.1.

Table 4.1 Comparison of sampling sites in Bayelva watershed including locations, areas and a basic description of their hydrology. *Discharge calculated for the 13 days period

Micro-catchment	**Location**	**Area [km^2]**	**Specific discharge [m]**		**Water regime**
			2009	**2010**	
Moraine (MM)	78°54.807N 11°50.647E	0.33	0.01*	0.16	Snowmelt, rainfall, ground ice melt including buried glacier ice
Talus (TM)	78°54.808N 11°51.630E	0.39	0.11	0.22	Snowmelt, rainfall, ground ice melt including rock glacier ice
Soil (SM1)	78°55.460N 11°49.903E	0.25	0.47	0.02	Snowmelt, rainfall, ground ice melt
Soil (SM2)	78°55.706N 11°48.040E	0.67	n/a	0.01	

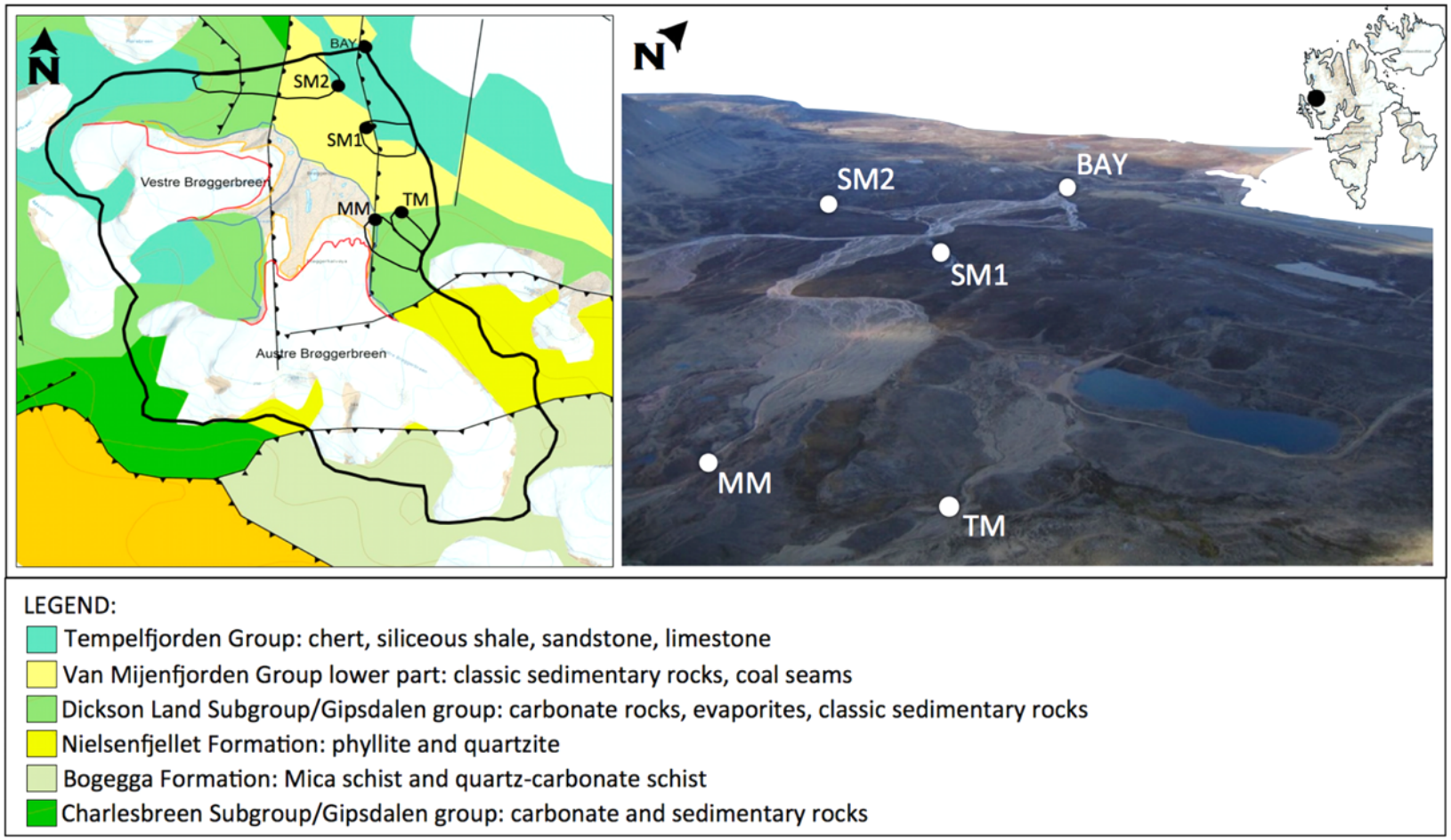

Fig. 4.1 The location of sampling sites in the Bayelva catchment on the Brøggerhalvøya, Svalbard and the geology of the watershed. Black lines indicate the borders of the soil, talus and moraine micro-catchments (SM1, SM2, TM, MM) with their sampling points (dots) and the whole Bayelva watershed (BAY). The map modified from Norwegian Polar Institute: www.svalbardkartet.npolar.no, 2013. Photo credit: A.Hodson

4.2.1 Moraine micro-catchment (MM)

The MM site was created in August 2009 when the main meltwater flowpath from Austre Brøggerbreen was changed due to glacier retreat (Nowak & Hodson, In Press). In consequence, a circa 1 km river channel draining about 74% of glacial meltwaters was abandoned (Fig. 4.2) and a small micro-catchment was created. It consists of Austre Brøggerbreen's ice-cored lateral moraine and the western slopes of Zeppelin mountain that includes a small sea bird breeding colony on the cliffs. The geology of MM comprised of clastic sedimentary rocks, evaporites and carbonates as well as poorly sorted rock debris such as red sandstone, quartzite, phyllite, mica and quartz-carbonate schists delivered by glacial meltwaters. No vegetation cover was recorded.

Fig. 4.2 Abandoned meltwater channel at MM (upper) and sampling location at MM (lower). Photo credit: A. Nowak

4.2.2 Talus micro-catchment (TM)

Similar to MM, TM consisted of poorly sorted rock debris that included carbonate rocks, evaporates and clastic sedimentary rocks. However, small patches of vegetation including mosses, *Dryas*, *Salix* and *Carex* communities were recorded in the vicinity of the stream (Fig. 4.3). Additionally, the southern part of the micro-catchment was

occupied by a rock glacier and northern part was covered by patterned ground that indicated frost heaving in the area.

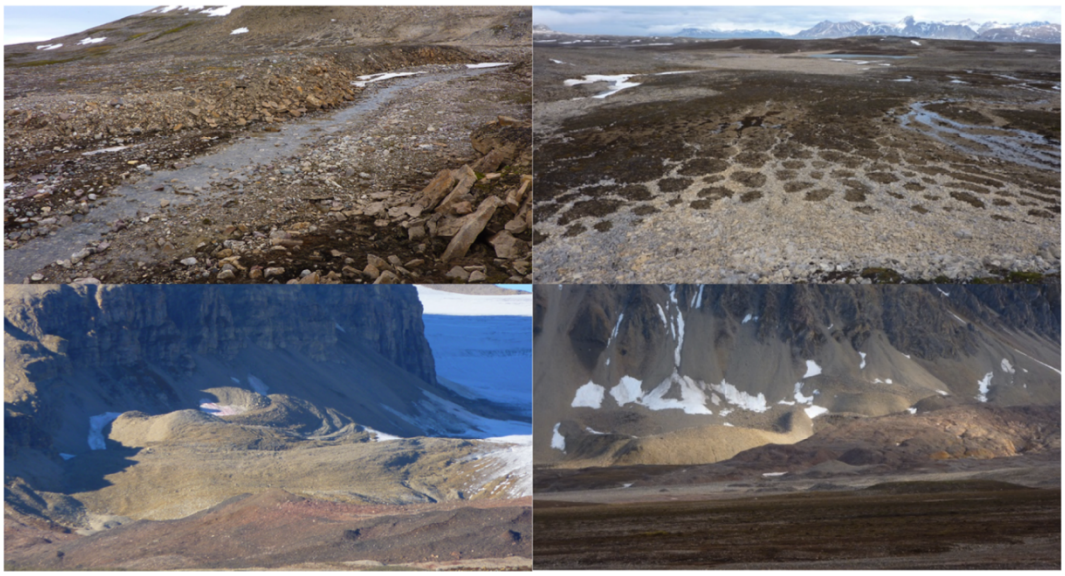

Fig. 4.3 Sampling location at TM (upper left), patterned ground in the northern part of the micro-catchment (upper right) and rock glacier in the southern part (lower left and right). Photo credit: A. Nowak

4.2.3 Soil micro-catchments (SM1, SM2)

The two soil micro-catchments SM1 and SM2 were selected on the basis of differences in geology, vegetation cover and the type of the river bed. The geology of the former consisted of chert, siliceous shale, sandstone, limestone, sedimentary rocks and coal seams. The micro-catchment was fully covered by a mixture of vegetation that included *Dryas*, *Salix* and *Carex* communities as well as variety of mosses also growing on the partially sandy bed of the stream. The geology of the SM2 additionally consisted of carbonate rocks and evaporates located at Schetelig mountain slopes. In contrast to SM1, SM2 was only partially covered by vegetation and had a rocky stream bed that was dominated by algae (Fig. 4.4).

Fig. 4.4 Sampling location at SM1 (upper left and right) and SM2 (lower left and right). Photo credit: A. Nowak

4.3 METHODS

Meteorological data for Ny-Ålesund area has been downloaded from eklima.met.no (2013) for weather station (no. 99910) located at 78.923N, 11.933E at 8 m a.s.l. (see Fig. 1.11 in Chapter One and Fig. 2.1 in Chapter Two). Precipitation types were deduced from T_a and classified as snow (when $T_a<0^oC$) or rain (when $T_a>0^oC$). Measured precipitation data were then corrected for catch by the value of 1.15 (rain) and 1.65 (snow) after Killingtveit (2004). Elevation gradient correction of 19% per 100m was used to further correct the data for elevation change. Detailed description of Bayelva catchment hydrology and meteorological conditions between 1974 - 2010 is provided in Chapter Two.

4.3.1 Hydrological monitoring

Campbell Scientific CR800 and CR1000 data loggers were used to monitor water stage, electrical conductivity and water temperature at sampling sites during both ablation seasons (see Table 4.2 and Figure 4.1 for details). Data were collected every 30 sec, averaged and then recorded every 15 min. The salt dilution method (Moore 2005) was performed after sampling at all four sites to estimate discharge rating curves. They were then used along with water stage to calculate hourly discharge at every micro-catchment with errors of ca. 10% (Hodson 1994). In order to collect representative water samples from the moraine, talus and tundra environments, each hydrological

monitoring station and water sampling point was located at the micro-catchment boundary, where water was draining the entire area of interest (see Figure 4.1 and Table 4.1).

4.3.2 Water sampling

In 2009 sampling was undertaken from the beginning of the ablation season when the streams were opening in the melting snowpack, until the cessation of flow. In 2010 the sampling commenced one week after the beginning of snowpack runoff and when most of the snowpack had melted at both SM sites. Water samples were collected with a pre-rinsed 250 mL polyethylene bottle and filtered within 12 hrs through a 0.45 µm Whatman cellulose nitrate filter papers using a Nalgene filtration unit. After filtration, samples were stored without air at +4^{o}C in 60 mL sterile, polypropylene bottles for no longer than 3 months. No contamination was detected in deionized water blanks collected and examined along with other streamwater samples. A comparison of hydrological monitoring and water sampling at every site during the 2009 and 2010 field campaigns is presented in Table 4.2.

4.3.3 Solute provenance and yields

Ion concentrations were separated into marine and crustally derived components (hereafter ssX and *X, where X is the solute of interest) after assuming that Cl^- was of marine (sea salt) origin. Therefore, ssX were calculated after Holland (1978) from standard marine ratios of ions to Cl^- in seawater. Then, *X were calculated by the subtraction of ssX from their total concentration. Lastly, the sum of rock and microbially produced SO_4^{2-} (hereafter $*SO_4^{2-}$) was calculated after subtraction of the sum of $ssSO_4^{2-}$ and atmospheric SO_4^{2-} from the total SO_4^{2-} concentrations. The sum of $ssSO_4^{2-}$ and atmospheric SO_4^{2-} was calculated using the average snowpack SO_4^{2-}/Cl^- ratio from snow samples collected at each micro-catchment (data not shown).

Ion yields were calculated according to Hodson et al. (2005) by summing the product of daily total stream discharge and ion concentration pairs, before dividing by the individual micro-catchment area. Since in some cases sampling was not undertaken every day, missing daily concentrations were estimated by either linear interpolation (when samples were collected every second day) or by best fit regression models of ion concentration and the stream discharge (when samples were collected every third and fourth day).

Table 4.2 The comparison of sampling strategies and hydrological monitoring within the pro-glacial area of the Bayelva watershed in Svalbard during 2009 and 2010 melt seasons. * -sampling after the snowmelt phase; ** - data logger was moved to another location when the main water flowpath from Austre Brøggerbreen changed due to glacier retreat

Site	Year	Sampling period		Sampling	Bayelva discharge period		Data logger	Manual stream flow measurement
		Dates	Days		Dates	Days		
MM	**2009**	13 June – 9 September	89	Daily, *every 2nd day	8 June – 26 September	111	CR 800, **n/a	Every 2nd day
TM				Daily, *every 2nd day			n/a	Every 2nd day
SM1				Daily			CR 800	Daily
MM	**2010**	29 June – 23 August	56	Every 4th day	18 June – 9 September	84	n/a	Every 4th day
TM				Daily, *every 2nd day			CR 800	Every 2nd day
SM1				Daily			CR 1000	Daily
SM2				Every 3rd day			n/a	Every 3rd day

4.3.4 Stable isotope analyses

To compare microbial activity among the micro-catchments, samples from 2010 were also analysed for $\delta^{15}N$ and $\delta^{18}O$ in NO_3^- at the School of Environmental Sciences, University of East Anglia using the bacterial denitrifier method following Kaiser et al. (2007). This allows determination of $\delta^{15}N$ and $\delta^{18}O$ with a precision of 0.2‰ for $\delta^{15}N$ and 0.5‰ for $\delta^{18}O$ in samples containing more than 10 nmol L^{-1} of NO_3^-. Full details are reported by Ansari et al. (2013), who discuss a set of samples from local snowpack and glaciers that were collected and analysed at the same time as the present study.

4.4 RESULTS

4.4.1 Meteorological conditions

The ablation season in 2009 was colder and wetter than 2010. Therefore, mean T_a during summer of 2009 were lower by between 1 and 1.5°C in May, June and October (when runoff was still occurring). Rainfall was the most dominant form of summer precipitation during both years however, nearly three times more rainfall was recorded during 2009. Additionally, in 2010, rainfall was mostly confined to October, which received nearly 50% of the total wet precipitation recorded during summer. Snowfall was recorded only in May and October during both ablation seasons. In May it accounted for 17% (2009) and 0.2% (2010) of the total precipitation, while in October for 66% (2009) and 16% (2010).

4.4.2 Meltwater characteristics

The time series of key solutes during the two observation periods at each micro-catchment are presented in Fig. 4.5. A full description of the same solutes recorded at BAY between 1991 and 2010 is given in Chapter Three and is used here for comparative purposes (years 2009 and 2010).

Moraine micro-catchment

A sudden increase in concentrations of solutes commonly associated with carbonate weathering (namely $*Ca^{2+}+*Mg^{2+}$ and HCO_3^-) was recorded around Day 217 (2009) and Day 207 (2010), which occurred when water discharge decreased markedly (see Fig. 5a). Interestingly, after those days, acquisition of $*Ca^{2+}+*Mg^{2+}$ did not follow the pattern in

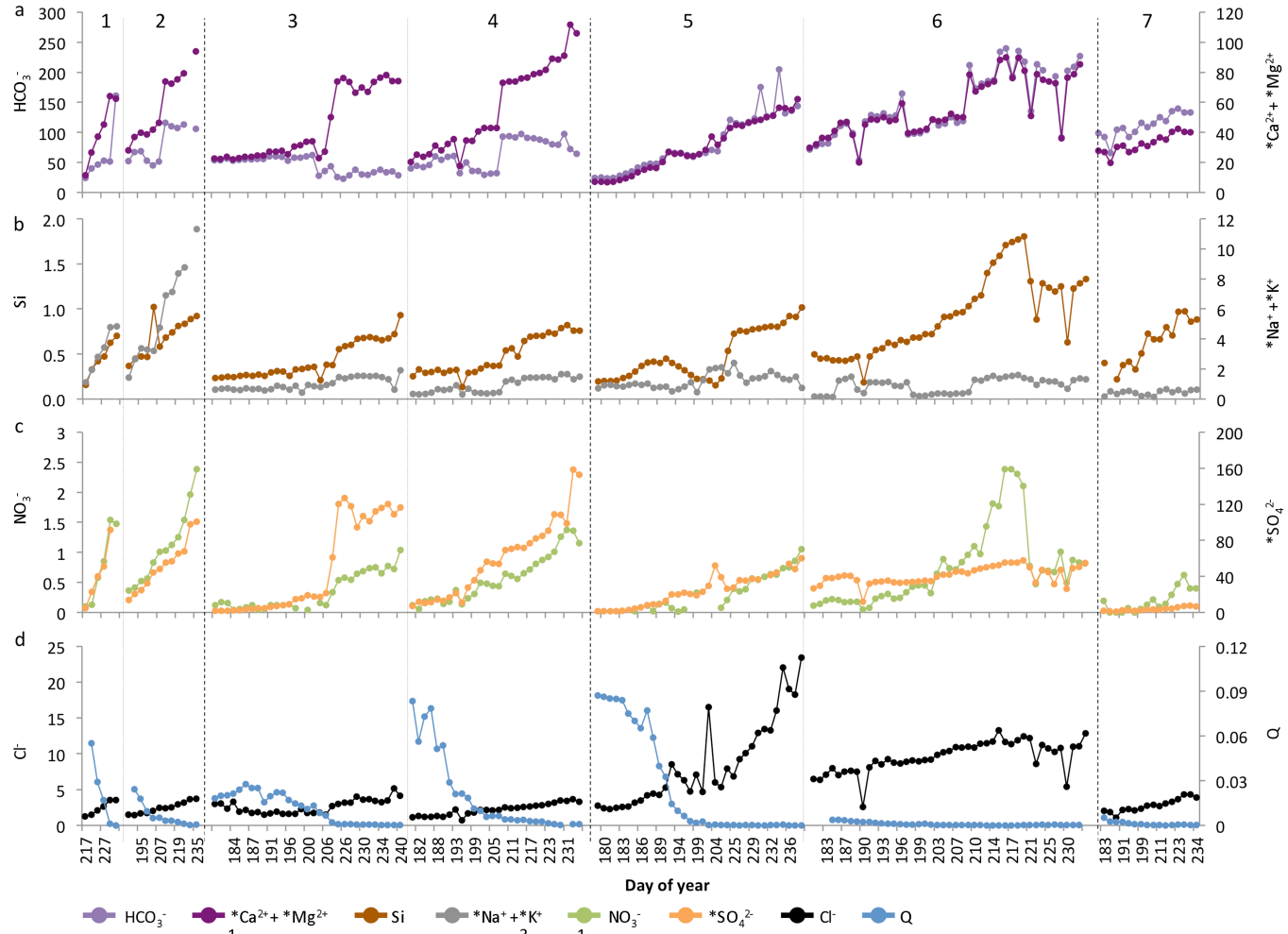

Fig. 4.5 Time series of ion concentrations (mg L^{-1}) and water discharge (m^3 sec^{-1}) at various sampling sites in the Bayelva watershed during 2009 and 2010 ablation seasons. Numbers 1 - 7 correspond to individual micro-catchments. Therefore, 1 – MM 2009, 2 – MM 2010, 3 – TM 2009, 4 – TM 2010, 5 – SM1 2009, 6 - SM1 2010, 7 - SM2 2010

HCO_3^- acquisition. Instead, changes in $*Ca^{2+}+*Mg^{2+}$ were accompanied by an increase in solutes associated with silicate weathering (namely Si, and $*Na^+ + *K^+$; see Fig. 5b) as well as $*SO_4^{2-}$ (Fig. 5c). The concentrations of $*Na^+ + *K^+$ and NO_3^- reached the highest levels recorded amongst all of the micro-catchments. NH_4^+ was recorded few times during July 2010 and ranged from 3 to 19 µg L^{-1}. No PO_4^{3-} was detected. Lastly, pH of the stream varied during both ablation seasons between 7.5 and 8.0 (Fig. 4.6).

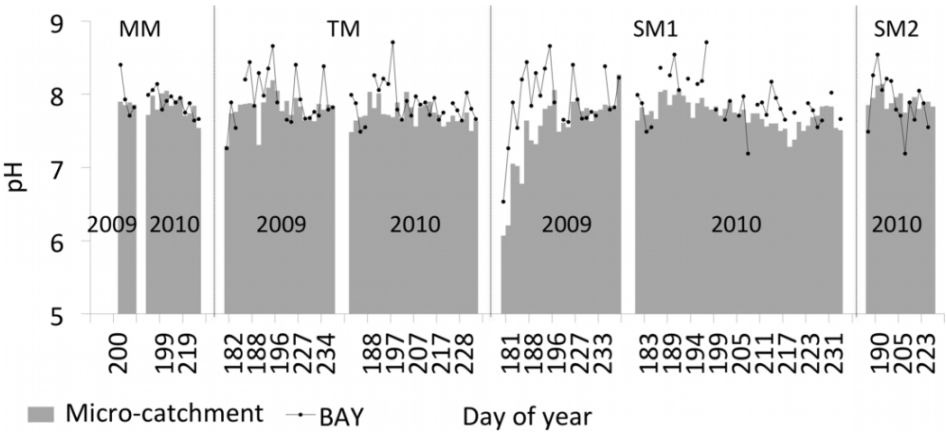

Fig. 4.6 The change in stream pH at all micro-catchments and in the Bayelva during 2009 and 2010 ablation seasons. Bayelva data are taken from Nowak & Hodson (In Press; Chapter Three)

Talus micro-catchment

Although the concentrations of ions recorded at TM were different to those recorded at MM, the behaviour of solute acquisition was similar. The same sudden increase in ion concentrations on Day 217 (2009) and 207 (2010) was also observed. The exceptions were HCO_3^- and $*Na^+ + *K^+$, whose concentrations increases were much less pronounced and even declined in the case of HCO_3^-. Additionally, concentrations of $*Ca^{2+}+*Mg^{2+}$ and $*SO_4^{2-}$ were amongst the highest recorded at all micro-catchments. NH_4^+ was only recorded a few times during July 2010 and ranged from 3 to 25 µg L^{-1}. Similarly to MM, no PO_4^{3-} was detected. pH varied between 7.3 and 8.2.

Soil micro-catchments

In contrast to MM and TM, concentrations of all ions recorded at SM1 and SM2 sites were characterized by a steady increase during the ablation season without any sudden changes as described above (the exception was Si in 2009 which will be discussed

below). No PO_4^{3-} was detected at either sites and pH values (were similar and varied between 6.1 and 8.3 (SM1) and 7.7 – 8.1 (SM2). Low pH values (< 7.7) at SM1, representing snowmelt, were recorded at the end of June 2009. Despite the similarities in temporal pattern of solute acquisition, differences in the solute concentrations were observed between the two soil micro-catchments. Therefore, concentrations of ions at SM1 were markedly higher than at SM2. For example, the concentrations of Si in 2010 were the highest observed in all of the micro-catchments. Also, a marked increase in Cl^- concentrations distinguished SM1 from all other micro-catchments. Such a marked and steady increase in Cl^- was a surprise to us and will be explored in detail later in the paper. Additionally, no NH_4^+ was recorded at SM1 while at SM2, similarly to TM and MM, NH_4^+ was recorded a few times during July 2010 and varied between 3 and 19 µg L^{-1}.

4.4.3 Solute yields

A comparison of solute yields from all micro-catchments and from the entire watershed (BAY) is presented in Table 3. Data for BAY was taken from Nowak & Hodson (In Press) and are used here as a basis for establishing the efficacy of solute export from the micro-catchments. The general characteristics in ion yields at all sites were similar. Therefore, HCO_3^-,*Ca^{2+} and SO_4^{2-} showed the largest yields and Si and NO_3^- the lowest (NH_4^+ is not presented). However, the magnitude of ion yields varied between the sites for reasons that are explored in the discussion. Variations between the years were also apparent, for example due to differences in snowmelt capture during our monitoring (for SM1) and the length of monitoring period (for MM).

Table 4.3 The comparison of ion yields from the micro-catchments and the whole Bayelva watershed during 2009 and 2010 ablation seasons. [1]Yields were calculated for 13 day period

Site	Year	HCO_3^-	Si	Cl^-	NO_3^-	*SO_4^{2-}	*Ca^{2+}	*Mg^{2+}	*K^+	*Na^+
						(kg km^2a^{-1})				
[1]**MM**	**2009**	922	3	19	7	443	264	71	15	24
TM		8023	46	306	21	2211	3495	833	67	48
SM1		18548	139	1667	19	2624	4412	1275	187	229
BAY		50931	149	2556	73	4321	13867	2387	404	210
MM	**2010**	24476	67	286	103	3665	4492	1566	250	266
TM		13107	82	374	58	5013	6430	1644	75	60
SM1		2444	13	183	7	831	750	241	11	3
SM2		1163	5	24	2	27	241	90	4	3
BAY		31981	91.1	686	26	2285	9108	1309	239	105

4.4.4 Stable isotopes

Variations in stable isotopes (expressed here as $\delta^{15}N$ and $\delta^{18}O$ values relative to atmospheric-N_2 and Vienna Standard Mean Ocean Water respectively) are presented in Fig. 4.7 and 4.8. A decreasing trend in $\delta^{18}O$ was observed at SM1 which was neither observed at TM nor accompanied by any trend in $\delta^{15}N$ (at either site, see Fig. 4.7).

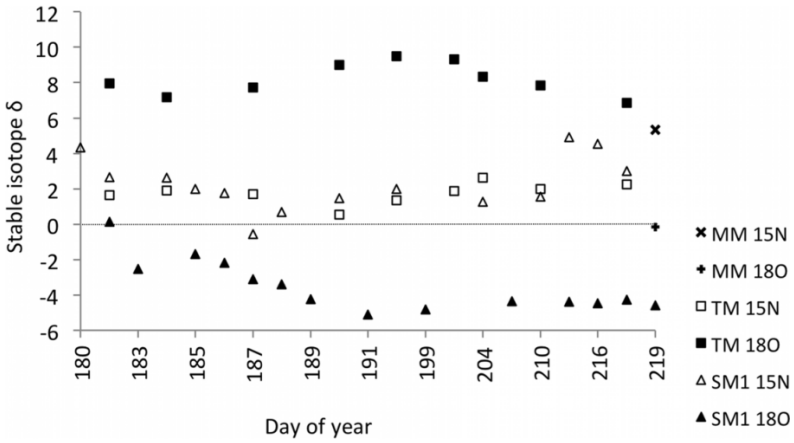

Fig. 4.7 Timeseries of stable isotopes $\delta^{15}N\text{-}NO_3^-$ and $\delta^{18}O\text{-}NO_3^-$ recorded at MM, TM, SM1 micro-catchments in 2010

Fig. 4.8 shows that the $\delta^{18}O$ values at this site were far lower than those observed in snowpack of this region, and in the BAY during early summer (the only available data being from before Day 186, when snowmelt caused high concentrations in the glacial outflow). The values at SM1 were also marginally lower than those from the other micro-catchments, although data was sparse at SM2 and MM. Interestingly, the $\delta^{18}O$ values from SM1 lay below the predicted range for microbial NO_3^- (Fig. 4.8) and estimated under the assumption that one atom of atmospheric oxygen ($\delta\ ^{18}O$ = 23.5 ‰) and two atoms of water oxygen (range used here: -15 to -6.8 ‰) are assumed to oxidise the N substrate during nitrification (Casciotti et al. 2002). For $\delta^{15}N$, the data was between -0.6 and + 6.0 ‰ at all sites except the BAY, where the range was greater (-6.0 to 3.2 ‰). Therefore the $\delta^{15}N$ values in the micro-catchments compare favourably to the range of $\delta^{15}N$ for soil organic matter and ammonium recorded by previous research in the area and used to define the range of microbial NO_3^- in Fig. 4.8.

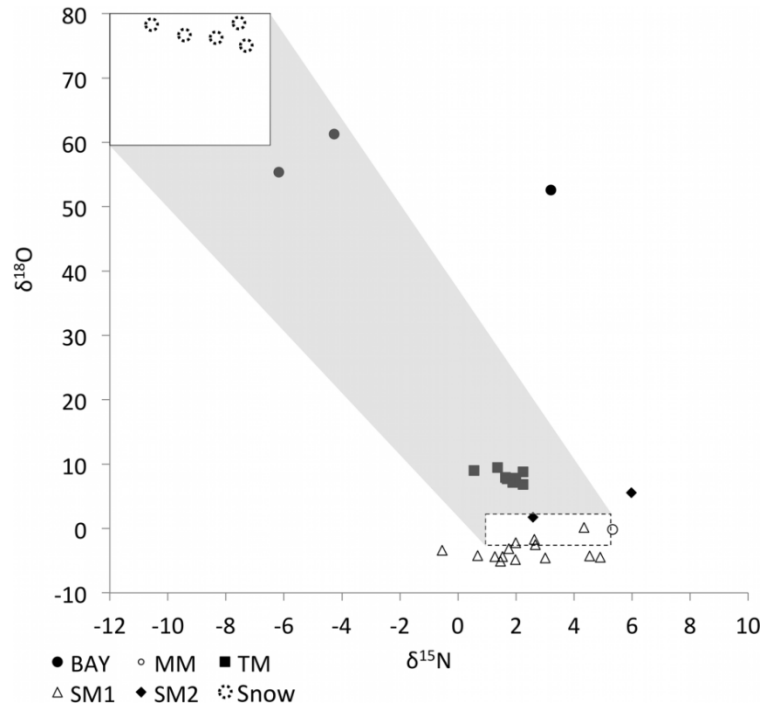

Fig. 4.8 Stable isotope results for $\delta^{15}N\text{-}NO_3^-$ and $\delta^{18}O\text{-}NO_3^-$ in the Bayelva and the micro-catchments during 2010. The solid line box represents the range of values for snow in the general study area as reviewed whilst the open circles represent snowpack samples from 2010 (after Ansari et al. 2013). The hatched rectangle is the range of "microbial NO_3^-" values estimated by assuming the nitrification of soil organic N or snowpack NH_4^+ with minimal fractionation (Eqn 1 in Ansari et al. 2013) and input ranges of $\delta^{18}O\text{-}H_2O$ (-15 to -6.8 ‰) and $\delta^{15}N\text{-}NO_3^-$ (1.2 to + 5.2 ‰) derived for local soils (Tye & Heaton 2007), ground ice (Budantseva et al. 2012) and non-ornithogenic, marine-derived soils (see discussion in Yuan et al. 2010). The grey shaded area is the hypothetical zone for mixed NO_3^- derived from the atmospheric and microbial sources

4.5 DISCUSSION

Here we focus on comparing solute acquisition and their transfer dynamics in the different micro-catchments using chemical weathering reactions that are already widely described in the literature (e.g. Tranter et al. 1993; Tranter et al. 1996; Anderson et al. 1997; Hodgkins et al. 1998; Brown 2002; Hodson et al. 2005). To establish the broad categories of chemical weathering processes we employ the statistical approach described by Nowak & Hodson (In Press) and Wadham et al. (2010). In so doing, a set of regression models between the solutes was produced and presented in Table 4.4. Scatterplots in Fig. 4.9 show the data used to define those models as well as the corresponding associations for main glacial meltwater channel (BAY).

4.5.1 Temporal and spatial changes in solute acquisition

Moraine micro-catchment

Two groups: *early* (pre-snowmelt, before days 217 in 2009 and 211 in 2010) and *late season* (post-snowmelt, after the above days) were distinguishable in the MM dataset (Fig. 4.5). Meltwater chemistry during the *early season* was dominated by carbonate carbonation (similarly to BAY). However, regression models presented in Table 4.4 indicated that other processes of ion acquisition were also operating in the environment. Those were most likely dissolution of gypsum/anhydrite as well as dissolution of carbonate and silicate minerals coupled to sulphide oxidation. Moreover, it is probable that weathering of dust supplied from the melting snowpack contributed to the initial ion concentration (see Tranter et al. 1996).

As the season progressed a marked change in solute acquisition was observed. Carbonate carbonation was no longer a major process supplying the ions. Instead, dissolution of gypsum was much more pronounced and accompanied by silicate dissolution coupled to sulphide oxidation (see also Fig 4.5a,b). A further interesting artefact of the silicate mineral weathering was revealed by *Model 8* (Table 4.4), where increase in slope during the *late season* indicated additional source of $*K^+$. We interpret this as a sign of K-feldspar weathering in the ice cored moraines which became an increasingly important source of base flow, due largely to the development of their active layer and the demise of the snow pack. A distinct feature of the moraines was the presence of fine, comminuted red sandstones transported down glacier from the southern part of the watershed. This feature was not present in any of the other micro-catchments and thus most likely explains why the concentrations of $*K^+$ were greatest here. Lastly, (unlike in BAY) *Models 6* and *7* (Table 4.4) suggested that NO_3^- production was concomitant with sulphide oxidation and silicate weathering. A case is therefore made for nitrification in the discussion below, when the isotope data are examined.

Table 4.4 The regression models between the aqueous products of well-known weathering processes recorded at various micro-catchments in the Bayelva watershed during 2009 and 2010 ablation seasons. R^2 values indicate the importance of the weathering process while slopes and intercepts indicate respectively stoichiometry of different weathering reactions and whether alternative mechanism(s) of chemical weathering supply any given solute

Site	Regression model	1	2	3	4	5	6	7	8	9
	X vs Y	HCO_3^- vs $*Ca^{2+}+*Mg^{2+}$	$*Mg^{2+}$ Vs $*Ca^{2+}$	$*Mg^{2+}$ vs $*SO_4^{2-}$	HCO_3^- vs $*SO_4^{2-}$	$*SO_4^{2-}$ vs $*Ca^{2+}$	$*SO_4^{2-}$ vs NO_3^-	Si vs NO_3^-	Si vs $*K^+$	Si vs $*SO_4^{2-}$
		($\mu Eq\ L^{-1}$)						($\mu mol\ L^{-1}$)		
SM1	R^2	0.96	0.97	0.90	0.73	0.80	0.54	086	0.62	0.60
	Slope	1.28±0.03	2.07±0.04	1.16±0.05	0.30±0.02	2.32±0.13	0.03±0.003	0.59±0.03	0.52±0.05	8.27±0.79
	Intercept	144±64.6	-81.6±41.3	48.9±35.7	141±44.9	83.1±103	-9.70±2.40	-7.22±0.97	4.97±1.40	135±23.8
SM2	R^2	1.00	0.36	0.54	0.83	0.83	0.85	0.75	0.57	0.85
	Slope	1.13±0.02	0.93±0.33	2.66±0.66	0.12±0.02	5.11±0.63	0.07±0.01	0.31±0.05	0.16±0.04	2.29±0.26
	Intercept	-161±32.7	586±229	474±57.8	-148±27.8	827±55.0	-1.98±0.64	-3.63±1.12	3.30±1.03	-11.7±6.01
TM early season	R^2	0.76	0.88	0.93	0.38	0.78	0.78	0.44	0.29	0.62
	Slope	1.73±0.16	2.23±0.14	0.48±0.02	0.74±0.16	1.04±0.09	0.01±0.001	0.64±0.12	0.94±0.25	60.0±7.99
	Intercept	-596±232	114±78.8	316±13.2	-593±229	828±55.3	0.85±0.30	-3.87±1.39	-0.51±2.85	-451±90.9
TM late season	R^2	0.09	0.37	0.23	0.05	0.81	0.01	0.92	0.46	0.04
	Slope	0.61±0.66	2.04±0.88	0.12±0.08	-0.45±0.65	0.76±0.12	-0.001±0.004	0.62±0.06	0.38±0.14	-5.51±9.14
	Intercept	3047±1205	199±1146	1017±176	3180±1200	1059±291	14.3±9.00	-3.57±1.52	14.6±3.33	1308±222
MM early season	R^2	1.00	0.98	0.97	0.92	0.91	0.95	0.81	0.69	0.85
	Slope	1.41±0.01	1.71±0.05	1.01±0.04	0.48±0.03	1.70±0.11	0.01±0.001	0.58±0.06	1.76±0.25	20.4±1.85
	Intercept	-16.4±13.1	251±26.2	92.1±16.7	-162±33.2	416±47.6	0.64±0.29	-1.89±0.78	1.78±3.24	-88.5±23.7
MM late season	R^2	0.78	0.99	0.99	0.67	0.98	0.97	0.90	0.98	0.95
	Slope	5.23±1.61	1.82±0.10	0.56±0.03	2.90±1.19	1.09±0.10	0.014±0.001	1.38±0.23	3.45±0.22	54.4±7.19
	Intercept	-1594±1163	343±81.5	111±27.0	-1160±859	520±104	-1.76±1.58	-9.52±3.92	-8.91±3.87	-336±110

Table 4.4 Continues on the next page

Table 4.4 Continued

Model 1. Establishes stoichiometry of carbonate weathering. For example, slope close to 1 indicates carbonation, while close to 2 indicates dissolution. However, additional sources of ions (in this case $*Ca^{2+}$ + $*Mg^{2+}$) can sometimes significantly increase the slope. Furthermore, an uptake of ions (for example creation of secondary mineral like gypsum) can decrease the slope. The judgment on which reaction is taking place depends on comparison to other regression models, catchment geology and chemical weathering kinetics. Significant, positive intercepts indicate that other processes are responsible for acquisition of ion(s) placed on *Y* axis, in this case $*Ca^{2+}$ + $*Mg^{2+}$ such as silicate weathering or gypsum/anhydrite dissolution, while significant negative intercepts indicate an additional source of ion(s) on *X* axis, in this case HCO_3^-

Model 2. Establishes relative importance of dolomite as a carbonate source of $*Mg^{2+}$

Model 3. Establishes importance of sulphide oxidation as a driver of the $*Mg^{2+}$sources presented above

Model 4 and ***Model 5.*** Establishes importance of sulphide oxidation coupled to carbonate dissolution, resulting in a slope close to 1. Large intercept identifies other processes nfluencing $*SO_4^{2-}$ concentrations such as gypsum/anhydrite dissolution

Model 6. Establishes relationship between NO_3^- production and $*SO_4^{2-}$ production, which are both largely assumed to be microbially-mediated

Model 7. Establishes relationship between NO_3^- production and longer residence time flowpaths conducive to silicate weathering, or uptake of both solutes during diatom blooms

Model 8. Establish stoichiometries of silicate weathering and/or relative importance of K-feldspars

Model 9. Establishes importance of sulphide oxidation as a driver of silicate weathering

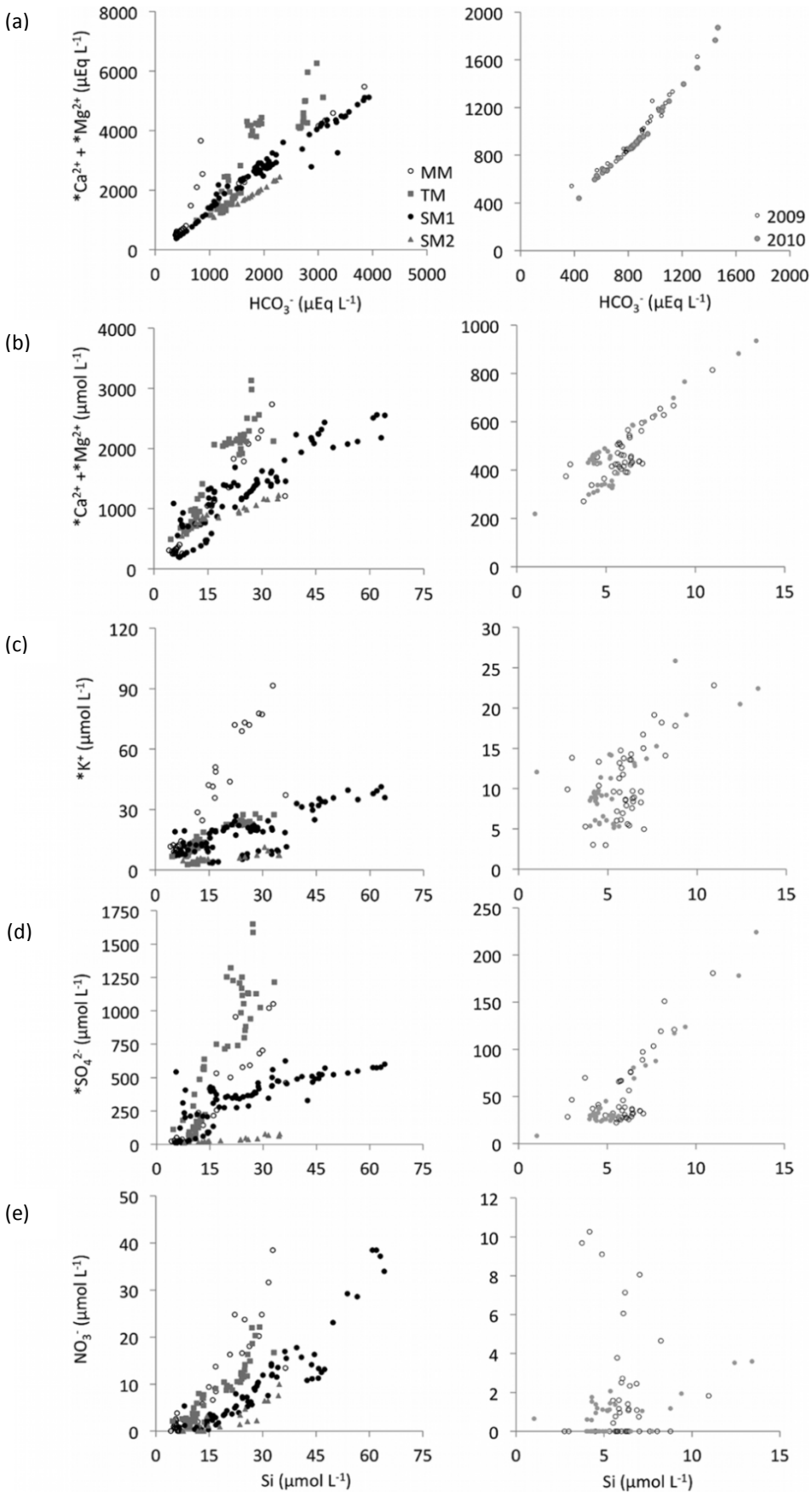

Fig. 4.9 The comparison of relationships between ions recorded at MM, TM, SM1, SM2 (left hand side) to those recorded at BAY (right hand side) during the 2009 and 2010 ablation seasons

Talus micro-catchment

Samples collected at TM were also divided into *early* and *late season* groups following the same justification as for MM. However, in contrast to MM and BAY, during the *early season*, carbonate carbonation was much less pronounced and the higher proportion of ions was also supplied by gypsum/anhydrite dissolution accompanied by a weak signal from silicate weathering. Interestingly, Fig. 4.5a,c clearly shows a distinct switch in chemical weathering between *early* and *late seasons* when ions were no longer acquired by carbonate carbonation at all, and the major reaction was gypsum/anhydrite dissolution. Considering the similarity in geological settings of both TM and MM, such a change in ion acquisition between those sites may be the result of different geomorphological characteristics (i.e. the presence of rock glacier and patterned ground at TM) and/or landscape maturity. Furthermore, *Model 7* (Table 4.4) and Fig. 4.9 indicated more pronounced nitrification than at MM, also resulting in greater nitrate flux (2009).

Soil micro-catchments

In contrast to both MM and TM, no marked change in solute concentrations were recorded on Days 217 (2009) and 211 (2010) at SM1 and SM2. Instead a steady increase of ions was captured from almost the beginning until the end of ablation seasons. In 2010, this was a consequence of post-snowmelt sampling and therefore, the results demonstrate only the chemistry typical of *late season*. However, sampling at SM1 in 2009 was undertaken throughout the whole ablation season, so the lack of the sudden transition in solute acquisition observed at TM and MM requires further explanation. We believe this was most likely related to the influences of runoff regime, geomorphology and biological activity. For example, in contrast to other sites, the SM1 stream collects water only very slowly from the surrounding low relief hill slopes. Consequently, water slowly draining through tundra soils caused increased the residence time and therefore enhanced solute acquisition for much of the observation period. Field observations showed that SM1 had the highest soil moisture (data not shown) of all the micro-catchments, with many fully saturated, expansive areas near the channel that maintained water saturation well into August (Fig. 4.4).

A decline in Si concentrations around Day 200 in 2009 coincided with a significant drop in concentrations of NO_3^-, a fall in water discharge (to $6x10^{-4}$ m^3 sec^{-1}) and an increase in water temperature to above 7^oC (data not shown). We believe this was linked to a diatom bloom at SM1 that was not observed at all the other micro-catchments where

faster-flowing drainage and lower water temperatures were unlikely to support such a phenomenon. After recovery from uptake by diatoms, temporal changes in Si acquisition recorded at SM1 mimicked those at TM and MM and thus reflected the transition from the *early to late season.*

The processes of ion acquisition also differed between SM1 and SM2 (Table 4.4, Fig. 4.5 and 4.9). At SM1, the main reaction supplying ions was calcite carbonation, whilst carbonation of dolomite also occurred at SM2, reflecting the geological heterogeneity of the watershed. Furthermore, the difference was also noticeable in the intensity of sulphide oxidation that was accompanied by almost stoichiometric silicate weathering (uncharacteristic for glacial meltwaters, e.g. at BAY; see Hodson et al. 2002). Both sulphide oxidation and silicate weathering were more pronounced at SM2 according to the slope values of regression *Model 9* (Table 4.4), in spite of lower concentrations than at SM1.

Lastly, a marked *late season* increase in Cl^- concentrations during both ablation seasons was unique to SM1. This cannot be attributed to the elution of snow because the snowpack retreated from this part of the catchment first and there were no persistent snowbanks. Marine aerosol inputs of Cl^- caused by high winds and evaporation effects were not responsible for such increase because these processes should have influenced streams across the entire proglacial area. Nor could the Cl^- inputs be attributed to rock weathering, as the geological conditions are not favourable and simple laboratory dissolution reactions using 10 g L^{-1} suspensions of freshly milled rock in deionised water showed no significant increase in Cl^- concentrations with time (Hodson, Unpublished Data). It should be noted however, that SM1 is the only micro-catchment that lies entirely within the former marine limits. For example, marine bivalve shells are abundant in the active layer (field observation; see also Fig. 4.10), and so we attribute the Cl^- increase to the release of marine salts from the permafrost of this former sea bed. The mobility of Cl^- is such that it may be rapidly leached into the stream as the active layer deepens, making its seasonal concentration increase a potentially sensitive indicator of marine permafrost degradation in low elevation catchments such as SM1.

Fig. 4.10 Bivalves in the uplifted marine sediments at SM1. Photo credit: A. Nowak

4.5.2 The fingerprint of microbial activity in the micro-catchments

The use of correlations between Si, NO_3^- and $*SO_4^{2-}$ to detect microbial activity in the micro-catchments (Table 4.4) was further supported by the $\delta^{15}N$ and $\delta^{18}O$ values for NO_3^- due to their proximity to the predicted range of microbial nitrate (Fig. 4.7 and 4.8). However, at TM, the $\delta^{18}O$ values were higher than the microbial NO_3^- range, implying a little more snowpack-derived NO_3^- was present (in agreement with the observed persistence of snow cover in the TM watershed). Further, low $\delta^{18}O$ values in SM1 NO_3^- show that nitrification was effective throughout the entire summer. This was surprising, because it was expected that assimilation of NO_3^- by vegetation would suppress the nitrification signal in runoff until senescence occurred (Tye et al. 2008). In addition, the $\delta^{18}O$ values in SM1 NO_3^- were in fact lower than the predicted range of microbial NO_3^-, as was observed by Tye et al. (2008) just outside the Bayelva watershed. In Casciotti et al's (2010) experimental study of oxygen isotope systematics during NH_4^+ oxidation, both fractionation and isotope exchange effects are plausible explanations for such low values. The most robust interpretation of the present study is therefore that nitrification dominates the production of the NO_3^- that is flushed from the SM1 micro-catchment by runoff very soon after the removal of the snowpack. The data from SM2 and MM, although sparse, also suggest that nitrification is important in these other micro-catchments, whilst the marginally higher values for the TM suggest that a small proportion of atmospheric NO_3^- also enters the system from the high elevation snow that is present here.

4.5.3 Productivity of the micro-catchments versus solute export from the watershed

The important differences in solute dynamics in the landscape units represented by the various micro-catchments are easily noticeable (e.g. in Fig. 4.5 and 4.9, Table 4.4), yet they are almost impossible to establish from measurements conducted at BAY (Nowak & Hodson 2013) and have not yet been detected in other watershed scale studies in Svalbard. For example, the average concentrations of ions recorded at BAY were up to two (HCO_3^-, $*Ca^{2+}$ + $*Mg^{2+}$), four (Si), seven (NO_{3-}) and ten times ($*SO_4^{2-}$) lower than those recorded at the micro-catchments (Fig. 4.9), because the water flux through Bayelva was almost two orders of magnitude greater and therefore significantly diluted by icemelt.

Water flux has a first order control over solute yields (Anderson et al. 1997) as is evident in their inter-annual variability (Table 4.3). The area-weighted solute yields of the micro-catchments were therefore used to see how they influence the solute flux from the entire watershed. In so doing, the different micro-catchments were assumed to be representative of the total moraine (area 3.06 km^2), talus (6.72 km^2) and tundra soils (4.18 km^2, 22% of which was similar to SM1 and 78% to SM2) in the deglacierized area (areas according to www.svalbardkartet.npolar.no, 2013). The solute yields for 2010 (Table 4.3) were then multiplied by the representative areas to estimate the solute fluxes from each landscape unit. Fig. 4.11 shows the combined solute fluxes expressed as a proportion of the total watershed solute flux at BAY.

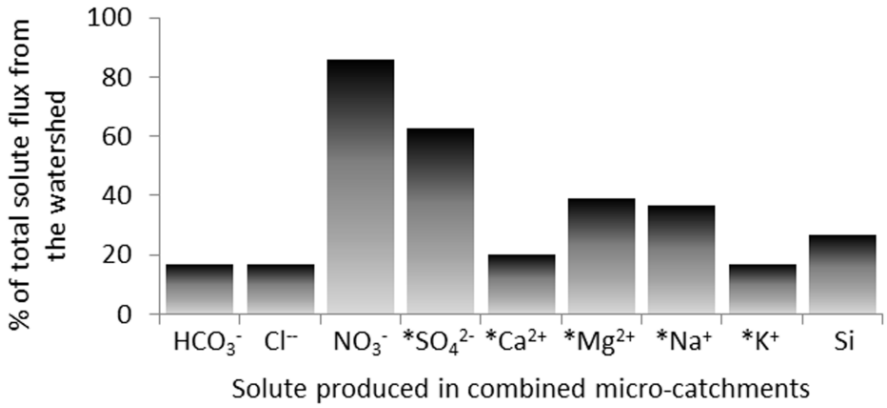

Fig. 4.11 Solute flux from combined micro-catchments expressed as a proportion of the total watershed solute flux measured at the BAY in 2010

As expected, the up-scaled solute fluxes from the aggregated micro-catchments never accounted for 100% of the solute flux due to missing terms in the balance calculations, namely large solute flux associated with the glacial inputs (not monitored in this study; see Nowak & Hodson In Press) and error (ca. 15 – 25% for each flux estimates following Hodson et al. 2005). For example, the sum of micro-catchments accounted for just 17% of the Cl^- flux during 2010, indicating a significant input from snowmelt. Hodson et al. 2005 have shown that the Cl^- budget for the watershed is easily "closed" by accounting for snowmelt in this case using the 1999 and 2000 dataset and applying it to the entire watershed (BAY). We confirmed that the glacial input could easily account for the difference in other hydrological years after estimating the product of summer melting (using glacier mass balance data) and average Cl^- concentrations reported in supraglacial streams at this site (1.23 mg L^{-1} Hodson et al. 2002). However, the same closure in the solute budgets could not be achieved with the other ions, especially with respect to those derived from carbonate and silicate weathering. Nor could error analysis account for the different solute budget calculations for these ions, since they would require changes in the mean composition of micro-catchment streams that were unacceptable when compared to the range of values reported by earlier work (Hodson, 1994 and Hodson et al. 2002). The "missing" HCO_3^-, Ca^{2+}, Mg^{2+}, K^+ and Si were therefore acquired by glacial meltwaters from paraglacial fine sediment weathering (c.f. Fairchild et al., 1999) and shallow groundwater exchange, most likely in the hyporheic zone of the floodplain. This is also supported by the resent work presented in Nowak & Hodson (In Press) where it is shown that even a watershed accommodating cold-based glaciers and underlain by continuous permafrost has significant chemical weathering potential due to the presence of fresh fine reactive sediments released by the retreat of the glacier and rock-water contact at a range of time scales. Furthermore, the study also indicates the importance of the hyporheic zone in generation of solutes. This was also explored in front of Antarctic cold-based glaciers of the McMurdo Dry Valleys where only glacial inputs of water to the glacier forefield are present (see Gooseff et al. 2013). Further research involving direct instrumentation and sampling of the proglacial sandur environment is therefore essential in order to better understand landscape solute fluxes during deglaciation.

The comparison of the solute flux from the entire watershed and the micro-catchments resulted in an unexpected discovery. Unlike crustally derived solutes described above, the aggregated micro-catchment flux estimates for NO_3^- and $*SO_4^{2-}$ represented more than 80% and 60% of the observed riverine flux at BAY, most of which was derived from

moraine and talus environments. This shows the importance of the microbial processes in these low water flux components of deglacierized part of the watershed.

Our study also shows for the first time that elevated concentrations of Cl^- can be used as a signal to record the biogeochemical consequences of melting permafrost of marine origin. This indicates that the legacy of glaciation is still strongly apparent through the impact upon sea level change and the slow, gradual release of marine solutes from parts of the landscape uplifted since the end of the last glacial maximum.

4.6 CONCLUSIONS

Our novel study of moraine, talus and soil micro-catchments within High Arctic watershed helps to understand landscape biogeochemical evolution following deglaciation and permafrost change. It also sheds light on how those environments contribute to solute export from the entire watershed and into the downstream marine ecosystem.

We show that seasonality in chemical weathering is strongest at sites where drainage is rapid and not restricted. Solute dynamics in different micro-catchments are also sensitive to other abiotic factors such as runoff volume, water temperature, geology, geomorphological controls upon hydrological flowpaths and landscape evolution following sea level and glacial changes.

Biotic factors influence the anionic composition of micro-catchment runoff via microbial $*SO_4^{2-}$ and NO_3^- production that is responsible for as much as 60 and 80 % (respectively) of the total $*SO_4^{2-}$ and NO_3^- fluxes from the entire watershed.

Young environments nearest to the retreating glacier are characterized by high yields of solutes such as $*Ca^{2+}$, HCO_3^-, $*Mg^{2+}$ and $*SO_4^{2-}$ due to the presence of fine reactive sediments. Those also provide an environment for microbially mediated chemical weathering reactions and the production of nutrients such as NO_3^-. Interestingly, nitrification is occurring with similar intensity at all micro-catchments, regardless landscape maturity. However, in younger environments, nutrients fluxes are larger and therefore can have a bigger effect on downstream marine ecosystem.

We also find that the change in permafrost has the most noticeable effect in the marine sediments uplifted since the last glacial maximum, which are now subjected to erosion,

chemical weathering and ground thaw and influence the levels of marine derived ions such as Cl^-.

Lastly, the comparison between the micro-catchments and solute fluxes exported from the entire watershed into High Arctic fjord indicates that, despite large $*SO_4^{2-}$ and NO_3^- yields from the aforementioned micro-catchments, a "glacial signal" dominates solute export from the watershed via a combination of quick weathering reactions of fine reactive sediments at the glacier terminus, rapid in-stream weathering of suspended sediments and processes occurring in the hyporheic zones of the floodplain.

Therefore, although climatically driven change in the proglacial area such as deepening of the active layer and melting of the permafrost has an influence on local ecosystems, the biogeochemical signal from the entire watershed (solute fluxes entering marine environment) is dominated by glacially derived products of rapid chemical weathering. Consequently only a study of micro-catchments existing within the watershed can uncover the landscape response to contemporary climate change.

CHAPTER FIVE:

CONCLUDING REMARKS

5.1 INTRODUCTION

This section summarises the work described in each chapter before presenting the key outcomes with respect to the objectives in Section 5.2 and suggestions for further research in Section 5.3.

This thesis utilizes meteorological, hydrological, mass balance and biogeochemical datasets based on respectively 35, 22, 43 and five years of monitoring in the Bayelva catchment (Svalbard) to advance our understanding of the response of a High Arctic glacierized watershed to the climate change. In addition, datasets collected from moraine, talus and soil micro-catchments during two consecutive ablation seasons, are used to reveal hydrological and biogeochemical processes occurring in those distinct environments that represent various stages of landscape transformation after glacier retreat. It is the first study to use such an extensive dataset to provide the knowledge on climatically driven changes in this harsh yet extremely vulnerable environment.

The introductory Chapter One presented the general conditions, trends and drivers in the Northern Hemisphere Arctic climate. The chapter discussed the importance and influence of atmospheric and oceanic circulations, the state of permafrost and general terrestrial responses to climatic changes. In so doing it was revealed how West Spitsbergen is an early warning site for Arctic coastal warming on account of its proximity to the Fram Straight, a crucial pathway for heat advection into the Arctic Basin. The state of Svalbard's cryosphere was then described, including glacier mass balance trends and permafrost changes, before introducing the hydrological and biogeochemical changes that follow glacier recession. The responses of both terrestrial and marine environments were also discussed. Emphasis was also given to how climate influences glacier thermal regime and how this in turn might affects watershed hydrology and geochemistry.

Thereafter, the chapter presented key study site details for the Bayelva watershed, where the study was undertaken. This was followed by an introduction to methodology used to quantify hydrological and biogeochemical changes within the watershed.

In Chapter Two close attention was given to the long term hydrological response of the Bayelva catchment to changing climate. Therefore, hydrological datasets collected over 22 years of Bayelva runoff monitoring were merged with meteorological data collected over 35 years from nearby Ny-Ålesund and glacier mass-balance monitoring from Austre Brøggerbreen that have been performed since 1969. Their integration was used to create an optimised water balance model for the Bayelva and to present a long term

water balance timeseries for analysis. In addition, an investigation of precipitation records was performed to uncover trends in climate, discover climatically driven changes in watershed hydrology and explain any water balance residuals that emerged when the time series were created.

In Chapter Three, an investigation of meltwater chemistry from the Bayelva main river over a 20 year period was performed. Particular emphasis was given to the thermal regime switch from polythermal to cold-based glaciation at Austre Brøggerbreen, a change that most likely occurred just prior to the 1990's. Old datasets collected by other scientists working in the Bayelva watershed from 1991 onwards were merged with new data collected by the author. Chemical analyses of water samples were used to depict changes in meltwater characteristics. Furthermore, this approach allowed recognition of various chemical weathering processes that occurred between the glacier margin and the fjord. Once identified the processes were used to indicate changes in solute acquisition in response to climatic forcing and glacial retreat.

Chapter Four was dedicated to the proglacial and paraglacial areas of the watershed. An investigation of hydrology and biogeochemistry in moraine, talus and soil micro-catchments was performed during two consecutive summers. Meteorological datasets were used to identify any climatic driven changes in micro-catchment hydrology. The spatial and temporal changes in water quantity and quality were used to depict solute cycling in the watershed and identify any signals from landscape maturation that follow deglaciation.

5.2 KEY OUTCOMES

5.2.1 Objective 1

A sensitivity study of the precipitation gradient with elevation identified an optimum value of 19 % (increase) in snowfall or rainfall per 100 m change in elevation. The modelling work first predicted annual river discharge volume, and was then used to produce a complete annual water balance for the period 1974/75 - 2009/10. In so doing, this study identified several crucial factors for accurate calculation of water balance. These are:

1. precipitation from June until September and all rainfall events responsible for early or late flow need to be carefully assigned to the correct hydrological year

because they can be quantitatively important;

2. a precipitation gradient correction of 19% per 100 m (for rain and snow) in addition to the catch correction (1.15 for rain and 1.65 for snow) must be applied;
3. glacier mass balance data are required for both snow accumulation and icemelt runoff in the upper part of the watershed;
4. water storage/release from ground icings in the active layer need to be assigned to the correct hydrological year and cannot be assumed negligible.

From this it was shown that hydrological changes within Bayelva watershed are most noticeable within the last 10 years, when winters have become warmer and wetter. The change is most significant during the shoulder months, especially September, when the transition from summer ablation to winter accumulation is taking place. Winter rainfalls, when extreme, produce ground icings and runoff outside the summer period. Dependent upon summer air temperatures, these icings may either melt and produce additional runoff, or persist until the following hydrological year. If the rate of the warming persists, more rain on snow events are expected, therefore more frequent icing formation and early/late river discharge events will be recorded.

These processes have a direct influence upon the water budget. They represent sources of error for water-balance calculations that either ignore winter runoff events and/or assume water storage is negligible. This study therefore shows that even when the watershed is underlain by permafrost and accommodates cold-based glaciers, storage can no longer be ignored.

Another finding is that despite sustained glacier retreat, annual runoff volume showed no trend during 1989 - 2010. Discharge was more variable and longer during the last decade due to the winter rainfalls. Changes in river discharge were driven by higher temperatures at the beginning of the ablation season, influencing timing of snowmelt, and by rainfall at the end when all the snow has melted and glacier melting is greatly reduced by low solar radiation and air temperature. Changes during September were also found to be important because they influence precipitation form and thus the timing of the transition from glacier ablation to accumulation. End of season rainfall was also found to have the capacity to offset any reduction in flow that might be caused by continued glacier shrinkage.

Finally, flow recession analyses revealed increasingly efficient evacuation of meltwater through the major channels within the catchment and the increasing occurrence of a

delayed flowpath through the glaciers' forefield. Therefore changes in both the water budget and the hydrograph form indicate the potential for changing rock-water contact dynamics, because they most likely occurred in the geochemically reactive active layer of the glacier forefield.

5.2.2 Objective 2

A long-term meltwater hydrochemistry dataset gave insights into the hydrochemical response of a glacierized watershed whose glaciers underwent their transition from a polythermal-based to a cold-based thermal regime. Earlier work in Svalbard has given much emphasis to the importance of subglacial rock-water contact as a source of solute to runoff and so, the loss of such processes as a consequence of the thermal regime change were explored.

The study indicates that on a long term scale, chemical weathering processes responsible for ion acquisition didn't change but became more productive. Due to the availability of fresh reactive sediments, the most chemically active part of the watershed was the glacier forefield. Such an environment makes high rates of weathering possible, even when ice losses have caused a switch to cold-based conditions with no delayed subglacial drainage flowpaths.

The release of sediments from the immediate glacier terminus and the further deposition of these fine sediments downstream from the ice margin also means that chemical weathering can be influenced for some time. Additionally, drainage system reorganization events are likely and can result in significant pCO_2 depletion in an otherwise high pCO_2 system. This further emphasises the importance of rock-water contact involving freshly exposed, reactive sediments at the immediate glacier margin, because the reorganisation was caused by ice retreat and the rapid erosion of a new flowpath at the immediate ice margin. As a consequence, a significant increase in annual crustal ion yields was observed, even in the following ablation season. The "flush" of crustally-derived ions can be meaningful for downstream terrestrial and marine ecosystems because the channel changes observed in the present study frequently occur in other glacierized watersheds. Therefore the study finds that the efficacy of chemical weathering in cold-based glacier basins can be readily compared to that observed in polythermal glacier basins where subglacial rock-water contact is important. The study also indicated that the end of ablation season meltwater chemistry is

characterized by reactions similar to those of subglacial environments, in spite of their absence in the watershed. They occur wherever long water residence times are present in the system, for example within the active layer, glacier moraines and the hyporheic zone of the proglacial floodplain.

In the light of the above, the following findings are pertinent:

1. long term/multiannual measurements are necessary for the accurate predictions of the hydrochemical response of a glacierized catchment to climate change, because significant perturbations may occur (e.g. channel change) that enhance solute fluxes for more than one ablation season;
2. during glacier retreat, the immediate vicinity of a cold-based glacier is the most chemically reactive part of the watershed;
3. the end of season chemical weathering makes an important contribution to solute concentrations via microbially mediated reactions such as sulphide oxidation, carbonate and silicate weathering and microbial production. Concentrated waters produced at the end of ablation season can be flushed out by the end of season rainfalls that, as the results from Objective 1 show, are occurring more frequently and might even be stored within the active layer until the next ablation season;
4. major reorganisations of the drainage system are typical as a result of glacier retreat and can occur suddenly, resulting in an "annual flush" of crustally-derived ions that is responsible for significant pCO_2 depletion in an otherwise high pCO_2 system;
5. although this enhanced geochemical weathering appears to be short-lived, its prolonged contribution to increased annual solute fluxes for shows that it can be significant for downstream terrestrial and marine ecosystems.

5.2.3 Objective 3

The study of moraine, talus and soil micro-catchments within the Bayelva watershed helped to develop an understanding of landscape biogeochemical evolution following deglaciation and permafrost change. Solute dynamics in different micro-catchments were found to be sensitive to abiotic factors such as runoff volume, water temperature, geology, geomorphological controls upon hydrological flowpaths, and landscape evolution following sea level and glacial changes. Young environments nearest to the retreating glacier were characterized by higher solute yields due to the presence of

reactive sediments. They were also found provide an environment for microbially mediated chemical weathering reactions and the production of NO_3^- and SO_4^{2-}, which became increasingly apparent throughout the summer season. Interestingly, nitrification appeared to be occurring with similar intensity in all micro-catchments, regardless landscape maturity. In younger environments, nutrients fluxes were larger and therefore had a bigger effect on downstream ecosystems. This most likely reflects the effect of residual ground ice or buried glacier ice.

Furthermore, changing permafrost had the most noticeable effect upon biogeochemistry in the lower part of the watershed, where former marine sediments have been uplifted since the last glacial maximum and are now subjected to erosion, chemical weathering and ground thaw. This was detectable through its influence upon levels of marine derived ions such as Cl^- during the latter half of the summer.

Despite large solute yields from the aforementioned micro-catchments, the "glacial signal" still seems to dominate solute export from the entire watershed via a combination of quick weathering reactions of fine reactive sediments at the glacier terminus, rapid in-stream weathering of suspended sediments and hyphoreic geochemical processes in the floodplain. Therefore, although climatically driven change in the proglacial area such as deepening of the AL and melting of the permafrost has an influence on local ecosystems, the signal from the entire watershed (solute fluxes entering marine environment) is largely dominated by glacially derived products of rapid chemical weathering. The exception is NO_3^- that is produced by nitrification at deglacierized parts of the watershed, whose signal is of sufficient strength to overcome that from the glacier and the floodplain. Consequently only a study of micro-catchments existing within the watershed can uncover the landscape response to contemporary climate change if a rapidly retreating glacier is present.

5.3 SUGESTIONS FOR FURTHER RESEARCH

This thesis has advanced the understanding how glacierized High Arctic watersheds respond to climate change by linking meteorological, hydrological and biogeochemical measurements.

Thanks to the above approach, as well as the extensive datasets that were available for analysis, the following knowledge gaps can be identified and are therefore presented here as profitable avenues for future research.

5.3.1 Improved water-balance modelling

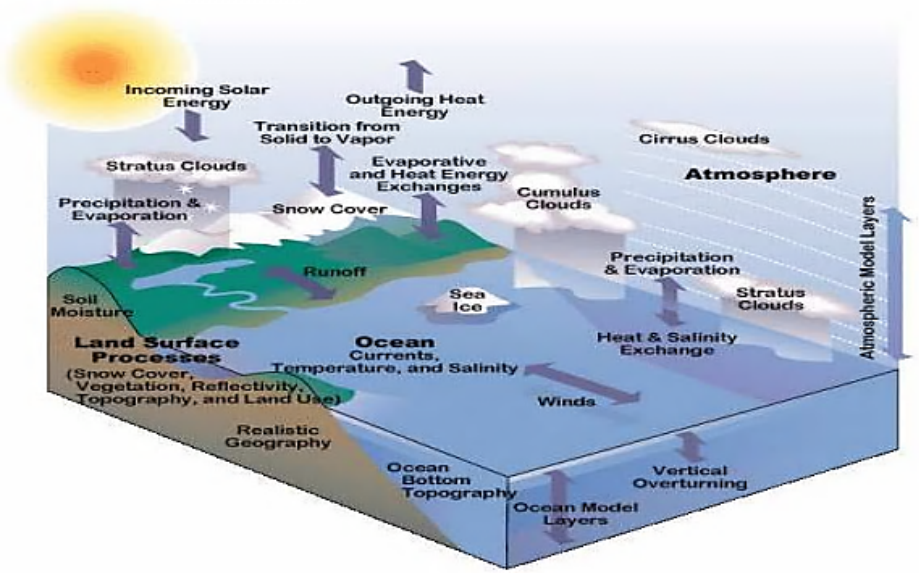

Plate 6 Major factors influencing water balance modelling. After Döscher 2010

Watershed hydrological and hydrochemical modelling is greatly restricted by a lack of precise precipitation data from various elevations, a failure to account for snow drifts and only very limited empirical understanding of how orographic precipitation gradients change with wind direction. Further problems include a lack of measurement of precipitation type (snow or rain) which, as shown in Chapter Two, is crucial for calculations of water balance. Also estimation of evapotranspiration suffers from a lack of data, especially on Svalbard, where the heterogeneity of the environment is substantial and uniform evaporation rates are often assumed by hydrologists. In addition, underestimating the importance of water storage within glacierized catchments has been highlighted by this work. These problems are likely to be even more significant in data-sparse areas of the Arctic, although it is particularly frustrating that they have yet to be addressed in one of the most important sites for monitoring.

While there are many pan-Arctic climate and hydrological models, their application to small scale systems is meaningless due to their coarse resolution and the fact that small scale complexity is so important in local ecosystems (e.g., Wilbanks & Kates 1999). For example, Arctic-Hype model covers 23 million km^2 with 700 km^2 resolution and 94 river mouth monitoring stations; ArcticRIMS with circa 25 km^2 resolution (www.eol.ucar.edu) or Polar MM5 with 60 km^2 resolution (Guo et al. 2003; Gutowski et al. 2003). Further, even smaller and downscaled GCM climate and hydrological models (e.g., Regional Arctic Model RCAO with circa 5 km^2 resolution) still require improvements in areas such

as albedo feedback, groundwater dynamics, and small scale runoff processes (see e.g., Fang et al. 2013). Furthermore, Leung et al. (2004) shows that some regional GCMs also suffer from poor incorporation of orographic forcing and rain-shadowing effect while others underestimate extreme events (Fowler et al. 2007).

Therefore, heterogeneity in various watersheds needs to be addressed because the variability in internal parameterization can be a source of considerable uncertainty in a model (Fowler et al. 2007). For example, the impact of heterogeneity upon active layer hydrology is crucial for understanding oxidation of permafrost carbon and its feedback to climate change. The TOPMODEL concept on sub-grid heterogeneity is therefore a popular tool for improving small scale heterogeneity of the active layer water table (Bohn et al. 2007; Zhu et al. 2013). However, at present, this protocol seems poorly equipped to forecast future changes in active layer water table dynamics because changes in the ground ice content are not accounted for. Moreover, the impact of watershed heterogeneity needs consideration with respect to freshwater inflow to fjords and the accurate prediction of its effect upon biotic (primary and secondary production) and abiotic (salinity, temperature and turbidity change) processes influencing coastal ecosystems. These are areas that contribute to the formation of Deep Atlantic Waters and therefore influence global thermohaline circulation, inducing changes in the climate. The complexity of interactions between quantity and quality of surface runoff and marine ecosystems were well presented by Dierssen et al. (2002). Although this study concerns coastal waters of Antarctic Peninsula, it can be expected that the drivers of change and the ecosystem responses will be similar in the Arctic. Examples include the adaptation of phytoplankton and zooplankton to changes in both salinity and water mixing. The complexity of the relationship between photosynthesis and meltwater inflow is well demonstrated by the fact that meltwater inflow may either enhance (via nutrient delivery) or limit (via turbidity and shading) primary production. Therefore, long term atmospheric and hydrological monitoring is crucial for accurate predictions of ecosystem change. However, on Svalbard it remains limited to only few locations.

5.3.2 Influence of surface runoff on the fjord ecosystem

The necessity for hydrological and biogeochemical monitoring due to its implications for watershed productivity emerged from the research presented in Chapters Three and Four.

Primary production in Svalbard fjords can be high in the summer, most likely when runoff maintains the delivery of essential nutrients, but to some degree it will depend on sediment loads that greatly restrict light penetration. At present, ecosystem research in West Spitsbergen fjords does not consider the role of nutrient supply by rivers during the summer, because the emphasis is given to primary production during the spring bloom of April and May (e.g., Hop et al. 2002; Hodal et al. 2012). Furthermore, studies that are carried out during summer (e.g., Piwosz et al. 2009 or Seuthe et al. 2011) point out the influence of turbidity and salinity upon primary and secondary production yet ignore the surface meltwater input and its characteristics.

However, the role of glaciers in elevating summer time nutrient levels (such as NO_3^- and Si) has been known for some time (e.g. Appolonio 1973). Furthermore, there is now compelling evidence showing that glacial dissolved organic carbon (DOC) can nourish marine bacterial production (Hood & Scott 2008). Therefore, since Fe, Si, N and P can be enhanced by river inputs to Svalbard fjord systems, studies of their role in fertilisation are long overdue. This thesis has shown that the nitrogen content of summer runoff is enhanced by nitrifying bacteria from almost all sedimentary environments. Furthermore, increased Si in the runoff from all micro-catchments, regardless of their stage of development, was also observed. The effect is most pronounced later in the summer, when nitrogen supply from snowpack is reduced and longer residence time water flowpaths are more pronounced. Additionally, Hodson et al. (2004) demonstrated that P export to the fjord is enhanced by glaciers and perhaps associated with iron III phases created by sulphide oxidation. In this work, sulphide oxidation was also found to be a major process occurring in sedimentary environments beyond the ice margin. The impact of glacial runoff upon fjord production should therefore be explored using incubation studies, perhaps isolating the effects of the nutrients from the turbidity influence upon shading and photosynthesis through the use of diffusion membranes (Westwood & Ganf 2004). The factor of salinity change should also be considered, as emphasised by Dierssen et al. (2002). Models of ablation and runoff will easily be able to provide quantitative estimates of the river inputs under a range of climate scenarios. Further, recent models show how sediment and nutrient inputs associated with the runoff can also be modelled (Fausto et al. 2012).

5.3.3 Solute dynamics – the Ice sheet perspective

Wadham et al. (2010a) used subglacial hydrochemistry data collected from several polythermal and temperate glaciers to indicate the importance of chemical weathering

in soft sediments partially driven by microbial activity. Additionally, the results were used as a proxy for chemical weathering and potential solute fluxes from the Antarctic Ice Sheet and ice streams. A similar approach was also employed for geochemical weathering by meltwaters from Northern Hemisphere ice sheets by Tranter, Huybrechts et al. (2002) and the implication of the above to ocean primary production, by supplying limiting nutrients such as iron, was explored by Raiswell et al. (2006; 2008).

The concept of using chemical weathering data from the subglacial environments of temperate glaciers as a proxy for sub-ice sheet weathering processes is therefore not new. However, when we consider deglaciation of the Barents Ice Sheet, the areas between active ice streams were more likely to have been frozen to the bed (Landvik et al. 2005), and weathering environments not unlike the conditions described at Bayelva in Chapter Three, would have been dominating at the margin.

The same conditions could apply to contemporary ice caps in North East Svalbard, Canada, parts of the Greenland Ice Sheet (GIS) and the Russian High Arctic islands eastwards from Franz Joseph land. Collectively, these dominate the ice cover of the Eurasian High Arctic and perhaps even the Northern Hemisphere (depending upon the unknown distribution of ice at the pressure melting point throughout the vast GIS). In such cases almost all of the waters are routed over the surface of the ice to reactive ice marginal sediments exposed by retreat.

It is therefore possible that polar ice sheets during deglaciation will produce solute fluxes from their cold based margins in a manner similar to the present study. Solute fluxes from ice marginal sediments will therefore join those from subglacial weathering environments of the manner described by Wadham et al. (2010a,b). However, the latter are characterised by lower water fluxes that are less likely to increase during deglaciation (because they are water fluxes controlled by the heat budget of the insulated glacier bed rather than its surface), than the ice marginal environments. For example, the assumed solute yields from Ross Ice Streams (LMR) presented in Wadham et al. (2010a), were nearly twice smaller than 2009 crustal ion yields from Bayelva because no surface melting takes place. It is reasonable to expect that weathering environments at the margin of Arctic ice caps will undergo a transition from being inactive on account of the cold basal ice at their margin, to contributing very significantly to the watershed geochemical budget during and after deglaciation. Chapter Three suggests that this transition is very sensitive to the hydrological system that is present in the young sediments. Here it was shown that water flowpath changes can occur

suddenly and result in an “annual flush” of crustally-derived ions. This placed the composition of Bayelva’s runoff between subglacial waters of polythermal glaciers such as Midre Lovénbreen (years 1991, 1992 and 2000) and Finsterwalderbreen (2009, 2010) presented by Wadham et al. (2010a). Clearly then, the efficacy of geochemical weathering at the margins of cold-based glaciers can no longer be assumed insignificant. Furthermore, Chapter Three shows that the weathering in such environments typically produces high pCO_2 solutions, resulting in significant atmospheric CO_2 sequestration only following major events that result in the reorganisation of the drainage system. Lastly, although this enhanced geochemical weathering appears to be short-lived, if considered in a large scale, it could be significant for the adjacent fiords and coastal waters.

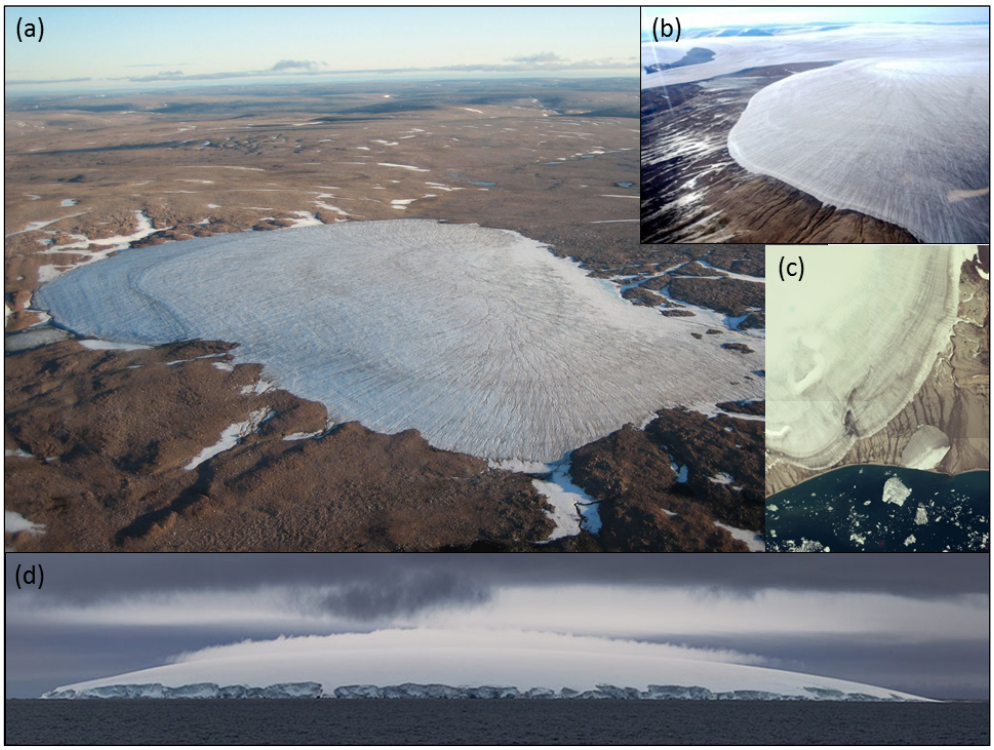

Plate 7 Examples of polar ice caps (a) Baffin Island, Canada (www.newscientist.com); (b) Lambert Land, Greenland (www.starofsophia.blogspot.co.uk); (c) Austfonna, Svalbard. (www.toposvalbard.npolar.no); (d) Storøya Island, Nordaustland, Spitsbergen. (www.mikereyfman.com)

Therefore, there is a need for an in depth study that would explore the implications of cold-based ice marginal weathering environments for regional biogeochemical cycling and land-ocean nutrient fluxes during deglaciation. Spatial extrapolation could include

data collected from other glacial catchments in Svalbard to account for different lithologies, ice conditions and meltwater fluxes. In so doing, a more representative picture of the geochemical coupling between Arctic ice sheets and the marine environment during glacial cycles would be derived.

REFERENCES

Aagaard K. & Carmack E.C. 1989. The role of sea ice and other fresh waters in the Arctic Circulation. Journal of Geophysical Research 94 (14): 1485-14498.

ACIA. 2005. Arctic Climate Impact Assessment. Cambridge University Press.

Åkerman H. 2005. Relations between slow slope processes and active-layer thickness 1972-2002, Kapp Linné , Svalbard. Norsk Geografisk Tidsskrift 59: 116-128.

AMAP. 1998. AMAP Assessment Report: Arctic Pollution Issues. Arctic Monitoring and Assessment Programme (AMAP), Oslo, Norway.

Anderson S.P., Drever J.I., Humphrey N.F. 1997. Chemical weathering in glacial environments. Geology 25 (5): 399-402.

Anderson S.P., Drever J.I., Frost C.D., Holden P. 2000. Chemical weathering in the foreland of a retreating glacier. Geochimica et Cosmochimica Acta 64 (7): 1173-89.

Anderson S.P., Dietrich W.E., Brimhall Jr. G.H. 2002.Weathering profiles, mass balance analysis, and rates of solute loss: linkages between weathering and erosion in a small, steep catchment. Geological Society of America Bulletin 114 (9): 1143–1158.

Anderson S.P. 2005. Glaciers show direct linkage between erosion rate and chemical weathering fluxes. Geomorphology 67: 47–157.

Anderson S.P. 2007. Biogeochemistry of glacial landscape systems. Annual Review of Earth and Planetary Sciences 35: 375-399.

Anisimov O.A., Vaughan D.G., Callaghan T.V., Furgal C., Marchant H., Prowse T.D., Vilhja´lmsson H., Walsh J.E. 2007. Polar regions (Arctic and Antarctic). In M.L. Parry et al. (eds.): Climate change 2007. Impacts, adaptation and vulnerability. Contribution of Working Group II to the fourth assessment report of the Intergovernmental Panel on Climate Change: 653685. Cambridge: Cambridge University Press.

Ansari A.H., Hodson A.J., Heaton T.H.E., Kaiser J., Marca-Bell A. 2013. Stable isotopic evidence for nitrification and denitrification in a High Arctic glacial ecosystem. Biogeochemistry 113: 341-357. DOI:10.1007/s10533-012-9761-9.

APHA, AWWA & WEF 1995. Standard Methods for Examination of Water and

Wastewater, 19th edition. American Public Health Association, New York.

APHA, AWWA & WEF 2005. Standard Methods for the Examination of Water and Wastewater (Method 2320 B). American Public Health Association, Washington.

Apollonio S. 1973. Glaciers and nutrients in Arctic seas. Science 180: 491-493.

Barnett T.P., Adam J.C., Lettenmaier D.P. 2005. Potential impacts of a warming climate on water availability in snow-dominated regions. Nature 438: 303-309.

Beldring S. 2009. Climate change impacts on hydrological processes in the Norwegian Arctic. Paper presented at the 17th International Northern Research Basins Symposium and Workshop. 12-18 August, Inqaluit-Pangnirtung-Kuujjuaq, Canada.

Benestad R.E. 2008. Empiricalstatistical downscaled Arctic temperature and precipitation series. Met.no Report 10/2008. Oslo: Norwegian Meteorological Institute.

Berner R.A., Lasaga A.C., Gerrels R.M. 1983. The carbonate-silicate geochemical cycle and its effect on atmospheric carbon dioxide over the past 100 million years. American Journal of Science 283: 641-683.

Berner R.A. &Lasaga A.C. 1989. Modelling the geochemical carbon cycle. Scientific American 260: 74-81.

Bælum K. & Benn D.I. 2011.Thermal structure and drainage system of a small valley glacier (Tellbreen, Svalbard), investigated by ground penetrating radar. The Cryosphere 5: 139-149.

Bjørnsson H., Gjessing Y., Hamran S., Hagen J.O., Palsson F., Erlingsson B. 1996. The thermal regime of sub-polar glaciers mapped by multi-frequency radio-echo sounding. Journal of Glaciology 42 (140): 23–32.

Bliss L.C. & Matveyeva N.V. 1992. Circumpolar Arctic vegetation. In: Chapin III S.F., Reynolds R.L., Shaver G.R., Svoboda J., Chu E.W. (eds.): Arctic Ecosystems in a Changing Climate. Academic Press, San Diego: 59-89.

Bogen J. 1991.Erosion and sediment transport in Svalbard. In: Gjessing Y., Hagen J.O., Hassel K.A., Sand K., Wold B. (eds.): Arctic Hydrology, Present and future tasks. Norwegian National Committee for Hydrology Report No. 23, Oslo.

Bogen J. & Bønsnes T. 2003. Erosion and sediment transport in High Arctic rivers, Svalbard. Polar Research 22: 175-189.

Bohn T.J., Lettenmaier D.P., Sathulur K., Bowling L.C., Podest E., McDonald K.C., Friborg T. 2007. Methane emissions from western Siberian wetlands: heterogeneity and sensitivity to climate change. Environmental Research Letters 2: 045015. DOI: 10.1088/1748-9326/2/4/045015.

Boike J. 2009. SPARC and disappearing permafrost – a story from Bayelva in Svalbard. Svalbard 25 Science Forum. http://ssf.npolar.no/pages/news318.htm.

Bourke R.H., Wiegel A.M., Paquette R.G. 1988. The westward turning branch of the West Spitsbergen Current. Journal of Geophysical Research 93: 14065-14077.

Boyd T.J. & D'Asaro E.A. 1994. Cooling of the West Spitsbergen Current – wintertime observations west of Svalbard. Journal of Geophysical Research 99: 22597-22618.

Brown J., Ferrians O.J.Jr., Heginbottom J.A., Melnikov E.S. 1997. Circum-Arctic Map of Permafrost and Ground-Ice Conditions. U.S. Geological Survey, Map CP-45, U.S. Department of the Interior.

Brown G.H., Sharp M.J., Tranter M., Gurnell A.M., Nienow P.W. 1994. Impact of post-mixing chemical reactions on the major ion chemistry of bulk meltwaters draining the Haut glacier d'Arolla, Valais, Switzerland. Hydrological Processes 8: 465–480. DOI: 10.1002/hyp.3360080509.

Brown G.H., Tranter M., Sharp M.J. 1998. Experimental investigations of the weathering of suspended sediment by alpine glacial meltwaters. In: Sharp M., Richards K.S., Tranter M. (eds.): Glacier hydrology and hydrochemistry, John Wiley and Sons, England.

Brown G.H. 2002. Glacial meltwater hydrochemistry. Applied Geochemistry 17: 855-883.

Brown R.D., 2000. Northern Hemisphere snow cover variability and change, 1915–1997. Journal of Climate 13: 2339-2355.

Bruland O. & Hagen J.O. 2002. Mass Balance of Austre Brøggerbreen (Spitsbergen), 1971-1999, modelled with the precipitation-run-off model. Polar Research 21: 109-121.

Budantseva N.A., Vasilchuk A.K., Zemskova A.M., Chizhova YuN, Vasilchuk YuK, Christiansen H.H. 2012. Delta 18 O variations in late Holocene ice-wedges and winter air temperature variability in the Yamal Peninsula, Russia and in Adventdalen, Svalbard. International Conference on Permafrost (ICOP) Proceedings 10 (2): 41-45.

Burn C.R. & Kokelj S.V. 2009. The environment and permafrost of the Mackenzie Delta area. Permafrost and Periglacial Processes 20 (2): 83-105.

Casciotti K.L., Sigman D.M., Galanter Hastings M., Bohlke J.K., Hilkert A. 2002. Measurement of the oxygen isotopic composition of nitrate in marine and fresh waters using the denitrifier method. Analytical Chemistry 74: 4905–4912.

Challinor A. 1967. The Structure of Brøggerhalvøya, Spitsbergen. Geological Magazine 104 (04): 322-336. DOI: 10.1017/S0016756800048913.

Chapin D.M. & Bledsoe C.S. 1992. Nitrogen fixation in Arctic plant communities. In: Chapin III S.F., Jeffries R.L., Reynolds J.F., Shaver G.R., Svoboda J., Chu E.W. (eds.): Arctic Ecosystems in a Changing Climate. Academic Press, San Diego: 301-319.

Chou L., Garrels R.M., Wollast R. 1989. Comparative study of the kinetics and mechanisms of dissolution of carbonate minerals. Chemical Geology 78, 269-282.

Christiansen H.H., Etzelmüller B., Isaksen K., Juliussen H., Farbrot H., Humlum O., Johansson M., Ingeman-Nielsen T., Kristensen L., Hjort J., Holmlund P., Sannel A.B.K., Sigsgaard C., Åkerman H.J., Foged N., Blikra L.H., Pernosky M.A. & Ødegår R.S. 2010. The thermal state of permafrost in the Nordic area during the International Polar Year 2007-2009. Permafrost and Periglacial Processes 21: 156-181.

Christiansen T.R., Ekberg A., Ström L., Mastepanov M., Panikov N., Őquist M., Svensson B.H., Nykänen H., Martikainen P.J., Oskarsson H. 2003. Factors controlling large scale variations in methane emissions from wetlands. Geophysical Research Letters 30 (7): 1414. DOI:10.1029/2002GL016848.

Christiansen T.R., Johansson ., Åkerman H.J., Mastepanov M., Malmer N., Friborg T., Crill P., Svensson B.H. 2004. Thawing sub-Arctic permafrost: effects on vegetation and methane emissions. Geophysical Research Letters 31: L04501.

Cooper R., Wadham J.L., Tranter M., Hodgkins R., Peters N.E. 2002. Groundwater hydrochemistry in the active layer of the proglacial zone, Finsterwalderbreen, Svalbard. Journal of Hydrology 269: 208-223.

Cooper R., Hodgkins R., Wadham J., Tranter M. 2011. The hydrology of the proglacial zone of a High-Arctic glacier (Finsterwalderbreen, Svalbard): sub-surface water fluxes and complete water budget. Journal of Hydrology 406: 88-96.

Covington M.D., Banwell A.F., Gulley J., Saar M.O., Willis I., Wicks C.M. 2012. Quantifying

the effects of glacier conduit geometry and recharge on proglacial hydrograph form. Journal of Hydrology 414: 59-71.

Croll J., 1870. On Ocean-currents, Part I: Ocean-currents in relation to the Distribution of Heat over the Globe. Philosophical Magazine and Journal of Science 39 (259): 81-106.

Degens E.T., Kempe S., Richey J.E. 1991. Summary: biogeochemistry of major world rivers. In: Degens E.T., Kempe S., Richey J.E. (eds.): Biogeochemistry of Major World Rivers. Wiley, Chichester, UK: 323– 347.

Dierssen H.M., Smith R.C., Vernet M. 2002. Glacial meltwater dynamics in coastal waters west of Antarctic peninsula. Proceeding of the National Academy of Sciences 99 (4): 1790-1795.

Dove P.M. 1994. The dissolution kinetics of quartz in sodium chloride solutions at 25^{o}C to 300^{o}C. American Journal of Science 294: 665-712.

Dowdeswell J.A., Drewry D.J., Liestøl O., Orheim O. 1984. Radio echo sounding of Spitsbergen glaciers: problems in the interpretation of layer and bottom returns. Journal of Glaciology 30: 16-21.

Döscher R. 2010. Arctic Climate Modelling. Source: www.baltrex-research.eu/ecosupport/events/climatesummerschool/arcticclimatemodelling_ralfdoscher. Accessed on 01.12.2013.

Eckerstorfer M. & Christiansen H.H. 2012. Meteorology, topography and snowpack conditions causing two extreme mid-winter slush and wet slab avalanche periods in High Arctic maritime Svalbard. Permafrost and Periglacial Processes 23: 15-25.

Engstrom D.R., Fritz S.C., Almendinger J.E., Juggins S. 2000. Chemical and biological trends during lake evolution in recently deglaciated terrain. Nature 408: 161-166.

Etzelmüller B., Schuler T., Isaksen K., Christiansen H., Farbrot H., Benestad R. 2011. Modelling the temperature evolution of Svalbard permafrost during the 20th and 21st century. The Cryosphere 5: 67-79.

Edlund S.A. & Garneau M. 2000. Overview of vegetation zonation in the Arctic. In: Garneau, M., Alt, B.T. (eds.): Environmental Response to Climate Change in the Canadian High Arctic. Geological Survey of Canada Bulletin: 113-127.

Fairchild I.J., Bradby L., Spiro B. 1994a. Reactive carbonate in glacial sediments: a

preliminary synthesis of its creation, dissolution and reincarnation. In: Deynoux M., Miller J.G., Domack E., Eyles N., Fairchild I.J. & Young G.M. (eds.): Earth's Glacial Record. Cambridge University Press.

Fairchild I.J., Bradby L., Sharp M., Tison J.L. 1994a. Hydrochemistry of carbonate terrains in alpine glacial settings. Earth Surface Processes and Landforms 19: 33-54.

Fairchild I.J., Bradby L., Spiro B. 1994b. Carbonate diagenesis in ice. Geology 21.

Fairchild I.J., Killawee J.A., Sharp M.J., Spiro B., Hubbard B., Lorrain R.D., Tison J.L. 1999. Solute generation and transfer from chemically reactive alpine glacial-proglacial system. Earth Surface Processes and Landforms 24: 1189-1211.

Fang X., Pomeroy J.W., Ellis C.R., MacDonald M.K. 2013. Multi-variable evaluation of hydrological model predictions for a headwater basin in the Canadian Rocky Mountains. Hydrology and Earth System Sciences 17. 1635-1659. DOI:10.5194/hess-17-1635-2013.

Fausto R.S., Mernild S.H., Hasholl B., Ahlstrøm A.P., Knudsen N.T. 2012. Modelling suspended sediment concentration and transport, Mittivakkat glacier, southeast Greenland. Arctic, Antarctic, and Alpine Research 44 (3): 306-318.

Forsberg C.F., O'Dwyer J., Karlöf L., Winther J.G. 2000. Frozen climate archives at the mouth of the Arctic Ocean. Cicerone 4. www.cicero.uio.no/media/547.pdf Accessed on 15.11.2013.

Fowler H.J., Blenkinsopa S., Tebaldib C. 2007. Review Linking climate change modelling to impacts studies: recent advances in downscaling techniques for hydrological modelling. International Journal of Climatology 27: 1547-1578.

Førland E., Hanssen-Bauer I., Nordli P.Ø. 1997a. Climate statistics and long-term series of temperature and precipitation at Svalbard and Jan Mayen. DNMI-Report 21/97. Oslo, Norway: Norwegian Meteorological Institute.

Førland E., Hanssen-Bauer I., Nordli P.Ø. 1997b. Orographic precipitation at the glacier Austre Brøggerbreen, Svalbard. Report 02/97 Klima. Oslo: Norwegian Meteorological Institute.

Førland E.J., Benestad F., Flatøy F. 2009. Climate development in north Norway and the Svalbard region during 1900-2100. Norsk Polarinstitutt Rapportserie 128. Tromsø, Norway: Norwegian Polar Institute.

Freitag T.E. & Prosser J.I. 2004. Differences between betaproteobacterial ammonia-oxidizing communities in marine sediments and those in overlying water. Applied Environmental Microbiology 70: 3789-3793.

French H.M. 1996. The Periglacial Environment. 2nd Edition, Addison Wesley Longman, Edinburgh Gate: 341.

Frey K. & McClelland J. 2009. Impacts of permafrost degradation on Arctic river biogeochemistry. Hydrological Processes 23: 169-182.

Fountain A.G., Nylen T.H., MacClune K.L., Dana G.I. 2006. Glacier mass balances (1993-2001), Taylor Valey, McMurdo Dry Valleys, Antarctica. Journal of Glaciology 52: 451-62.

Gao X., Schlosser A.C., Sokolov A., Anthony K.W., Zhuang Q., Kicklighter D. 2013. Permafrost degradation and methane: low risk of biogeochemical climate warming feedback. Environmental Research Letters 8. 035014. DOI:10.1088/1748-9326/8/3/035014.

Garneau M.E., Vincent W.F., Alonso-Sáez L., Gratton Y., Lovejoy C. 2006. Prokaryotic community structure and heterotrophic production in a river-influenced coastal Arctic ecosystem. Aquatic Microbial Ecology 42: 27-40.

Gillett N.P., Stone D.I.A., Stott P.A., Nozawa T., Karpechko A.Y.U., Hegerl G.C., Wehner M.F., Jones P.D. 2008. Attribution of polar warming to human influence. Nature Geoscience 1: 750- 754.

Gillett N.P., Arora V.K., Flato G.M., Scinocca J.F., von Salzen K. 2012. Improved constraints on 21st-century warming derived using 160 years of temperature observations. Geophysical Research Letters 39: L01704. DOI:10.1029/2011GL050226.

Gislason S.R., Oelkers E.H., Snorrason A. 2006. Role of river-suspended material in the global carbon cycle. Geology 34 (1): 49-52.

Gooseff M.N., Barrett J.E., Levy J.S. 2013. Shallow groundwater systems in a polar desert, McMurdo Dry Valleys, Antarctica. Hydrogeology Journal 21 (1): 171-183.

Groisman P.Y., Karl T.R., Knight R.W. 1994. Observed impact of snow cover on the heat balance and the rise of continental spring temperatures. Science 263: 198-200.

Gutowski W.J.Jr., Wei H., Vorosmarty C., Fekete B. 2003. Regional climate simulation for the pan-Arctic region using MM5.

http://www.mmm.ucar.edu/mm5/workshop/ws00/Gutowski.pdf Accessed on 1st December 2013.

Guo Z., Bromwich D.H., Cassano J.J. 2003. Evaluation of Polar MM5 Simulations of Antarctic Atmospheric Circulation. Monthly Weather Review 131: 384-411. DOI: http://dx.doi.org/10.1175/1520-0493(2003)131<0384:EOPMSO>2.0.CO;2.

Gulley J.D., Benn D.I., Screaton E., Martin J. 2009. Mechanisms of englacial conduit formation and their implications for subglacial recharge. Quaternary Science Reviews 28; 1984-1999.

Gurnell A.M. 1993. How many reservoirs? An analysis of flow recessions from a glacier basin. Journal of Glaciology 39: 132.

Hagen J.O., Korsen O.M., Vatne G. 1991. Drainage pattern in a sub-polar glacier, Brøggerbreen, Svalbard. In: Gjessing U., Hagen J.O., Hassel K.A., Sand K., Wold B. (eds.): Arctic Hydrology. Present and Future Tasks. Norwegian National Committee for Hydrology Report No. 23, Oslo. 121-131.

Hagen J.O. & Sætrang A. 1991. Radio-echo soundings of sub-polar glaciers with low frequency radar. Polar Research 9: 99-107.

Hagen J.O. & Lefauconnier B. 1995. Reconstructed runoff from the High Arctic Basin Bayelva based on mass-balance measurements. Nordic Hydrology 26: 285296.

Hagen J.O., Melvold K., Pinglot F. Dowdeswell J.A. 2003. On the net mass balance of the glaciers and ice caps in Svalbard, Norwegian Arctic. Arctic Antarctic and Alpine Research 35: 264–270. DOI:10.1657/1523-0430(2003)035[0264:OTNMBO]2.0.CO2.

Hannah D.M., Gurnell A.M., McGregor G.R. 1999. A methodology for investigation of the seasonal evolution in proglacial hydrograph form. Hydrological Processes 13: 2603-2621.

Hannah D.M., Gurnell A.M., McGregor G.R. 2000. Spatio-temporal variation in micro-climate, the energy balance and ablation over a cirque glacier. International Journal of Climatology 20: 733-758.

Hannah D.M., Kansakar S.R., Gerrard A.J. 2005a. Identifying potential hydrological impacts of climatic variability and change for Himalayan basins of Nepal. Regional Hydrological Impacts of Climate Change—Impact Assessment and Decision Making, Proceedings of Symposium S6 during the VIIth IAHS Assembly at Foz do Iguaçu. IAHS. Publication 295: 120–130.Brazil.

Hannah D.M., Kansakar S.R., Gerrard A.J., Rees G. 2005b. Flow regimes of Himalayan rivers of Nepal: their nature and spatial patterns. Journal of Hydrology 308: 18–32.

Hanssen-Bauer I. 2002. Temperature and precipitation in Svalbard 19122050 measurements and scenarios. Polar Record 38 (206): 225232.

Hedges J.I. & Keil R.G. 1995. Sedimentary organic matter preservation: an assessment and speculative synthesis. Marine Chemistry 49: 81-115.

Hegerl G.C., Zwiers F.W., Braconnot P., Gillett N.P., Luo Y., Marengo Orsini J.A., Nicholls N., Penner J.E., Stott P.A. 2007. Understanding and attributing climate change. In S. Solomon et al. (eds.): Climate Change 2007: The Physical Science Basis. Contribution of Working Group 1 to the Fourth Assessment Report of the Intergovernmental Panel on Climate Change. Cambridge University Press, Cambridge, UK. 663–745.

Hjelle A. 1993. The geology of Svalbard. Polarhåndbook 7. Oslo: Norwegian Polar Institute.

Hobbie J.E., Peterson B.J., Bettez N., Deegan L., O'Brien W.J., Kling G.W., Kipphut G.W., Bowden W.B., Hershey A.E. 1999. Impact of global change on the biogeochemistry and ecology of an Arctic freshwater system. Polar Research 18 (2): 207-214.

Hoch A.R., Reddy M.M., Drever J.L. 1999. The importance of mechanical disaggregation in chemical weathering in cold, alpine environment, San Juan Mountains, Colorado. Geological Society of America Bulletin 111: 304-314.

Hodal H., Falk-Petersen S., Hop H., Kristiansen S., Reigstad M. 2012. Spring bloom dynamics in Kongsfjorden, Svalbard: nutrients, phytoplankton, protozoans and primary production. Polar Biology 35: 191-203.

Hodgkins R., Tranter M., Dowdeswell J.A. 1997. Solute provenance, transport and denudation in a High Arctic glacierized catchment. Hydrological Processes 11: 1813-1832.

Hodgkins R., Tranter M., Dowdeswell J.A. 1998. The hydrochemistry of runoff from a 'cold-based' glacier in the High Artic (Scott Turnerbreen, Svalbard). Hydrological Processes 12 (1): 87-103.

Hodgkins R., Hagen J.O., Hamran S. 1999. 20th Century mass balance and thermal regime change at Scott Turnerbreen, Svalbard. Annals of Glaciology 28: 216-220.

Hodgkins R., Tranter M., Dowdeswell J. 2004. The characteristics and formation of a High-Arctic proglacial icing. Geografiska Annaler 86 A: 265-275.

Hodgkins R., Cooper R., Wadham J., Tranter M. 2009. The hydrology of the proglacial zone of a High-Arctic glacier (Finsterwalderbreen, Svalbard): atmospheric and surface water fluxes. Journal of Hydrology 378: 150-160.

Hodson A.J. 1994. Climate, hydrology and sediment transfer process interactions in a sub-polar glacier basin. PhD thesis, University of Southampton, UK.

Hodson A., Gurnell A., Tranter M., Bogen J., Hagen J.O., Clark M. 1998a. Suspended sediment yield and transfer processes in a small High-Arctic glacier basin, Svalbard. Hydrological Processes 12 (1): 73–86.

Hodson A.J., Gurnell A.M., Washington R., Tranter M., Clark M.J., Hagen J.O. 1998. Meteorological and runoff time-series characteristics in a small, high-Arctic glaciated basin, Svalbard. Hydrological Processes 12 (3): 509-526.

Hodson A., Gurnell A., Tranter M., Bogen J. Hagen J.O. & Clark M. 1998b. Meteorological and runoff time series characteristics in a small high-Arctic glacier basin, Svalbard. Hydrological Processes 12: 509–526.

Hodson A., Tranter M., Vatne G. 2000. Contemporary rates of chemical denudation and atmospheric CO2 sequestration in glacier basins: an Arctic perspective. Earth Surface Processes and Landforms 25: 1447-1471.

Hodson A., Tranter M., Gurnell A., Clark M., Hagen J.O. 2002. The hydrochemistry of Bayelva, a High Arctic proglacial stream in Svalbard. Journal of Hydrology 257: 91-114.

Hodson A., Mumford P., Lister D. 2004. Suspended sediment and phosphorus in proglacial rivers: bioavailability and potential impacts upon the P status of ice-marginal receiving waters. Hydrological Processes 18 (13): 2409-2422.

Hodson A.J., Mumford P.N., Kohler J., Wynn P.M. 2005. The High Arctic glacial ecosystem: new insights from nutrient budgets. Biogeochemistry 72: 233-256.

Hodson A.J., Anesio A.M., Tranter M., Fountain A., Osborn M., Priscu J., Laybourn-Parry J., Sattler B. 2008. Glacial Ecosystems. Ecological Monographs 78 (1): 41-67.

Holland H.D. 1978. The Chemistry of the Atmosphere and Oceans. Wiley, New York.

Hollibaugh J.T., Bano N., Ducklow H.W. 2002. Widespread distribution in polar oceans of

a ^{16}S rRNA gene sequence with affinity to Nitrosospira-like ammonia-oxidizing bacteria. Applied Environmental Microbiology 68: 1478-1484.

Hood E. & Scott D.T. 2008. Riverine organic mater and nutrients in southeast Alaska affected by glacial coverage. Nature Geoscience 1: 583-587. DOI:10.1038/ngeo280.

Hop H., Pearson T., Hegseth E.N., Kovacs K.M., Wiencke C., Kwasniewski S., Eiane K., Mehlum F., Gulliksen B., Wlodarska-Kowalczuk M., Lydersen C., Weslawski J.M., Cochrane S., Gabrielsen G.W., Leakey R.J.G., Lønne O.J., Zajaczkowski M. et al. 2002. The marine ecosystem of Kongsfjorden, Svalbard. Polar Research 21 (1): 167-208.

Høj L., Olsen R.A., Torsvik V.L. 2005. Archaeal communities in High Arctic wetlands at Spitsbergen, Norway (78^{o}N) as characterized by 16S rRNA gene fingerprinting. FEMS Microbiology Ecology 53 (1): 89-101.

IPCC 2007. The Physical Science Basis. Contribution of Working Group I to the Fourth Assessment Report of the Intergovernmental Panel on Climate Change. Cambridge, United Kingdom and New York, NY, USA, Cambridge University Press.

Irvine-Fynn T.D. & Hodson A.J. 2010. Biogeochemistry and dissolved oxygen dynamics at a subglacial upwelling, Midtre Lovénbreen, Svalbard. Annals of Glaciology 51 (56): 41-46.

Irvine-Fynn T.D.L., Hodson A.J., Moorman B.J., Vatne G., Hubbard A.L. 2011. Polythermal glacier hydrology: a review. Reviews of Geophysics 49: RG4002. DOI:10.1029/2010RG000350.

Isaksen K., Sollid J., Holmlund P., Harris C. 2007. Recent warming of mountain permafrost in Svalbard and Scandinavia. Journal of Geophysical Research, Earth Surface 112: F02S04. DOI:10.1029/2006JF000522.

Iversen T. 1996. Atmospheric transport pathways for the Arctic. In: E.Wolff and R.C. Bales (eds.): Chemical exchange between the atmosphere and polar snow. Global Environmental Change. NATO ASI 1 (43): 71-92. Springer-Verlag, Berlin and Heidelberg,Germany.

Jansson P. 1999. Effect of uncertainties in measured variables on the calculated mass balance of Storglaciären. Geografiska Annaler 81 A: 633-642.

Jia W., Meibing J., Takahashi J., Suzuki T., Polyakov I.V., Mizobata K., Ikeda M., Saucier F.J., Meier M. 2008. Modelling Arctic Ocean heat transport and warming episodes in the

20th century caused by the intruding Atlantic Water. Chinese Journal of Polar Science 19 (2): 159-167.

Johannessen O.M., Shalina E.V., Miles M.W. 1999. Satellite evidence of or an Arctic sea ice cover in transformation. Science 286: 1937-1939.

Jorgenson M.T., Shur Y.L., Pullman E.R. 2006. Abrupt increase in permafrost degradation in Arctic Alaska, Geophysical Research Letters 25: L02503. DOI:10.1029/2005GL024960.

Jóhannesson T., Raymond C., Waddington, E. 1989.Time-scale for adjustment of glaciers to changes in mass balance. Journal of Glaciology 35: 355–369.

Kaiser J., Hastings M.G., Houlton B.Z., Röckmann T., Sigman D.M. 2007. Triple oxygen isotope analysis of nitrate using the denitrifier method and thermal decomposition of N_2O. Analytical Chemistry 79: 599-607.

Keil R.G., Tsamakis .E, Bor Fuh C., Giddings J.C., Hedges J.I. 1994. Mineralogical and textural controls on the organic composition of coastal marine sediments: hydrodynamic separation using SPLITT-fractionation. Geochimica et Cosmochimica Acta 58: 879-93.

Keller K., Blum J.D., Kling G.W. 2010. Stream geochemistry as an indicator of increasing permafrost thaw depth in an Arctic watershed. Chemical Geology 273 (1-2): 76-81.

Killingtveit A., Pettersson L.E., Sand K. 2003. Water balance investigations in Svalbard. Polar Research 22: 161-174.

Killingtveit A. 2004. Water balance studies in two catchments on Spitsbergen. In D.L. Kane & D. Yang (eds.): Northern research basins water balance. Proceedings of a workshop held at Victoria, Canada, March 2004. IAHS Publishing 290: 120-128. Wallingford: International Association of Hydrological Sciences Press.

Kohler J., Nordli Ø., Brandt O., Isaksson E., Pohjola V., Martma T. & Aas H.F. 2002. Svalbard temperature and precipitation, late 19th century to the present. Final report on ACIA-funded project. 483-491. Oslo: Norwegian Polar Institute.

Kohler J. 2010. Mass balance measurements of glaciers in Svalbard. Tromsø, Norway: Norwegian Polar Institute.

Kokelj S.V., Pisaric M.F.J., Burn C.R. 2007. Cessation of ice-wedge development during the 20th century in spruce forests of eastern Mackenzie Delta, Northwest Territories, Canada. Canadian Journal of Earth Sciences 44: 1503–1515.

Krause P., Boyle D., Base F. 2005. Comparison of different efficiency criteria for hydrological model assessment. Advances in Geoscience 5: 89-97.

Krawczyk W.E., Lefauconnier B., Pettersson L. 2003. Chemical denudation rates in the Bayelva catchment, Svalbard, in the Fall of 2000. Physics and Chemistry of the Earth 28: 1257-1271.

Krawczyk W.E. & Pettersson L. 2007. Chemical denudation rates and carbon dioxide drawdown in a ice-free polar karst catchment: Londonelva, Svalbard. Permafrost and Periglacial Processes 18: 337-350.

Krawczyk W.E. & Bartoszewski S.A. 2008. Crustal solute fluxes and transient carbon dioxide drawdown in the Scottbreen basin, Svalbard in 2002. Journal of Hydrology 362: 206-219.

Kump L.R., Brantley S.L., Arthur M.A. 2000. Chemical weathering, atmospheric CO_2, and climate. Annual Review of Earth Planetary Sciences 28: 611-67.

Kwok R. & Untersteiner R. 2011. The thinning of Arctic sea ice. Physics Today 64 (4). http://dx.doi.org/10.1063/1.3580491.

Landvik J.Y., Ingólfsson Ó., Mienert J., Lehman S.J., Solheim A., Elverhøi A., Ottesen D. 2005. Rethinking Late Weichselian ice-sheet dynamics in coastal NW Svalbard. Boreas 34: 7-24.

Lawler D.H., McGregor G.M., Phillips I.D. 2003. Influence of atmospheric circulation changes and regional climate variability on river flow and suspended sediment fluxes in southern Iceland. Hydrological Processes 17: 3195-3223.

Lawrence D.M., Slater A.G., Tomas R.A., Holland M.M., Deser C. 2008. Accelerated Arctic land warming and permafrost degradation during rapid sea ice loss. Geophysical Research Letters 35: 11506. DOI:10.1029/2008GL033985.

Liestøl O. 1976. Pingos, springs, and permafrost in Spitsbergen. Nor. Polarinst. Årb.: 7-29.

Le Fouest V., Babin M., Tremblay J. E. 2013. The fate of riverine nutrients on Arctic shelves. Biogeosciences, 10:3661-3677.

Lemke P., Ren J., Alley R.B., Allison I., Carrasco J., Flato G., Fujii Y., Kaser G., Mote P., Thomas R.H. and Zhang T. 2007. Observations: Changes in Snow, Ice and Frozen Ground.

In: Solomon S. et al. (eds.): Climate Change 2007: The Physical Science Basis. Contribution of Working Group I to the Fourth Assessment Report of the Intergovernmental Panel on Climate Change. Cambridge University Press, Cambridge, United Kingdom and New York, NY, USA.

Lliboutry L.A. 1971. Permeability, brine content and temperature of temperate ice. Journal of Glaciology 10 (58): 15-29.

Lliboutry L.A. 1976. Physical processes in temperate glaciers. Journal of Glaciology 16 (74): 151-158.

Lobbes J., Fitznar H.P., Kattner G., 2000. Biogeochemical characteristics of dissolved and particulate organic matter in Russian rivers entering the Arctic Ocean. Geochimica et Cosmochimica Acta 64: 2973-2983.

Leung L.R., Qian Y., Bian X., Washington W.M., Han J., Roads J.O. 2004. Mid-century ensemble regional climate change scenarios for the Western United States. Climatic Change 62: 75-113.

Mackay J.R. 1992. Lake stability in an ice-rich permafrost environment: examples from the western Arctic coast. In: Roberts R.D. & Bothwell M.L. (eds.): Aquatic ecosystems in semi-arid regions: Implications for resource management. NHR1 Symp. Ser. 7. Saskatoon: 1-26.

Magnuson J.J., Robinson D.M., Wynne R.H., Benson B.J., Livingstone D.M., Arai T., Assel R.A., Barry R.D., Card V., Kuusisto E., Granin N.G., Prowse T.D., Stewart K.M., Vuglinski V.S. 2000. Ice cover phenologies of lakes and rivers in the Northern Hemisphere and climate warming. Science 289: 1743-1746.

Marsz A.A & Styszyńska A. 2009. Oceanic control of the warming processes in the Arctic – a different point of view for the reasons o changes in the Arctic climate. Problemy Klimatologii Polarnej 19: 7-31.

Marsz A.A. 2010. Rola międzystrefowej cyrkulacji południkowej nad wschodnią częścią Atlantyku Północnego w kształtowaniu niektórych cech klimatu Arktyki Atlantyckiej. Problemy Klimatologii Polarnej 20: 7-29.

Matthews J.A. 1992. The Ecology of Recently Deglaciated Terrain: A Geoecological Approach to Glacier Forelands and Primary Succession. Cambridge: Cambridge University Press.

Mercier D. 2001. Le Ruissellement au Spitsberg. (Runoff on Spitsbergen.) Clermont-Ferrand, France: Blaise Pascal University Press.

Miethe A & Hergesell H. 1911. Mit Zeppelin nach Spitzbergen. Bilder von der Studienreise der deutschen arktischen Zeppelin Expedition. Deutches Verlagshaus BONG & Co. Berlin.

Milner A.M. & Petts G.E. 1994. Glacial rivers: physical habitat and ecology. Freshwater Biology 32: 295-307.

Milner A.M., Fastie C.L., Chapin III F.S., Engstrom D.R., Sharman L.C. 2007. Interactions and linkages among ecosystems during landscape evolution. BioScience 57 (3): 237-247.

Milner A.M., Brown L.E., Hannah D.M. 2009. Hydroecological response of river systems to shrinking glaciers. Hydrological Processes 23: 62-77.

Mitchell A.C., Lafrenière M.J., Skidmore M.L., Boyd E.S. 2013. Influence of bedrock mineral composition on microbial diversity in a subglacial environment. Geology. DOI: 10.1130/G34194.1.

Moore R.D. 2005. Slug injection using salt in solution. Watershed Management Bulletin 8 (2): 1-6.

Moulton K.L. & Berner R.A. 1998. Quantification of the effect of plants on weathering: studies in Iceland. Geology 26 (10): 895-898.

Mysak L., Manak D.K., Marsden R.F. 1990. Sea ice anomalies observed in the Greenland and Labrador Seas during 1901-1984 and their relation to an Interdecadal Climate Cycle. Climate Dynamics 5: 111-133.

Newman A.C.D. & Brown G. 1969. Delayed exchange of potassium from some edges of mica flakes. Nature 223: 175-176.

Nilsen F., Gabrrielsen T.M., Søreide J.E., Vader A., Skoghset R. 2013. www.unis.no/60_NEWS/6085_Archive_2013/n_13_01_04_warm_water/dominates_Svalbard_fjords_news_04012013.html accessed on 28.11.2013.

NSIDC (National Snow and Ice Data Centre). 2013. www.nsidc.org/arcticseaicenews accessed on 20.11.2013.

Nold S.C., Zhou J.Z., Devol A.H., Tiedje J.M. 2000. Pacific Northwest marine sediments contain ammonia-oxidizing bacteria in the beta subdivision of the Proteobacteria.

Applied Environmental Microbiology 66: 4532-4535.

Nowak A. & Hodson A. 2013. Hydrological response of a High Arctic catchment to changing climate over the past 35 years; a case study of Bayelva watershed, Svalbard. Polar Research 32: 19691, http://dx.doi.org/10.3402/polar.v32i0.19691.

Nuth C., Kohler J., König M., von Deschwanden A., Hagen J.O., Kääb A., Moholdt G., Pettersson R. 2013. Decadal changes from a multi-temporal glacier inventory of Svalbard. The Cryosphere 7: 1603–1621. DOI: 10.5194/tc-7-1603-2013.

Orvin A.K. 1934. Geology of the Kings Bay region, Spitsbergen. Skrifter om Svalbard og Ishavet 57. Oslo: Norway's Svalbard and Arctic Ocean Survey (Norwegian Polar Institute).

Østrem G. & Haakensen N. 1999. Map comparison or traditional mass-balance measurement: which method is better? Geografiska Annaler 81 A: 703-711.

Paterson W.S.B. 1971. Temperature measurements in Athabasca Glacier, Alberta, Canada. Journal of Glaciology 10 (60): 339-349.

Pecher K. 1994. Hydrochemical analysis of spatial and temporal variations of solute composition in surface and subsurface waters of a High Arctic catchment. Catena 21: 305-327.

Pettersson R.2004. Dynamics of the cold surface layer of polythermal Storglaciären, Sweden. PhD thesis, Stockholm University, Sweden.

Piechura J., Beszczynska-Moller A., Osinski R. 2001. Volume, heat and salt transport by the West Spitsbergen Current. Polar Research 20: 233-240.

Piwosz K., Walkucz W., Hapter R., Wieczorek P., Hop H., Wiktor J. 2009. Comparison of productivity and phytoplankton in a warm (Kongsfjorden) and a cold (Hornsund) Spitsbergen fjord in mid-summer 2002. Polar Biology 32 (4): 549-559.

Porter P., Vatne G., Ng F. & Irvine-Fynn T. 2010. Ice-marginal sediment delivery to the surface of a High-Arctic glacier: Austre Brøggerbreen, Svalbard. Geografiska Annaler 92 A: 437-449.

Prowse T.D., Wrona F.J., Reist J.D., Gibson J.J., Hobbie J.E., Lévesque L.M.J., Vincent W.F. 2006. Climate Change effects on hydroecology of Arctic freshwater ecosystems. Journal of the Human Environment 35 (7): 347-358.

Rachlewicz G. & Szczuciński W. 2008. Changes in thermal structure of permafrost active layer in a dry polar climate, Petuniabukta, Svalbard. Polish Polar Research 29 (3): 261-27.

Raiswell R. 1984. Chemical models of solute acquisition in glacial melt waters. Journal of Glaciology 30 (104): 49-57.

Raiswell R. & Thomas A.G. 1984. Solute acquisition in glacial melt waters I. Fjallsjokull (south-east Iceland): bulk melt waters with closed-system characteristics. Journal of Glaciology 30: 35-43.

Raiswell R., Tranter M., Benning L.G., Siegert M., Déath R., Huybrechts P., Payne T. 2006. Contribution from glacially derived sediment to the global iron (oxyhydr)oxide cycle: Implications for iron delivery to oceans. Geochimica Cosmochimica Acta 70: 2765-2780.

Raiswell R., Benning L.G., Davidson L., Tranter M. 2008. Nanoparticulate iron minerals in icebergs and glaciers. Mineralogy Magazine 72 (1): 345-348.

Räisänen O. 2008. http://commons.wikimedia.org/wiki/File:Topographic_map_of_Svalbard.svg. Accessed on 5.12.2013.

Repp K. 1988. The hydrology of Bayelva, Spitsbergen. Nordic Hydrology 4: 259-268.

Riebe C.S., Kirchner J.W., Finkel R.C. 2003. Long-term rates of chemical weathering and physical erosion from cosmogenic nuclides and geochemical mass balance. Geochimica et Cosmochimica Acta 67 (22): 4411-4427.

Riseborough D.W. 1990. Soil latent heat as a filter of the climate signal in permafrost. Proceedings of the Fifth International Conference on Permafrost. Colection Nordicana 54: 199-206. Univ. Laval, Quebec, Canada.

von Rohr M.R. 2007. The role of microbially mediated weathering on glacier forefields. Term Paper. Swiss Federal Institute of Technology, Zurich. Paper downloaded from www.up.ethz.ch/education/term_paper/Final_Version_M.R.vonRohr.pdf in October 2013.

Romanovsky V.E., Smith S.L., Christiansen H.H. 2010. Permafrost thermal state in the Polar Northern Hemisphere during the International Polar Year 2007-2009: a Synthesis. Permafrost and Periglacial Processes 21: 106-116.

Roth K. & Boike J. 2001. Quantifying the thermal dynamics of a permafrost site near Ny-Ålesund, Svalbard. Water Resources Research 37: 2901-2914.

Rouse W.R., Douglas M.S.V., Hecky R.E., Hershey A.E., Kling A.E., Lesack L., Marsh P., McDonald M., Nicholson B.J., Roulet N.T., Smol J.P. 1997. Effects of climate change on the freshwaters of Arctic and Subarctic North America. Hydrological Processes 11: 873-902.

Rovansek R.J., Hinzman L.D., Kane D.L. 1996. Hydrology of a tundra wetland complex on the Alaskan Arctic Coastal Plain,U.S.A. Arctic and Alpine Research 28 (3): 311-317.

Rutter N., Hodson A., Irvine-Fynn T., Solas M.K. 2011. Hydrology and hydrochemistry of a deglaciating High-Arctic catchment, Svalbard. Journal of Hydrology 410: 39-50.

Saloranta T.M. &Haugan P.M. 2001. Interannual variability in the hydrography of Atlantic water north west of Svalbard. Journal of Geophysical Research 106: 13931-13943.

Sand K., Winther J.G., Mare´chal D., Bruland O., Melvold K. 2003. Regional variations of snow accumulation on Spitsbergen, Svalbard, 199799. Nordic Hydrology 34: 17-32.

Schimel J.P., Bilbrough C., Welker J.M. 2004. The effect of increased snow depth on microbial activity and nitrogen mineralization in two Arctic tundra communities. Soil Biology and Biochemistry 36: 217-227.

Schuur E.A.G., Vogel J.G., Crummer K.G., Lee H., Sickman J.O., Osterkamp T.E. 2009. The effect of permafrost thaw on old carbon release and net carbon exchange from tundra. Nature 459. DOI: 10.1038/nature08031.

Sekar A., Fuchs B.M., Amann R., Pernthaler J. 2004. Flow sorting of marine bacterioplankton after fluorescence in situ hybridization. Applied Environmental Microbiology 70: 6210-6219.

Serreze, M.C., Walsh J.E., Chapin III F.S., Osterkamp T., Dyurgerov M., Romanovsky V., Oechel W.C., Morison J., Zhang T., Barry R.G. 2000. Observational evidence of recent change in the northern high latitude environment. Climatic Change 46: 159-207.

Seuthe L., Iversen K.R., Narcy F. 2011. Microbial processes in a high-latitude fjord (Kongsfjorden, Svalbard): II Ciliates and dinoflagellates. Polar Biology 34: 751-766.

Sharp M., Tranter M., Brown G.H., Skidmore M. 1995. Rates of chemical denudation and

CO2 drawdown in a glacier-covered alpine catchment. Geology 23: 61-64.

Sharp M. & Wolken G. 2010. Glaciers outside Greenland. In J. Richter-Menge & J.E. Overland (eds.): Arctic report card: update for 2010. 48-54. Darby, PA: Diane Publishing.

Skidmore M.L., Foght J.M., Sharp M.J. 2002. Microbial life beneath a High Arctic glacier. Applied Environmental Microbiology 66 (8): 3214-3220.

Skidmore M.L., Anderson S.P., Sharp M., Foght J., Lanoil B.D. 2005. Comparison of microbial community compositions of two subglacial environments reveals a possible role for microbes in chemical weathering processes. Applied Environmental Microbiology 71 (11): 6986-6997.

Skretteberg R. 1991. Discharge measurement structure under Arctic conditions. Design and construction considerations. In Y. Gjessing et al. (eds.): Arctic hydrology. Present and future tasks. 167-174. Oslo: Norwegian National Committee for Hydrology.

Smith L.C., Sheng Y., MacDonald G.M., Hinzman L.D. 2005. Disappearing arctic lakes. Science 308: 1429.

Smith S.L., Romanovsky V.E., Lewkowicz A.G., Burn C.R., Allard M., Clow G.D., Yoshikawa K., Throop J. 2010. Thermal state of permafrost in North America: a contribution to the International Polar Year. Permafrost and Periglacial Processes 21: 117-135. DOI:10.1002/ppp.690.

Stahl K., Moore R.D., Shea J.M., Hutchinson D., Cannon A.J. 2008. Coupled modelling of glacier and streamflow response to future climate scenarios. Water Resources Research 44: W02422.

Stallard R.F. 1995. Tectonic, environmental, and human aspects of weathering and erosion: A global review using a steady-state perspective. Annual Reviews of Earth and Planetary Science 23: 11-39.

Stuart G., Murray T., Gamble N., Hayes K., Hodson A. 2003. Characterization of englacial channels by ground-penetrating radar: An example from Austre Brøggerbreen, Svalbard. Journal of Geophysical Research-Solid Earth 108 (11): EPM 7-1-EPM 7-13.

Sturm M., Schimel J., Michaelson G, Welker J.M., Oberbauer S.F., Liston G.E.,Fahnestock J., Romanovsky V.E. 2005. Winter biological processes could help convert Arctic tundra to shrubland. BioScience 55 (1): 17-26.

Stutter M. & Billett M. 2003. Biogeochemical controls on streamwater and soil solution chemistry in a High Arctic environment. Geoderma 113: 127-146.

Styszyńska A. 2005. Przyczyny i mechanizmy współczesnego (1982-2002) ocieplenia atlantyckiej Arktyki. Wydawnictwo Uczelniane Akademii Morskiej w Gdyni: 109.

Styszyńska A. 2007. Zmiany klimatyczne w Arktyce a procesy oceaniczne. Zmiany klimatyczne w Arktyce i Antarktyce w ostatnim pięćdziesięcioleciu XX wieku i ich implikacje środowiskowe. Wydawnictwo Uczelniane Akademii Morskiej w Gdyni: 111-144.

Sujono J., Shikasho S., Hiramatsu K. 2004. A comparison of techniques for hydrograph recession analysis. Hydrological Processes 18: 403-413.

Sund M. 2008. Polar hydrology. Norwegian Water Resources and Energy Directorate's work in Svalbard. NVE Report 2. Oslo: Norwegian Water Resources and Energy Directorate.

Symon C., Arris L. & Heal B. (eds.): 2005. Arctic climate impact assessment. New York: Cambridge University Press.

Tank S.E., Manizza M., Holmes R.M., McClelland J.W., Peterson B.J. 2012. The Processing and Impact of Dissolved Riverine Nitrogen in the Arctic Ocean. Estuaries and Coasts 35:401-415.

Tranter M., Brown G.H., Raiswell R., Sharp M.J., Gurnell A.M. 1993. A conceptual model of solute acquisition by Alpine glacial meltwaters. Journal of Glaciology 39: 573-581.

Tranter M., Brown G.H., Hodson A.J., Gurnell A.M. 1996. Hydrochemistry as an indicator of subglacial drainage system structure: A comparison of Alpine and sub-polar environments. Hydrological Processes 10 (4): 541-556.

Tranter M., Sharp M.J., Lamb H.R., Brown G.H., Hubbard B.P., Willis I.C. 2002. Geochemical weathering at the bed of Haut Glacier d'Arolla, Switzerland – a new model. Hydrological Processes 16: 959-993.

Tranter M., Huybrechts P., Munhoven G., Sharp M.J., Brown G.H., Jones I.W., Hodson A.J., Hodgkins R., Wadham J. 2002. Direct effect of ice sheets on terrestrial bicarbonate, sulphate and base cation fluxes during the last glacial cycle: minimal impact on atmospheric CO_2 concentrations. Chemical Geology 190 (1-4): 33-44.

Tranter M., Skidmore M., Wadham J. 2005. Hydrological controls on microbial communities in subglacial environments. Hydrological Processes 19: 995-998.

Tveit J. & Killingtveit Å. 1994. Snow surveys for studies of water budget on Svalbard 19911994. In K. Sand & Å Killingtveit (eds.): Proceedings of the 10th International Northern Research Basins Symposium and Workshop, Spitsbergen, Norway. SINTEF Report 22 A96415. 489-509. Trondheim: Norwegian Institute of Technology.

Tye A. & Heaton T. 2007. Chemical and isotopic characteristics of weathering and nitrogen release in non-glacial drainage waters on Arctic tundra. Ceochimica et Cosmochimica Acta 71: 4188-4205.

Vatne G. 2001. Geometry of englacial water conduits, Austre Brøggerbreen, Svalbard. Norsk Geografisk Tidsskrift 55: 85-93.

Wadham J.L., Tranter M., Dowdeswell J.A. 2000. Hydrochemistry of meltwaters draining polythermal based high-Arctic glacier, south Svalbard II: Winter and early spring. Hydrological Processes 14: 1767-1786.

Wadham J.L., Cooper R.J., Tranter M., Hodgkins R. 2001. Enhancement of glacial solute fluxes in the proglacial zone of a polythermal glacier. Journal of Glaciology 47 (158): 378-386.

Wadham J.L., Tranter M., Skidmore M., Hodson A.J., Priscu J., Lyons W.B. 2010a. Biogeochemical weathering under ice: Size matters. Global biogeochemical Cycles 24: GB3025. DOI:10.1029/2009GB003688.

Wadham J.L., Tranter M., Hodson A.J., Hodgkins R., Bottrell S., Cooper R. 2010b. Hydro-biogeochemical coupling beneath a large polythermal Arctic glacier: Implications for sub ice sheet biogeochemistry. Journal of Geophysical Research 115: F04017. DOI: 10.1029/2009JF001602.

Wadham J.L., Bottrell, S., Tranter M., Raiswell, R. 2004. Stable isotope evidence for microbial sulphate reduction at the bed of a polythermal High Arctic glacier. In: Earth and Planetary Science Letters 219 (3-4): 341-355.

Wadham J.L., Tranter M., Skidmore M., Hodson A.J., Priscu J., Lyons W.B. 2010. Biogeochemical weathering under ice: Size matters. Global biogeochemical Cycles 24: GB3025. DOI: 10.1029/2009GB003688.

Walsh J.E., Kattsov V., Portis D., Meleshko V. 1998. Arctic precipitation and evaporation: Model results and observational estimates. Journal of Climate 11: 72-87.

Wells L.E. & Deming J.W. 2003. Abundance of Bacteria, the Cytophaga–Flavobacterium cluster and Archaea in cold oligotrophic waters and nepheloid layers of the Northwest Passage, Canadian Archipelago. Aquatic Microbial Ecology 31: 19-31.

Westermann S., Lüers J., Langer M., Pier K., Boike J. 2009. The annual surface energy budget of a high-Arctic permafrost site on Svalbard, Norway. The Cryosphere 3: 245-263.

Westermann S., Wollschläger U., Boike J. 2010. Monitoring of active layer dynamics at a permafrost site on Svalbard using multi-channel ground-penetrating radar. The Cryosphere 4: 475-487.

Westermann S., Boike J., Langer M., Schuler T.V., Etzelmuller B. 2011. Modeling the impact of wintertime rain events on the thermal regime of permafrost. The Cryosphere Discussion 5: 1697-1736.

Westermann S., Langer M., Boike J. 2011b. Spatial and temporal variations of summer surface temperatures of high-Arctic tundra on Svalbard – Implications for MODIS LST based permafrost monitoring. Remote Sensing of Environment 115: 908-922.

Westwood K.J. & Ganf G.G. 2004. Effect of cell flotation on growth of Anabaena circinalis under diurnally stratified conditions. Journal of plankton research 26 (10): 1183-1197.

White A.F. & Blum A.E. 1995. Effects of climate on chemical weathering in watersheds. Geochimica et Cosmochimica Acta 59 (9): 1729-1747.

Wilbanks T.J. & Kates R.W. 1999. Global change in local places: How scale matters. Climatic Change 43: 601-628.

Williams M.W., Knauf M., Caine N., Liu F., Verplanck P.L. 2006. Geochemistry and source waters of rock glacier outflow, Colorado Front Range. Permafrost and Periglacial Processes 17 (1): 13-33. DOI: 10.1002/ppp.535.

Williams P.J. & Smith M.W. 1989. The Frozen Earth: Fundamentals of Geocryology. Cambridge University Press: Cambridge. 306.

Wolf-Gladrow D.A., Zeebe R.E., Klaas C., Körtzinger A., Dickson A.G. 2007. Total alkalinity: The explicit conservative expression and its application to biogeochemical processes. Marine Chemistry 106: 287-300.

Wollast R. 1967. Kinetics of the alteration of K-feldspar in buffered solutions at low temperature. Geochimica et Cosmochimica Acta 3: 635-648.

Woo M.K., Lewkowicz A.G., Rouse W.R. 1992. Response of the Canadian permafrost environment to climatic change. Physical Geography 134: 287-317.

Woo M.K. & Young K.L. 2006. High Arctic wetlands: Their occurrence, hydrological characteristics and sustainability. Journal of Hydrology 320: 432-450.

www.eol.ucar.edu/projects/arcss/ArcticRIMS/AAR/4_0.htm. Accessed on 1st December 2013.

www.mikereyfman.com/photo/photo.php?Gallery=Arctic-Landscape-Svalbard-Spitsbergen-Norway&ImageNumber=MR0112&No=12&Name=Storoya_Island_covered_by_an_ice_cap._Svalbard_(Spitsbergen)_Archipelago,_Norway._81st_parallel_North. Accessed on 15th December 2013.

www.newscientist.com/blog/environment/2008/01/land-that-never-melts.html. Accessed on 15th December 2013.

www.starofsophia.blogspot.co.uk/2012/03/map-exercise-greenland-and-iceland.html. Accessed on 15th December 2013.

Wynn P.M., Hodson A., Heaton T. 2006. Chemical and isotopic switching within the subglacial environment of a High Arctic glacier. Biogeochemistry 78 (2): 173-193.

Yershov E.D. 1998. General Geocryology. Cambridge University Press: Cambridge. 580.

Yuan L., Sun L., Long N., Xie Z., Wang Y., Liu X. 2010. Seabirds colonized Ny-Ålesund, Svalbard, Arctic ~ 9,400 years ago. Polar Biology 33: 683-691.

Zarnetske J.P., Gooseff M.N., Brosten T.R., Bradford J.H., McNamara J.P., Bowden W.B. 2007. Transient storage as a function of geomorphology, discharge, and permafrost active layer conditions in Arctic tundra streams, Water Resources. Research 43: W07410. DOI:10.1029/2005WR004816.

Zemp M., Hoelzle M., Haeberli W. 2009. Six decades of glacier mass-balance observations: a review of the worldwide monitoring network. Annals of Glaciology 50: 101-111.

Zhu X., Zhuang Q., Lu X., Song L. 2013. Spatial scale-dependent land-atmospheric methane exchange in the northern high latitudes from 1993 to 2004. Biogeosciences

Discussions 10 (11): 18455-18478.

Zhu X., Zhuang Q., Qin Z., Glagolev M., Song L. 2013. Estimating wetland methane emissions from the northern high latitudes from 1990 to 2009 using artificial neutral networks. Global Biogeochemical Cycles 27 (1-13). DOI: 10.1002/gbc.20052.